Scaling and mean reversion in foreign exchange time series

Maria Elisabeth Boeker

Thesis submitted for the degree of
Doctor of Philosophy

University College London
Department of Computer Science

Primary Supervisor: Dr. Guido Germano
Secondary Supervisor: Prof. Jessica James

25 August 2021

Declaration

I, Maria Elisabeth Boeker, confirm that the work presented in this thesis is my own. Where information has been derived from other sources, I confirm that this has been indicated in the thesis.

Abstract

This thesis aims to further our understanding of the statistical properties of foreign exchange rate time series. We propose a model of nominal exchange rates as following an Ornstein–Uhlenbeck process with a time-dependent reversion level and test this model against real-world data with a particular focus on the scaling properties of the series. In doing so, we aim to contribute towards the development of a stochastic model of FX rates which combines the mean-reverting behaviours predicted by economic models and trading strategies with the multifractal properties of foreign exchange time series well-known in econophysics. Our findings may be used to improve models of foreign exchange time series as well as trading strategies.

The research analyses real-world foreign exchange time series and synthetic data sets and comprises the following three parts:
Part 1 explores the scaling of the volatility of exchange rates under the premise of the series having a mean-reverting component. Using simulated data, we show that our model is as good at reproducing the volatility scaling of the real data as a random walk.
Part 2 examines two aspects of Ornstein–Uhlenbeck parameter estimation. First, the accuracy of the estimators in the case of incomplete or irregular finite samples is numerically investigated. Second, a novel parameter estimation method for Ornstein–Uhlenbeck processes with unknown time-dependent reversion level is proposed, and this and an existing method are tested. Neither of these topics are well-represented in the literature, yet they have numerous applications, within and beyond the field of finance.
Part 3 calibrates our model to real-world FX data using the method proposed in Part 2. We give an empirical relationship between the calibrated parameters of the model and the way the underlying trend is defined. We show that this dependence can be described by the Hurst exponent of the series. This finding may help inform the construction of models of FX rates as well as parameter estimation and calibration methods where unknown time-dependent reversion levels are involved.

This thesis contributes to science in a number of ways:

- we have extended the range of intervals for which the scaling of FX volatility has been shown to hold;
- we have shown that this scaling law may be compatible with a mean reversion based model of FX rates;
- we have gathered some insight into the reliability of parameter estimation of the Ornstein–Uhlenbeck process under imperfect conditions;
- a novel calibration method for an Ornstein–Uhlenbeck process with time-dependent mean has been proposed and an existing method has been tested;
- a relationship between the calibrated parameters of a mean-reverting model of FX rates and the self-similarity of the series was found.

Impact statement

With this thesis we contribute towards the development and refinement of stochastic models of nominal exchange rates. The foreign exchange market is the largest financial market in the world, and therefore directly and indirectly affects a great number of people worldwide. There are of course many financial applications of a model of exchange rates, including in trading strategies, risk management, option pricing, and informing government regulations. Additionally, there are well-known similarities between the behaviours of foreign exchange rates and quantities in other fields within and outside of finance. Thus, findings in the foreign exchange market may contribute towards advances in these related fields too.

We also present some insight into the parameter estimation and calibration of the Ornstein–Uhlenbeck process with constant and time-dependent reversion level. While our primary interest in these findings is with regard to foreign exchange data, the Ornstein–Uhlenbeck process finds applications in a wide range of fields including physics and neuroscience. Anywhere where this process is used, a deeper understanding of the parameter estimators will help improve methods.

Acknowledgments

I would like to thank my supervisors Dr. Guido Germano and Prof. Jessica James. I am grateful to the EPSRC Doctoral Training Centre in Financial Computing and Data Science at UCL, and Prof. Philip Treleaven in particular, for funding and supporting my PhD. Further thanks go to my initial supervisor Prof. Byron Cook, as well as Dr. Stephen Pasteris, Dr. Kiki Leutner, Tom Mayne, my family, my friends, my cat, Antifolk, and anyone who's ever got me a VDCNLNI or similar. Most of all I thank my dad for his support and help throughout this PhD.

Contents

List of Figures

List of Tables

Chapter 1

Introduction

In this chapter we present the motivation for this thesis, the research objectives, the methodologies employed in the research for all three parts, as well as a preview of the contributions to science made. Finally, we explain how the thesis is structured.

1.1 Research motivation

This thesis is concerned with statistical properties of the Foreign Exchange market. The FX market is the largest financial market in the world. There has been a large increase in high-frequency trading in recent years, and thus a large amount of high-frequency data has become available to research. This data is different both in the processes that generate it and in its properties. In particular, there is a much larger involvement of algorithmic trading, and traders are able to create a higher turnover than they have in the past. This consistent growth and evolution of the FX market means that there is a wealth of open research questions, and the financial importance of these questions ensures a demand for answers.

Due to the complexity of the factors that affect the FX market, short of a complete understanding of the causalities in the FX market the market may be best described through models. While there are of course many different disciplines seeking to model the market in different ways, for example from economic, political, or behavioural perspectives, this thesis aims to model FX rates as stochastic processes, with a basis in some of the stylized facts of FX rates found in the literature. In particular, we are concerned with a model of nominal FX rates following a mean-reverting process with time-dependent reversion level, with a particular focus on the self-similarity of the series under such a model. The model is consistent with economic models of foreign exchange rates, as well as with the models underlying many popular trading strategies. Meanwhile, the fractality, and indeed multifractality, of FX rates is a well-established fact in the literature of econophysics. The motivation of this thesis was to unite these two seemingly disparate aspects.

We chose an Ornstein–Uhlenbeck process (OUP) as the foundation for the mean-reverting model. However it is a well-known fact that the estimators of the OUP are

biased. But how unreliable are they? While there is much literature giving the analytically derived variances and biases of the estimators of the OUP, these are mostly concerned with regularly observed data, and often infinite sample sizes. In real-world applications samples are of course finite, and financial data presents additional problems, such as only being recorded during market opening hours, and high-frequency data being irregularly spaced in time. We wanted to test the performance of the parameter estimators of the standard Ornstein–Uhlenbeck process in practical application to imperfect data sets. We therefore, using synthetic data, tested the effect of the process and observation parameters and irregularity in observation on the bias and accuracy of the parameter estimators.

The literature on the calibration or parameter estimation of an OUP with unknown time-dependent reversion level is very scarce, and thus, we tested one method we found in the literature against an alternative proposed by us. As we calibrate this model in a purely data-driven way, we are faced with the problem of separating the processes into the "underlying" and the "overlayered" components. But how does the calibration of the model depend on how we define this separation? In order to answer this question, we tested different ways of defining the underlying trend and found a dependence of the calibrated model parameters on the way the trend was defined.

We next hypothesized that this dependence was related to the fractality of the data. We tested this hypothesis by describing the dependence of the calibrated parameters on the underlying value as a scaling law, which we then compared to the scaling relationship found by conducting a detrending moving average analysis, which is a type of scaling analysis that measures the roughness of a series. In doing so, we not only shed light on our model of FX rates, but also gathered further evidence of the fractality of FX time series. While the self-similarity of FX rates is well-documented, re-confirming it is nonetheless of interest due to the fact that new time scales become available, with larger time scales becoming available as the FX market as we know it ages, and smaller time scales becoming available due to technological advances.

A greater statistical understanding of FX rates is of course always of use, and may help inform many kinds of real-world decisions. The model we propose and any insight associated with our research, like many findings in econophysics, may also be applicable to other fields, but it is also directly relevant to mean-reversion based trading strategies, which assume a mean reversion to a time-dependent fundamental value, which in many cases is obtained in a purely data-driven way, for example through a moving average. Many trading strategies use "moving average crossovers" to determine buying/selling signals. However, in some cases, particularly in what is referred to as "technical analysis", there tends to be a lack of theoretical foundation for these strategies. How can crossovers of and mean reversion to moving averages in FX be described and predicted statistically? With this research we hope to contribute to a stochastic model of FX rates to provide a statistical foundation to some of these methods.

Thus, our motivation for this thesis was to

- reconcile models of FX rates being mean-reverting to an underlying reversion level with the known fractality of the market;
- update the literature on the scaling of mean absolute log returns in FX using a novel data set;
- improve our understanding of parameter estimation of the Ornstein–Uhlenbeck process under imperfect conditions;
- propose and test a way of estimating the parameters of an OUP with unknown time-dependent reversion level;
- find out how the calibration of such a model to foreign exchange data depends on the Hurst exponent of the time series;
- use DMA to find the Hurst exponent of FX time series.

1.2 Research objectives

Our first research objective was to confirm the validity of the well-known scaling law describing a linear relationship between the logarithm of mean absolute log returns and the logarithm of the time intervals over which they are measured using our novel data sets, to see if the scaling law would extend to a greater range of time intervals and to newer data than previously tested, as well as to estimate the scaling exponent of the series.

The next goal was to generate two synthetic data sets as models of logarithmic FX rates, one following Brownian motion, and the other following an Ornstein–Uhlenbeck process with time-dependent reversion level, and to see whether these two models would obey the same scaling law as we observed in the real-world FX data.

Since our model was of log FX rates following a mean-reverting process with time-dependent reversion level, which might be interpreted as a trend, we next wanted to test how "detrending" the data would affect the mean absolute log returns. The hypothesis based on the model was that the mean absolute returns of the detrended log data would depend on the time intervals in the same way as the mean absolute returns of an OUP. This was to be tested by detrending the data before again computing the mean absolute returns as a function of the time intervals over which they were observed, and comparing the results to those obtained by conducting the same analysis on the two synthetic data sets.

We next aimed to shed some light on the reliability of standard parameter estimation methods of the OUP in the case of finite samples, and in particular in the case of small reversion strengths. Secondly, we wanted to determine how the reliability of the estimators would be affected by irregularity of observations. We were particularly interested in the effect that estimating irregularly observed data as regular would have on the estimation accuracy, as well as in the effect of observational gaps such as weekends on parameter

estimation in the case of interpolation or estimating the parameters using a business time scale. This was done by simulating sets of time series following standard Ornstein–Uhlenbeck processes with a variety of parameters, and then sampling the process regularly, irregularly, or with major gaps in the observation sequence, before testing the performance of the parameter estimators in the different scenarios.

The next goal was to test a parameter estimation method we found in the literature, which estimates the parameters of an Ornstein–Uhlenbeck process with unknown time-dependent reversion level, against an alternative method proposed by us. We did this by simulating such a process and then comparing the performance of the two methods to the results of applying the standard parameter estimation method to the simulated data.

Since both of these methods include an arbitrary parameter, which affects the accuracy of the estimator of the underlying reversion level, and since the accuracy of all other estimators relies on the estimation of the reversion level, we hypothesized that the calibration of the model of an OUP with time-dependent reversion level to a time series using either of the methods would heavily rely on the choice of this parameter. Furthermore, our hypothesis was that this dependence could be described by the Hurst exponent, which is a measure of the memory of the process. Thus our final objective was to determine a scaling relationship between the calibrated parameters and the parameter of the reversion level estimation, and then compare this scaling exponent to the Hurst exponent found via a detrending moving average analysis.

1.3 Research methodology

In the following subsections we will give an overview of the data sets our research is based on and the methodology employed in producing the three parts of the research.

1.3.1 Data sets

In addition to the simulated synthetic data sets, two different real-world data sets were used in this research. Both contained historical foreign exchange data.

The first data set was obtained from the Thomson Reuters Eikon platform. It contained the 17 currency pairs USD/CAD, USD/GBP, USD/JPY, EUR/AUD, EUR/CAD, EUR/CHF, EUR/GBP, EUR/JPY, EUR/USD, EUR/NOK, EUR/SEK, GBP/AUD, GBP/CAD, GBP/CHF, GBP/EUR, GBP/JPY and CHF/JPN. Historical close prices captured at six different frequencies were downloaded, with the time intervals between consecutive observations being 24 hours, 60 minutes, 30 minutes, 10 minutes, 5 minutes and 1 minute. This data reached back between 40 years for daily data and about 40 days for minutely data. The data was mostly regularly spaced, but contained some gaps.

The second data set was obtained from Commerzbank. It contained irregularly spaced high-frequency bid and ask quotes for 63 currency pairs for the time period between 1 January 2015 and 15 December 2016. Each quote had as its source either London or

New York, and for the most liquid currency pairs the frequency of the data reached about 150,000 values per source per day. After cleaning this data set we were left with one series per source for the currency pairs AUD/JPY, AUD/USD, EUR/USD, EUR/BRL, USD/CAD, USD/CHF, USD/CNH.

1.3.2 Part 1: Scaling of log returns

The first goal of this part of the research was to test if a well-known scaling law of FX mean absolute log returns would hold in more recent data and over a wider range of intervals than previously reported in the literature. This was done by sampling each log FX series at different sampling frequencies, producing a set of series with different observation steps. For each of these sampled series we then computed the mean absolute return and then conducted a line fit to the log mean absolute log returns as a function of the log observation steps to find the slope and correlation coefficient. Then, in order to see if this behaviour would be predicted by our model of log FX rates following an OUP with a smoothed Brownian motion as reversion level, we simulated such a process, as well as a time series following a Brownian motion, and conducted the same analysis on these two series. Next, motivated by our model, we detrended the log FX series as well as both simulated series by subtracting a range of moving averages, before again computing the mean absolute returns of these detrended series and comparing them to the mean absolute returns of a standard Ornstein–Uhlenbeck process.

1.3.3 Part 2: OUP parameter estimation under various conditions

The goal of Part 2 of the research was to gain some insight into the reliability of the standard parameter estimators of the standard OUP based on imperfect observations, and to test methods for estimating the parameters of an OUP with time-dependent mean. This was done by first simulating multiple paths of standard OUPs with a variety of parameters and then computing the mean errors and mean squared errors of the standard estimators over the paths for each parameter set. We then simulated irregularly sampled OUPs by simulating standard OUPs at higher frequencies and then sampling a subset of the simulated points of each path. We tested a number of different sampling scenarios. Firstly, we simulated an OUP with a constant sampling step, but with regular major gaps in the data to represent weekends. We then estimated the parameters of these series first by interpolating the missing values, and then by treating the data as a complete data set, and compared the MEs and MSEs of these estimators to those obtained from the complete observation. Secondly, we sampled the process at a random point within a certain window centred around each regular sampling point, and then at a set of entirely randomly selected sampling points. We again compared the MEs and MSEs of the estimators in all these cases.

We then used a technique we found in the literature to estimate the parameters of an OUP with a time-dependent reversion level. We simulated such a process with a sine

function as reversion level, and then applied this technique to find the estimators along with their MEs and MSEs. We then implemented an alternative method proposed by us, which subtracts a moving average from the sampled series and then applies standard OUP parameter estimation techniques to the detrended series. We generated parameter estimates along with MEs and MSEs with this method on the same process and compared the performance of these estimators to the performance of standard estimators based on the original, non-detrended series.

1.3.4 Part 3: Time-dependent OUP reversion levels and the Hurst exponent

In Part 3, our method tested in Part 2 was used to calibrate a model of an OUP with time-dependent reversion level to real-world FX data. Our goal was to see how the calibrated parameters would depend on the time constant used to compute the moving average. We used simple and exponentially weighted moving averages, with a range of time constants, and for each detrending method we applied our estimation technique to calibrate the reversion strength and diffusion coefficient of the model. We fitted a curve of the shape $f(x) = a/x$ to the relationship between the reversion strength parameter and the time constant, and a curve of the shape $g(\tau) = b\tau^c$ to the relationship between the long-term variance of the calibrated model and the time constant. Finally, we conducted a detrending moving average analysis to find the Hurst exponent of the series and compared the Hurst exponent to the scaling exponent of the long-term variance to see if there was a dependence.

1.4 Contributions to science

There are a number of ways in which this thesis hopes to contribute to science.

In Part 1, the scaling law relating the volatility of exchange prices to the time interval over which it is measured is verified using a novel data set and a greater range of intervals than we have found reported in the literature. We thus have extended our knowledge of the ranges of intervals over which the scaling law holds. We also show that the scaling law may be consistent with a model of FX rates reverting to a time-dependent underlying value, and that the mean absolute returns of detrended FX data resemble those of an Ornstein–Uhlenbeck process. This helps bridge the gap between this scaling behaviour, which has so far been reported as a stylized fact in the literature, and models and trading strategies based on FX rates being mean-reverting.

In Part 2, we present numerical findings regarding the accuracy of standard parameter estimators of the Ornstein–Uhlenbeck process in the case of irregular observations. As far as we know, the effect of the true parameters of the OUP on estimator accuracy in the case of irregular observations and interpolation has not been reported before. These findings are extremely relevant wherever OUP parameters are estimated on imperfect data, as we

have shown significant effects of the irregularity, and a qualitative difference between the effect of parameters on estimator accuracy between the regular, irregular, interpolated and business time cases. Secondly, we have proposed a method of estimating the parameters of OUPs with time-dependent reversion level which we have not found reported elsewhere, and have tested this method against another method reported in the literature, showing that the two methods perform similarly. There is currently very little literature on the subject of estimating the parameters of an OUP with unknown time-dependent reversion level, and our research may help in developing and refining such methods, which have a great number of potential applications not only in finance but also in other areas such as physics.

In Part 3, we show that the calibration of a model of an OUP reverting to a time-dependent reversion level, which relies on detrending the process, is heavily dependent on the detrending method used, and show empirically the relationships between the calibrated parameters and the detrending parameter. These findings are relevant not only to the calibration of OUPs with time-dependent reversion level, but also to the parameter estimation of such processes. We also conduct a detrending moving average analysis on FX series and determine the Hurst exponent of the series and show that the dependence of the calibrated parameters on the detrending parameter is directly related to the Hurst exponent. To the best of our knowledge, this has never been done before, and we suggest that it may be of great use for improving trend-following trading strategies and models of FX time series.

1.5 Structure of the thesis

The presentation of our research is preceded by the background and literature review, which gives an extensive overview of the background and existing literature regarding the themes covered in this thesis, with a deeper look at the most relevant literature. The background and literature review is followed by the research, which is divided into three parts. We refer to these as Parts 1–3. Each research chapter contains several related analyses. The research chapters start with a description of the overarching research question before presenting the methodology, followed by the results of each of the analyses contained in the chapter and then concluding with a discussion, where we evaluate and interpret results, point out weaknesses of the research, and discuss ideas for further study. In the final chapter of the thesis we summarize our conclusions and areas for further research. The appendix contains additional graphs and tables of the same type but greater scope than those included in the main research chapters.

Chapter 2

Background and literature overview

This chapter presents the theoretical and contextual background for this research and reviews relevant existing literature.

The foreign exchange market is the world's largest [1, 2] and most liquid [3] capital market. As such, it provides a wealth of data, and equally the demand for information that can be used for trading is very high. Compared with many fields, finance is still young, and with the continued advancements in computing and technology, its nature is constantly evolving, and the volume and frequency of trading are ever-increasing [2]. There is therefore a steady opportunity for research, both in gaining new knowledge about the market, and in seeing whether previously established properties still hold.

In particular, algorithmic trading has seen a rapid rise. Instead of trading decisions being made based on knowledge of external factors, more and more trades are executed based purely on a statistical analysis of the time series the market provides. One well-known trading strategy which can be algorithmized is the trend following strategy, which assumes that there are periods when prices have a tendency to continue moving in their current direction. An alternative strategy, which is in some ways complementary to the trend following strategy, is the mean reversion strategy, which assumes a tendency of prices to return to a long-term equilibrium. These strategies are sometimes summed up as "buy winners, sell losers" and "buy low, sell high" respectively. For trading strategies such as these to be studied and improved, a thorough knowledge of the statistical properties of the financial market in which one is trading is imperative.

Numerous theories have been proposed to describe financial markets in general and the foreign exchange market in particular. One of the oldest of these is the random walk hypothesis, first proposed in 1863 by Jules Regnault and in 1900 by Louis Bachelier, which assumes that no information about future price movement can be gained from past data. Related to this is the efficient market hypothesis (EMH), developed in the 1960s concurrently by Paul Samuelson and Eugene Fama, which assumes that all available information about a commodity will be reflected in its current price [4]. An example of a model con-

forming to the EMH is the theory that prices follow Brownian or geometric Brownian motion. The EMH itself has by now widely been rejected [5] and efficiency is viewed as a relative concept, with the foreign exchange market being arguably the most efficient of the financial markets. However, stylized facts regarding foreign exchange market data consistently show a number of scaling behaviours not compatible with a geometric Brownian motion of exchange rates. Exchange rates are also sometimes modelled by mean reverting stochastic processes, with one example of such a process being the Ornstein–Uhlenbeck (OU) process [6].

Some of the topics that this thesis builds on are presented in some more detail in this chapter: We start with some background information on the foreign exchange market, as this is the setting and area of application of our research. We then give some information about the Ornstein–Uhlenbeck process and its parameter estimation, before looking at some extensions of the process. Finally we review the topic of scaling and self-similarity, both in general and with regard to foreign exchange data.

2.1 The foreign exchange market

To provide some context to the research conducted in this thesis, we start out by providing some general information about the FX market, before briefly describing some of the FX rate and trading models relevant to our work.

2.1.1 Background

The FX market of today originated in the 1970s with the end of the Bretton Woods system, and today is the largest capital market of all, continuing to evolve at a rapid pace [7]. According to the Bank for International Settlements (BIS), the average daily trading volume as of April 2019 was US$6.6 trillion, having grown by US$1.5 trillion since April 2016 [8].

The FX market is decentralized and for the most part unregulated. It is open continuously, from about 10pm GMT on Sunday until about 10pm GMT on Friday, with varying levels of activity depending on the times of day in its various locations in Australia, Asia, Europe and New York [9]. The two main locations are London and New York, where roughly one third and one fifth of trades take place respectively [10]. The four most heavily traded currencies, which are sometimes referred to as "the majors" or "G4", in descending order are the US dollar (USD), the euro (EUR), the Japanese yen (JPY) and the British pound (GBP) [10]. Currency prices are usually quoted against the US dollar. Pairs that do not involve the US dollar are referred to as "cross rates" [11]. While we study only spot rates in this thesis, which are the immediate currency exchange rates and accounted for 30% of global FX turnover in April 2019 [8], there are of course also markets within the FX market for other instruments, such as swaps, options [12, 13], forwards and futures.

While the original purpose of the FX market was to facilitate international trading of goods and services, it is now also used to make money through speculation as well as to hedge investments, and participants in the FX market include central banks, commercial banks, FX brokers, private companies, investors, as well as individuals [14]. Nowadays, just like in other markets, a large proportion of trades is algorithmic, and the frequency of trading has skyrocketed with the evolution of technology, with a 2011 BIS report estimating about a quarter to a third of trades being high-frequency [15].

Trades are executed based on quotes given by the major dealers. Quotes in the FX market are given as separate "ask" and "bid" prices. A bid quote is the price for which the dealer is prepared to buy the pair, and an ask quote is the price for which they are prepared to sell [14]. In other words, there is an implied transaction cost, which is the bid-ask spread, from which the dealer profits. When the spot rate is modelled as a single time series it is therefore necessary to find a mid price.

The granularity with which currencies are traded is measured in "pips", short for price increment points [10] or price interest points. Usually pairs are quoted with an accuracy of four decimal points. For pairs involving the Japanese yen a pip is 0.01 of the pair. By pair, we mean the price of one currency expressed in terms of another.

We speak of "nominal" and "real" exchange rates. The nominal exchange rate (NER) is equivalent to the spot rate, i.e. the rate at which a currency pair can be exchanged on the FX market, while the real exchange rate (RER) is a theoretical quantity determined from the domestic prices of goods in the respective countries and the NER. Note that some currency rates are fixed by governments, but throughout this thesis we are concerned with floating rates. We discuss FX rate determination in the following section.

2.1.2 Models of foreign exchange rate determination

There are many different ways in which the determination of FX rates has been modelled, with separate models for nominal and real exchange rates. In this thesis we study the NER, and we focus on macro models, which do not incorporate the detailed effects of trading [16]. While until the 1970s models of FX rate determination were more commonly based on flow based approaches, such as the Mundell–Fleming model, this has been superseded by asset based models [17], which is what we will focus on in this section. One concept central to this branch of models is that of purchasing power parity (PPP), which has a number of definitions [17], but roughly stipulates that there should be no arbitrage opportunity through the costs of goods or assets in different countries [18]. The PPP rate therefore may be determined by assuming that some "identical" bundle of goods in two different countries in their respective domestic currencies should cost the same amount of "money" [19]. With regard to individual items, this assumption is referred to as the law of one price [18]. This is directly related to the RER R, which in its simplest form is defined as the

ratio between the NER N and the PPP rate P:

$$R = \frac{N}{P}\,. \tag{2.1}$$

Note that this means for the logarithmic NER, which is the quantity we analyse in this thesis, that

$$\log N = \log R + \log P\,. \tag{2.2}$$

The RER is constant if PPP holds [19]. Note that due to economic factors as well as varying ways of computing the PPP rate it is not necessarily 1.

The most popular model of the NER is the monetary model, which assumes that an equilibrium of exchange rates is based on free flow of capital, but not free flow of bonds. This is in contrast with the portfolio balance model, which assumes both capital and bonds to be free-flowing [17]. Within the monetary model there are the flexible price model and the sticky price model. According to the latter, which is also sometimes called the overshooting model or Dornbusch model, PPP holds in the long run, i.e. real FX rates, and thus log real FX rates, revert to a constant, meaning that log nominal FX rates revert to a constant plus the log PPP rate, in the long run but not in the short run, making them mean-reverting to a time-dependent value. In reality, the RER has indeed been found to be not constant but mean reverting [18], supporting this model, and in the short and medium run spot exchange rates are commonly modelled as random walks [20]. The idea that FX prices display different behaviour at different frequencies, which relates to the topic of scaling, discussed in Section 2.5, is also treated by Gençay et al. [1] amongst others, and is reflected in the use of separate models for long-run and short-run exchange rates. We look at evidence of mean reversion in FX rates in the next section.

More generally, one aspect that many FX rate determination models have in common is that they assume an underlying fundamental rate, such as the PPP rate, which may change over time as influenced by a variety of economic factors such as trade, production, inflation and interest rates, and upon which the NER depends. This thesis conducts only a statistical analysis of FX rates, but like many of these models assumes a mean reversion of the logarithmic NER to an underlying, slowly changing reversion level, which, depending on the macroeconomic model, may be interpreted as being a function of the PPP rate.

For the following chapters of this thesis we investigate FX rates as stochastic processes, rather than from an economic perspective.

2.1.3 Mean reversion in foreign exchange

While mean reversion can be found in a great variety of fields, such as physics, neuroscience, and various areas of finance, such as stock prices [21], interest rates, and stochastic volatility models, the reason why it is central to this thesis is its applicability to FX rates.

There is no universal definition of mean reversion, especially as it is a concept interpreted differently in different contexts, but even within finance different definitions have

been proposed [22]. For the purpose of this section, when we refer to a mean reverting process we very generally mean any stochastic process which has a tendency to, if disturbed, revert towards some constant or varying long-run "mean" or equilibrium. Note that this equilibrium may or may not be constant, and may or not be the mean of the process. The phenomenon of mean reversion is also sometimes referred to as the "value effect" when referring to a price's tendency to return to its "long-run value" [23].

A popular example of a mean reverting process is the Ornstein–Uhlenbeck process, which is the process we focus on in this thesis, and which we will introduce in more detail in Section 2.2. Other examples of mean reverting processes are the Feller-square-root process and the autoregressive process of order 1, commonly referred to as the AR(1) process, which is the discrete analogue of the Ornstein–Uhlenbeck process as described in Section 2.2.3. Given a time series and a statistical model, it is possible to test for mean reversion through unit root tests such as the Dickey–Fuller test. The Dickey–Fuller test tests the null hypothesis of the series having a unit root, which means it is neither stationary nor trend-stationary.

As discussed in Section 2.1.2, there has been much research and discussion of different models for the FX market, and in the following we shall have a look at some of the evidence in the literature for the theory of log NERs being mean-reverting to the sum of a constant and the log PPP rate, which implies a reversion of the RER to a constant equilibrium level [24].

One paper that studies such a model is that by Lothian and Taylor [25], analysing about 200 years' worth of annual RERs for FRF/GBP and USD/GBP. They predict a long-run reversion of the RERs to an equilibrium level, and test this hypothesis by applying a unit root test and fitting the series to an AR(1) process. They determine that an AR(1) model is suitable from evaluating autocorrelations of the time series, and fit it to the data with a small but positive reversion strength. They find that this model is a good fit for the data and performs much better than non-stationary models for RERs.

Da Fonseca et al. [26] analyse daily nominal FX rates against the US dollar for 23 different countries and find that while the standard Ornstein–Uhlenbeck process is not suitable to describe the data, a time-homogeneous Ornstein–Uhlenbeck process, which is a potentially non-Gaussian generalization of the Ornstein–Uhlenbeck process, appears in fact to be an appropriate model.

In a review of literature on the subject of PPP and the RER, Sarno and Taylor [19] found in 2002 that the model of real FX rates reverting to a long-run equilibrium was currently generally supported for the major currencies. There is some evidence that this adjustment may be non-linear, as the reversion to the long-run mean may be stronger for greater deviations from the equilibrium.

2.1.4 Trading strategies

One of the reasons why we strive to understand financial markets better is to find more profitable ways of trading, and much of the trading in financial markets, including the FX market, is based on trading strategies. These may be in the form of a set of rules based on some indicators upon which a trader acts, or it may be in the form of algorithmic trading. Two classic types of trading strategies, which form the basis for many more complex ones, are trend following and mean reversion strategies.

Trend following (sometimes called momentum-based) trading strategies are strategies which attempt to identify the current trend of a security, and make a buying or selling decision based on the assumption that this trend will continue [27]. There are a number of methods that can be used to determine the current trend of a security, such as using trend lines or the relative strength index (RSI) [28]. However the most common method is to look for moving average crossovers. These are points where a moving average (MA), calculated in some way over the preceding data points, crosses over or under either the current price, or an MA computed over a shorter period. In fact, the difference between two MAs in this context may be referred to as the "momentum" or "differential" [1]. The theory behind this strategy is that if a price, or a short-term ("fast") MA, crosses a longer-term ("slow") MA from below, referred to as a "golden cross", the momentum of the security is now upward, and it should therefore be bought. Inversely, if the price or short-term MA crosses the longer-term MA from above, referred to as a "death cross", the security is trending downward, and should therefore be sold [28]. There are many different ways in which the MA may be calculated. Firstly, there is the question of how large the time interval should be over which the longer-term MA is calculated, as well as whether a short-term MA or the current price should be used as an indicator of the current trend. A common and very simple version of the strategy would to use the current price and the 50-period simple moving average (SMA), i.e. the arithmetic mean of the 50 previous data points, or the 50-period and the 200-period simple MAs. An example of alternative types of MA is the exponential moving average (EMA), where the values used to calculate the MA are weighted exponentially, with more recent values being weighted more heavily. It has been found that some, but not all, currency pairs are suited to trend following trading [29].

Another very popular, but in its assumptions opposite, trading strategy is mean-reversion-based, or contrarian, trading. The underlying assumption of this strategy is that prices will eventually return to a long-run "mean", which may be a fundamental value and does not have to be constant, and therefore when a price has diverged from this reversion level to a certain degree, it is likely to reach some extremum and a reversion of the price towards the mean is likely to take place. The reversion level is usually approximated by an MA, which may be calculated over any length of time, and as a simple or weighted MA. Trading signals tend to be divergences from an MA, rather than crossover points with it. Ways in which a sufficient divergence may be determined are, amongst

others, Bollinger bands, the duration of a trend, RSIs and many more. As an example, Bollinger bands can be created by determining the MA and standard deviation of the time series over a certain period, and calculating the lines which lie some multiple of the standard deviation above and below the MA for each point in time, and the area between these lines is then thought of as the "band" within which prices will tend to move.

While the choice between mean reversion and trend following strategies may be based on many complex factors, such as the asset traded, the market conditions, and technical indicators, generally mean reversion strategies are favoured for short-term trades, while trend following strategies are used by longer-term traders. Mean reversion strategies and trend following strategies may of course also be combined, and this has been shown to work in FX [30]. In the case of FX trading this may be interpreted as in accordance with the idea of short-term volatility and a long-run mean as in the Dornbusch model. The existence of the phenomena of momentum and long-run value in a variety of assets including FX data spanning a total of 32 years is also confirmed by Asness, Moskowitz and Pedersen [23]. Another trading strategy which combines trend following and contrarian strategies is described by Gençay et al. [1]. The model follows the trend most of the time, but goes against the trend "in the case of extreme foreign exchange movements", which is roughly two to three times out of the 60 to 70 deals executed in a year. They test this strategy on 5-minute frequency data for three major currency pairs and one cross rate for the years 1990–1996, with the model taking into account human reaction times, opening hours of the geographical FX markets, transaction costs, and risk, and find that the model generates positive returns.

2.2 Ornstein–Uhlenbeck process

The Ornstein–Uhlenbeck (OU) process is a mean reverting diffusion process which may be thought of as a standard Brownian motion tending towards a long-term reversion level. It was first introduced in 1930 by Leonard Ornstein and George Eugene Uhlenbeck [31].

2.2.1 Diffusion processes

Diffusion processes are continuous stochastic processes with no memory, or, in other words, they are Markov processes with no jumps [32]. A classic example of a real-world diffusion is the movement of particles in fluids [33], which is described by Brownian motion. Other examples of diffusion processes are geometric Brownian motion, Feller-square-root (FSR) processes, Bessel processes, and the OU process. For comparison, examples of stochastic processes which are not diffusions are Poisson and Bernoulli processes.

Brownian motion was first described mathematically around 1900 is possibly the most well-known stochastic process of all, and as such we shall familiarize ourselves a little more with it. Standard Brownian motion, also referred to as the Wiener process $\{W(t)\}_{t\in\mathbb{R}_0^+}$, is defined as a continuous stochastic process with starting value $W(0) = 0$, and independent,

Gaussian increments [34]. Its probability density function (PDF) at time t is

$$P(W(t) = x) = \frac{1}{\sqrt{2\pi t}} e^{-\frac{x^2}{2t}}, \tag{2.3}$$

i.e. $W(t) \overset{d}{=} N(0,t)$ for $t \geq 0$, where $\overset{d}{=}$ denotes equality of distribution. Throughout this thesis we will treat time as being dimensionless. The expected value and variance of the Wiener process at time t are therefore described by $\mathrm{E}[W(t)] = 0$ and $\mathrm{Var}[W(t)] = t$. The process can also be obtained as the continuous limit of a random walk. The Wiener process is self-similar, since if $\{W(t)\}_{t\in\mathbb{R}_0^+}$ is the Wiener process then for any $c \in \mathbb{R}^+$, $\{W'(t)\}_{t\in\mathbb{R}_0^+}$ defined by $W'(t) = \frac{1}{\sqrt{c}} W(ct)$ is also the Wiener process [32]. We will discuss this property in Section 2.5.1. Note that, in the context of a one-dimensional diffusion, the variance of the Wiener process means that the mean square displacement (MSD) of particles following standard Brownian motion starting at point $x\,(0)$ increases with time proportionally to t:

$$\overline{(x(0) - x(t))^2} \propto t. \tag{2.4}$$

The Wiener process forms the basis for many other stochastic processes, such as arithmetic Brownian motion, geometric Brownian motion, and fractional Brownian motion, all of which we will present in some more detail in the following, as well as some mean reverting processes, including the OU process.

Arithmetic Brownian motion (ABM) is a Wiener process with added drift $\mu_A \in \mathbb{R}$. We will define this process $\{A(t)\}_{t\in\mathbb{R}_0^+}$ in terms of its stochastic differential equation (SDE) as

$$dA(t) = \mu_A dt + \sigma dW(t), \tag{2.5}$$

where $\sigma \in \mathbb{R}^+$ is the volatility, with some starting value $A(0) \in \mathbb{R}$. This means the Wiener process is a special case of ABM with $\mu_A = 0$ and $\sigma = 1$.

A quantity is said to follow geometric Brownian motion (GBM), or exponential Brownian motion, if its logarithm follows a Wiener process with drift, i.e. an ABM. One of the properties of GBM is therefore that, unlike the Wiener process, it cannot take negative values, which is one of the reasons it is generally favoured for many quantities in finance, maybe most famously in the Black–Scholes model. The SDE of a GBM $\{G(t)\}_{t\in\mathbb{R}_0^+}$ with starting value $G(0) \in \mathbb{R}^+$, drift $\mu_G \in \mathbb{R}$ and volatility $\sigma \in \mathbb{R}^+$ is

$$dG(t) = \mu_G G(t) dt + \sigma G(t) dW(t), \tag{2.6}$$

where $\{W(t)\}_{t\in\mathbb{R}_0^+}$ is the Wiener process. The parameters of ABM and GBM are related by $\mu_A = \mu_G - \frac{\sigma^2}{2}$ if $A(t) = \log \frac{G(t)}{G(0)}$. Throughout this thesis, by $\log x$ we mean the natural logarithm of x.

Fractional (or fractal) Brownian motion is a generalization of Brownian motion where the process is allowed to have a scaling exponent H, which describes the self-similarity of the process, anywhere between 0 and 1. If $H \neq 0.5$ the increments of the process are

non-independent, and therefore inconsistent with the Wiener process, and also meaning the process is no longer a diffusion. We discuss the scaling exponent in more detail in Section 2.5.1.

2.2.2 Ornstein–Uhlenbeck process properties

The SDE of a standard OU process $\{X(t)\}_{t\in\mathbb{R}_0^+}$ with reversion level $\mu \in \mathbb{R}$, reversion strength (or reversion speed) $\alpha \in \mathbb{R}^+$, and volatility coefficient $\sigma \in \mathbb{R}^+$ is

$$dX(t) = \alpha\left(\mu - X(t)\right)dt + \sigma dW(t), \tag{2.7}$$

where $\{W(t)\}_{t\in\mathbb{R}_0^+}$ is the Wiener process. The solution to this SDE, which may be obtained by variation of parameters, with starting value $X(0)$, is

$$X(t) = X(0)e^{-\alpha t} + \mu\left(1 - e^{-\alpha t}\right) + \sigma\int_0^t e^{-\alpha(t-s)}dW(s) \tag{2.8}$$

[34]. Given $X(0)$, at time t, $X(t)$ will therefore have a Gaussian distribution with expectation

$$\mathrm{E}[X(t)|X(0)] = X(0)e^{-\alpha t} + \mu\left(1 - e^{-\alpha t}\right) \tag{2.9}$$

and variance

$$\mathrm{Var}[X(t)|X(0)] = \left(1 - e^{-2\alpha t}\right)\frac{\sigma^2}{2\alpha}, \tag{2.10}$$

and the long-term limits of these values are

$$\lim_{t\to\infty}\mathrm{E}[X(t)] = \lim_{t\to\infty}\mathrm{E}[X(t)|X(0)] = \mu \tag{2.11}$$

and

$$\lim_{t\to\infty}\mathrm{Var}[X(t)] = \lim_{t\to\infty}\mathrm{Var}[X(t)|X(0)] = \frac{\sigma^2}{2\alpha}. \tag{2.12}$$

Note that any point $t' \geq 0$ may be defined as the starting point of the process, so that the above equations may be generalized to

$$\mathrm{E}[X(t'+\tau)|X(t')] = X(t')e^{-\alpha\tau} + \mu\left(1 - e^{-\alpha\tau}\right) \tag{2.13}$$

and

$$\mathrm{Var}[X(t'+\tau)|X(t')] = \left(1 - e^{-2\alpha\tau}\right)\frac{\sigma^2}{2\alpha}. \tag{2.14}$$

Therefore the process is wide-sense stationary or quasi-stationary. In fact, the OU process is the only Gaussian, wide-sense stationary Markov process.

By some definitions, the above process, either as defined or with $\mu > 0$ [35], is a Vasicek process, and the Ornstein–Uhlenbeck process is the special case of the Vasicek process where $\mu = 0$ [36]. In this thesis, however, we allow the reversion level μ of the OU process to be any real number. Similarly, while some definitions allow the reversion

strength α to take any real value, we restrict it to strictly positive values, in order to ensure the mean reverting property of the process.

2.2.3 Discretization

Since in practice we can only observe and simulate the OU process discretely, it is necessary to discretize the process. The Euler–Maruyama discretization $\{X_i\}_{i\in\mathbb{N}_0}$ of the OU process $\{X(t)\}_{t\in\mathbb{R}_0^+}$ with discretization step Δt is

$$\begin{aligned} X_0 &= X(0) \\ X_{i+1} &= X_i + \alpha\left(\mu - X_i\right)\Delta t + \sigma\epsilon_i, \end{aligned} \tag{2.15}$$

where $\epsilon_i \overset{d}{=} N(0, \Delta t)$ for $i \in \mathbb{N}_0$ [37]. In this case, X_i is an approximation of $X(i\Delta t)$, since the deterministic part of the process is split into linear increments. The approximation therefore may be used only for sufficiently small discretization steps Δt. An exact discretization is obtained instead by using the analytic moments from Eqs. 2.13 and 2.14. We get

$$\begin{aligned} X_0 &= X(0) \\ X_{i+1} &= X_i e^{-\alpha\Delta t} + \mu\left(1 - e^{-\alpha\Delta t}\right) + \sigma\sqrt{\frac{1 - e^{-2\alpha\Delta t}}{2\alpha}}\epsilon_i, \end{aligned} \tag{2.16}$$

with $\epsilon_i \overset{d}{=} N(0, 1)$ for $i \in \mathbb{N}_0$ [37]. This discretization may be used for any size of discretization step Δt.

The OU process is sometimes called the CAR(1) process [38], where the 'C' signifies a continuous process, since the AR(1) process is its discrete-time analogue. Each value X_t of the AR(1) process $\{X_t\}_{t\in\mathbb{N}_0}$ at time $t \geq 1$ only depends on the previous value X_{t-1}, the noise term ϵ_t, the reversion level $c \in \mathbb{R}$ and the reversion parameter $a \in \mathbb{R}$, as, given some starting value X_0,

$$X_t = c + aX_{t-1} + \epsilon_t, \tag{2.17}$$

with $\{\epsilon_t\}_{t\in\mathbb{N}_0}$ being a white noise process and $|a| < 1$, for the stationary, i.e. mean reverting, version of the process.

2.2.4 Other applications

In addition to its original use as a model of the velocity of particles under friction, the OU process has long been popular as a model for interest rates, as first introduced by Vasicek [39]. Several extensions to the Vasicek model have also been made. The extended Vasicek model, also called the Hull–White model [40], first proposed in 1990, allows for a time-dependent reversion level $\mu(t) : \mathbb{R}_0^+ \mapsto \mathbb{R}$, reversion strength $\alpha(t) : \mathbb{R}_0^+ \mapsto \mathbb{R}^+$, and

volatility $\sigma(t) : \mathbb{R}_0^+ \mapsto \mathbb{R}^+$, and has the SDE

$$dX(t) = \alpha(t)\left(\mu(t) - X(t)\right)dt + \sigma(t)dW(t). \tag{2.18}$$

While interest rates are probably the most common financial application of the OU process, it is also commonly used in pairs trading, stochastic volatility models, and to model FX rates.

Another common application of the OU process is in neuroscience, where it is commonly employed to model neuron membrane potential [41, 42]. These are just some examples, and other quantities the OU process has been used to model range from temperatures [43] to oil and gas prices [44].

2.3 Parameter estimation for the Ornstein–Uhlenbeck process

There is much literature on the subject of parameter estimation of different variants of OU processes observed in different ways. The models in this thesis are based on a standard OU model observed discretely and regularly, and so we may choose between maximum likelihood estimation (MLE) and least squares estimation (LSE), as these are mostly equivalent in the case of Gaussian noise [45]. We nonetheless introduce both methods, as both may be built on for different variants of the model.

2.3.1 Maximum likelihood estimation

In order to find the maximum likelihood (ML) estimators of the parameters of the OU process $\{X(t)\}_{t\in\mathbb{R}_0^+}$ observed at regular intervals of size Δt over the observation window $[0, T]$ with $T = (n-1)\Delta t$, giving the n samples $\{x_i\}_{i\in\mathbb{N},0\leq i<n}$ where x_i is the observation made at time $t = i\Delta t$, we first find the conditional PDF of making an observation $x_i = x$ given the previous observation x_{i-1}. From Section 2.2.3 we know that X_i has a normal distribution with expected value

$$\mathrm{E}[X_i|X_{i-1} = x_{i-1}] = x_{i-1}e^{-\alpha\Delta t} + \mu\left(1 - e^{-\alpha\Delta t}\right) \tag{2.19}$$

and variance

$$\mathrm{Var}[X_i|X_{i-1} = x_{i-1}] = \sigma^2\frac{1 - e^{-2\alpha\Delta t}}{2\alpha} \tag{2.20}$$

[34], and therefore

$$P\left(X_i = x|X_{i-1} = x_{i-1}\right) = \frac{1}{\sqrt{2\pi s^2}}e^{-\frac{\left(x - x_{i-1}e^{-\alpha\Delta t} - \mu\left(1-e^{-\alpha\Delta t}\right)\right)^2}{2s^2}}, \tag{2.21}$$

where

$$s^2 = \sigma^2\frac{1 - e^{-2\alpha\Delta t}}{2\alpha}. \tag{2.22}$$

From this, we can find the joint PDF of all observations $\{X_i\}_{i\in\mathbb{N},0\leq i<n}$. In order to maximize this function with respect to the three parameters of the process we find the log likelihood function

$$\begin{aligned}\ell(\mu,\alpha,s) &= \log\mathcal{L}\left(\mu,\alpha,s|\, x_0,x_1,...,x_{n-1}\right) = \log P\left(x_1,x_2,...,x_{n-1}|x_0,\mu,\alpha,s\right)\\ &= -\frac{n}{2}\log\left(2\pi\right) - n\log s - \frac{1}{2s^2}\sum_{i=1}^{n}\left[x_i - x_{i-1}e^{-\alpha\Delta t} - \mu\left(1-e^{-\alpha\Delta t}\right)\right]^2. \end{aligned} \tag{2.23}$$

By setting the partial derivatives with respect to the three parameters to zero we may now find the ML estimators.

2.3.2 Least squares estimation

Since the discretization with analytic moments means that each observation is a linear function of the previous observation with added Gaussian noise, it is also possible to use linear regression in order to derive the parameter estimators of the standard OU process:

If, again, we have n discrete observations $\{x_i\}_{0\leq i<n}$ made at times $\{i\Delta t\}_{0\leq i<n}$ with $T=(n-1)\Delta t$, then $y=\{x_1,x_2,...,x_{n-1}\}$ is the vector of evenly spaced observed values of the dependent variable, and $z=\{x_0,x_1,...,x_{n-2}\}$ is the vector of values of the independent variable, and according to Eq. 2.16 they have the relationship

$$y_i = a + bz_i + \epsilon_i, \tag{2.24}$$

where $a=\mu(1-e^{-\alpha\Delta t})$, $b=e^{-\alpha\Delta t}$, and $\epsilon_i \overset{d}{=} N(0,s^2)$ for $1\leq i\leq n-1$ with $s=\sigma\sqrt{\frac{1-e^{-2\alpha\Delta t}}{2\alpha}}$. We want to find estimates $\hat{a}$ for a and $\hat{b}$ for b, such that the sum of the squares of the residuals for all observed values is minimized, i.e. we want to minimize the sum of squared residuals $R=\sum_{i=1}^{n-1}\left(x_i-\left(\hat{a}+\hat{b}x_{i-1}\right)\right)^2$.

It is easily determined from this formula that the estimators which minimize R are given by

$$\hat{a} = \frac{\sum_{i=1}^{n-1}x_i - \hat{b}\sum_{i=0}^{n-2}x_i}{n-1} \tag{2.25}$$

and

$$\hat{b} = \frac{(n-1)\sum_{i=0}^{n-2}\left[x_ix_{i+1}\right] - \sum_{i=0}^{n-2}x_i\sum_{i=1}^{n-1}x_i}{(n-1)\sum_{i=0}^{n-2}\left[x_i{}^2\right] - \left[\sum_{i=0}^{n-2}x_i\right]^2}. \tag{2.26}$$

From these values we then obtain the estimators for the parameters of the OU process by

$$\hat{\alpha} = -\frac{\log\hat{b}}{\Delta t}, \tag{2.27}$$

$$\hat{\mu} = \frac{\hat{a}}{1-\hat{b}}. \tag{2.28}$$

2.3.3 Estimators

Both of these methods lead to the following parameter estimators for the reversion level μ and reversion strength α:

$$\hat{\mu} = \frac{\sum_{i=1}^{n-1} x_i \sum_{i=0}^{n-2} \left[{x_i}^2\right] - \sum_{i=0}^{n-2} x_i \sum_{i=0}^{n-2} \left[x_i x_{i+1}\right]}{n\left(\sum_{i=0}^{n-2} \left[{x_i}^2\right] - \sum_{i=0}^{n-2} \left[x_i x_{i+1}\right]\right) - \left(\left[\sum_{i=0}^{n-2} x_i\right]^2 - \sum_{i=0}^{n-2} \left[x_i x_{i+1}\right]\right)}, \tag{2.29}$$

$$\hat{\alpha} = -\frac{1}{\Delta t} \log \frac{\sum_{i=0}^{n-2} \left[x_i x_{i+1}\right] - \hat{\mu} \sum_{i=0}^{n-2} x_i - \hat{\mu} \sum_{i=1}^{n-1} x_i + n\hat{\mu}^2}{\sum_{i=0}^{n-2} \left[{x_i}^2\right] - 2\hat{\mu} \sum_{i=0}^{n-2} x_i + n\hat{\mu}^2}. \tag{2.30}$$

Via the MLE method we also obtain the following estimator for the volatility coefficient σ:

$$\hat{\sigma} = \hat{s}\sqrt{\frac{2\hat{\alpha}}{1 - e^{-2\hat{\alpha}\Delta t}}} \tag{2.31}$$

where

$$\begin{aligned} \hat{s}^2 = \frac{1}{n-1} \Bigg[& \sum_{i=1}^{n-1} \left[{x_i}^2\right] - 2e^{-\hat{\alpha}\Delta t} \sum_{i=0}^{n-2} \left[x_i x_{i+1}\right] + e^{-2\hat{\alpha}\Delta t} \sum_{i=0}^{n-2} \left[{x_i}^2\right] \\ & -2\hat{\mu}\left(1 - e^{-\hat{\alpha}\Delta t}\right)\left(\sum_{i=1}^{n-1} x_i - e^{-\hat{\alpha}\Delta t} \sum_{i=0}^{n-2} x_i\right) + n\hat{\mu}^2 \left(1 - e^{-\hat{\alpha}\Delta t}\right)^2 \Bigg]. \end{aligned} \tag{2.32}$$

These are the estimators we will use throughout this thesis.

2.3.4 Literature on Ornstein–Uhlenbeck process parameter estimation

In practice, estimating the parameters of the OU process is by no means trivial. One issue is that of sampling, as in reality an OU process cannot be observed continuously and infinitely. It is therefore not surprising that there is a large amount of literature on the topic, some of which we will discuss below.

It is known that the estimation of the reversion strength parameter in particular is difficult, as the estimators based on discrete observations are heavily biased, in particular if the reversion strength is small (the near-unit-root case). Tang and Chen [46] find the bias and the variance of the ML parameter estimators of the OU process, as well as some related processes, based on discrete, regular observations over some observation window $[0, T]$. They find that with n samples and sampling interval Δt so that $(n-1)\Delta t = T$, with $n \to \infty$ and either Δt fixed or $\Delta t \to 0$, and $T \to \infty$ in both cases, the bias and variance of the ML estimators of the reversion strength α are at the order of $\frac{1}{T}$. In addition, they also find the other estimators to be biased, but the estimation of the reversion strength parameter remains the most problematic.

A method advocated by Phillips and Yu [47], which reduces the bias of the ML estimator of the reversion strength parameter based on finite samples, is the jackknife technique.

Here, an estimate $\hat{\alpha}_{\text{whole}}$ of the reversion strength over the whole series is first found, then the series is partitioned (the number n of partitions proposed is 2, although 3 and 4 are also Monte Carlo tested) and then a reversion strength parameter estimator $\hat{\alpha}_{\text{partition},i}$ is found for each of the n partitions. The new estimator $\hat{\alpha}_{\text{jackknife}}$ is then found by calculating

$$\hat{\alpha}_{\text{jackknife}} = \frac{n}{n-1}\hat{\alpha}_{\text{whole}} - \frac{\sum_{i=1}^{n}\hat{\alpha}_{\text{partition},i}}{n^2-n}. \tag{2.33}$$

When testing this technique on simulated data, Smith [48] concludes that while it leads to a significantly smaller bias than the standard estimation techniques, it also leads to a larger standard deviation of the reversion strength estimator, making it an appropriate choice only when several sample paths are available. Phillips and Yu [47] also acknowledge this trade-off, noting that a larger n leads to a smaller variance of the estimator, but also a smaller reduction of the bias.

More recently, Tang and Chen [46] proposed using a bootstrap method for estimating the parameters of the OU and other diffusion processes, which in a simulation study they find to be more effective than Phillips and Yu's [47] jackknife technique, with the bootstrap causing a smaller increase in the variance than the jackknife technique, including in the the near-unit-root case. Their technique consists of finding an estimate $\hat{\theta}$ of the parameter vector $\theta = (\mu, \alpha, \sigma^2)$ from the original process observed at a sampling interval Δt and then generating a bootstrap sample path of the process with parameter vector $\hat{\theta}$ and discretization step Δt. From this sample path, the bootstrap estimator $\hat{\theta}'$ is determined. This procedure is then repeated an additional $(n-1)$ times, yielding n bootstrap estimators $\{\hat{\theta}'_i\}_{1\leq i\leq n}$ in total. From this, the bias-corrected estimator $\hat{\theta}_B$ is found by

$$\hat{\theta}_B = 2\hat{\theta} - \frac{1}{n}\sum_{i=1}^{n}\hat{\theta}'_i. \tag{2.34}$$

Some papers that also explore the parameter estimation of the OU process in more detail and under different aspects are the following: Arató, Kuki and Szabó [49] give an ML estimator of the reversion strength and Arató and Fegyverneki [50] ML estimators for the reversion level and the reversion strength for an OU process observed continuously over a closed interval with a focus on the near-unit-root case. Florens-Landais and Pham [51] analyse the ML estimator for the reversion strength of a continuously observed OU process with known reversion level and reversion strength, with a focus on the tails of the distributions of the estimators. Yu [52] approximates the bias of the ML estimator (which is equivalent to the LS estimator) of the reversion strength of an OU process with known reversion level based on discrete observations, and in particular they treat the near-unit-root case. Rieder [53] explores how to make the OU process parameter estimation more robust against outliers, using the so-called M-estimation. Zapranis and Alexandridis [43] apply neural networks to the parameter estimation for the OU process.

2.4 Extensions of the Ornstein–Uhlenbeck process

There are many generalizations, extensions and variants of the OU process and its parameter estimation. These may arise from relaxing restrictions on the parameters of the process, from allowing the noise to take different forms, or from observing the process indirectly, such as through an integration, a function of the process, or any observable created by the process. Some examples of such variants are explosive OU processes, fractional OU processes, arithmetic OU processes, Lévy-driven OU processes, and OU processes with time-dependent parameters.

We give an overview of the literature regarding some of these variants below. We then focus on variants with time-dependent reversion level, as these are what we shall use to model FX rates in this thesis.

2.4.1 Variants of the Ornstein–Uhlenbeck process

As a very common application of the OU process is in modelling interest rates, it is not surprising that many other interest rate models use processes related to the OU process. In this context the OU process is more commonly referred to as the Vasicek process, and the FSR process as the Cox–Ingersoll–Ross (CIR) process [54], both of which are special cases of the CKLS model [55], which nests a number of interest rate models in the process $\{X(t)\}_{t\in\mathbb{R}_0^+}$ with SDE

$$dX(t) = \alpha(\mu - X(t))dt + \sigma X(t)^\gamma dZ(t), \tag{2.35}$$

with $\{Z(t)\}_{t\in\mathbb{R}_0^+}$ being the noise process and α, μ, σ and γ being the parameters of the model, which may be restricted in various ways to generate different special cases. Note that, if $\{Z(t)\}_{t\in\mathbb{R}_0^+}$ is the Wiener process, $\{X(t)\}_{t\in\mathbb{R}_0^+}$ is the generalized Bessel process [56]. Nowman [57] deals with parameter estimation of the CKLS interest rate models, including Vasicek and CIR, based on discrete observations. Yu and Phillips [58] improve on Nowman's parameter estimation by proposing an alternative way of discretizing these processes to allow Gaussian estimation in the case of non-Gaussian noise, making their method more exact than Nowman's. Sanchez and Palacio [44] provide another alternative to Nowman's method.

Outside of interest rate modelling, maybe the most widely studied generalization is the Lévy-driven OU process, which is often referred to as a process of Ornstein–Uhlenbeck type [59], or even simply as the generalized Ornstein–Uhlenbeck process [38], although other types of noise may be substituted to create different generalizations of the OU process.

Barndorff-Nielsen and Shephard [60] explore Lévy-driven OU processes, which allow the noise component of the OU process to be non-Gaussian Lévy noise, which they use to model the volatility of financial assets. The parameter estimation of discretely observed Lévy-driven OU processes is discussed by Sun and Zhang [59] and parameter estimation of their reversion strength in particular is discussed by Mai [61], Zhang and Zhang [62]

and Hu and Long [63, 64]. Other types of noise that drive variants of the OU process include fractional Brownian motion. Quasi OU processes, which are OU processes where the noise process has stationary, dependent increments, such as the fractional OU process, are discussed by Barndorff-Nielsen and Basse-O'Connor [65]. Kubilius et al. [66] use MLE to estimate the reversion strength of an OU process driven by fractional Brownian motion based on discrete observations.

Allowing the reversion strength to be non-positive yields the non-stable, or unstable, OU process, where the reversion strength is 0, and the explosive OU process, where the reversion strength is negative [67]. Bercu, and Coutin and Savy [67] give the ML estimator for the reversion strength based on a continuous observation over some closed interval of the process in all three cases, where reversion level and volatility coefficient are known. (Note that while in this terminology, a stable OU process is a standard OU process as defined in Section 2.2.2, i.e. with a strictly positive reversion strength [67], a different definition of a stable OU process is an OU type process where the noise distribution is stable [68].)

Many variants of the OU process prevent the process from taking on negative values, which is a property often required to model real-world data, including in finance, such as if the process is used to model raw prices rather than log prices. An example is the reflected OU process, which is treated by Hu et al. [69], who also give an estimator for the reversion strength parameter based on discrete observations. Another variant of the OU process which is suitable where negative values are not desired is the FSR process. The SDE for this process $\{X(t)\}_{t\in\mathbb{R}_0^+}$ is

$$dX(t) = \alpha\left(\mu - X(t)\right)dt + \sqrt{X(t)}\sigma dW(t), \tag{2.36}$$

with reversion level $\mu \in \mathbb{R}$, reversion strength $\alpha \in \mathbb{R}^+$, volatility coefficient $\sigma \in \mathbb{R}^+$, and $\{W(t)\}_{t\in\mathbb{R}_0^+}$ the Wiener process. It is therefore an OU process with a volatility scaled in relation to the size of the current value.

There are also papers that treat parameter estimation of an OU process that is not directly observed. For example, Gloter [70] estimates the volatility coefficient and reversion strength of an integrated OU process with known reversion level observed at discrete regular intervals using the Whittle estimator, which is an approximation of the ML estimator. They compare this with the maximum likelihood split data estimator, which splits the series into multiple consecutive series of an equal, short length, and then applies MLE to each of these sub-series before finding the likelihood for the whole series. In another paper Gloter estimates parameters of integrated diffusion processes including the OU process, the FSR process, and others [71]. They do this based on discrete regular observations where the sampling rate tends to infinity. Matulewicz [72] explores the parameter estimation of a multi-dimensional OU process based on a continuous observation of a graph produced by the OU process according to an algorithm.

Dehay [73] explores the parameter estimation of an OU process where the reversion

strength is a parameter α multiplied by a known periodic function. They give the ML estimator of the reversion strength based on a continuous observation of the process. Brandes [38] explores CARMA processes with random Lévy coefficients. A special case of this is the CARMA(1,0) process, which is an OU process with random Lévy coefficients.

2.4.2 Time-dependent reversion level

We have a particular interest in OU processes with time-dependent reversion levels, and shall therefore present some of the literature on this topic below.

It should first of all be noted that there is a minor difference between an OU process where the drift is determined by the current value's distance from the time-dependent reversion level and a process defined as the sum of a time-dependent value and an OU process with constant reversion level. However, there does not appear to be a formal distinction in the literature, and both processes are referred to as OU processes with time-dependent reversion level. One application of this is in the Hull–White model [40] described in Eq. 2.18, which is an extension of the Vasicek model. This model assumes that interest rates follow an OU process with time-dependent reversion level, and sometimes other time-dependent parameters. However, when calibrating this model, it is generally assumed that the reversion level is known prior to estimating the other parameters of the model.

Thierfelder [74] explores the trending OU process $\{X(t)\}_{t\in\mathbb{R}_0^+}$, which is an OU process where the reversion level is a linear function of time. The process is defined as

$$X(t) = X(0) + \mu t + \sigma \int_0^t e^{\alpha(s-t)} dW(s), \tag{2.37}$$

for $t \geq 0$, with reversion strength $\alpha \in \mathbb{R}^+$, volatility coefficient $\sigma \in \mathbb{R}^+$ and drift $\mu \in \mathbb{R}$ with $\{W(t)\}_{t\in\mathbb{R}_0^+}$ being the Wiener process. The process has the SDE

$$dX(t) = (\mu - \alpha\left[X(t) - (X(0) + \mu t)\right])\, dt + \sigma dW(t), \tag{2.38}$$

meaning that $(X(t) - \mu t - X(0))$ follows a standard OU process with no initial displacement reverting to 0. They also treat the dependence of the average return measured over a certain interval on the interval. They show that if log prices follow a trending OU process then the log return $r_{\Delta t}(t)$ at time t measured over the preceding time interval of size Δt has expected value

$$\mathrm{E}\left[r_{\Delta t}\left(t\right)\right] = \mu \Delta t \tag{2.39}$$

and the variance of the log return as t tends to infinity is given by

$$\lim_{t\to\infty} \mathrm{Var}[r_{\Delta t}(t)] = \frac{\sigma^2}{\alpha}\left(1 - e^{-\alpha \Delta t}\right). \tag{2.40}$$

Sanchez and Gallego [75] propose a parameter estimation method for a discretely

observed mean reverting process where the reversion level is an unknown, deterministic function of time. They analyse the continuous processes $\{X(t)\}_{t\in\mathbb{R}_0^+}$ given by

$$dX(t) = \alpha\left(\mu\left(t\right) - X(t)\right)dt + \sigma X(t)^{\gamma}dW(t) \tag{2.41}$$

with constant parameters $\alpha \in \mathbb{R}^+$, $\sigma \in \mathbb{R}^+$, $\gamma \in [0, 3/2]$ for some initial condition $X(0) = x(0)$, where $\{W(t)\}_{t\in\mathbb{R}_0^+}$ is the Wiener process, and $\mu(t) : \mathbb{R}_0^+ \mapsto \mathbb{R}$ is the deterministic, time-dependent reversion level. This is a generalization of CKLS, and for $\gamma = 0$ it is the OU process with a time-dependent reversion level with SDE

$$dX(t) = \alpha\left(\mu\left(t\right) - X(t)\right)dt + \sigma dW(t), \tag{2.42}$$

which is what we are working with in this thesis. They show that the expected value $m(t)$ of the process at time t is

$$m(t) = \mathrm{E}[X(t)] = \mathrm{E}[X(0)]e^{-\alpha t} + e^{-\alpha t}\int_0^t e^{\alpha s}\mu(s)ds. \tag{2.43}$$

The relationship between $\mu(t)$ and $m(t)$ is given by

$$\mu\left(t\right) = m(t) + \frac{\dot{m}(t)}{\alpha}, \tag{2.44}$$

where $\dot{m}(t)$ is the first derivative of $m(t)$. In order to find parameter estimators $\hat{\alpha}$ for α and $\hat{\sigma}$ for σ given $n+1$ discrete observations $\{x_i\}_{0\leq i\leq n}$ made at some constant sampling interval Δt with x_i being the observation of the sample path $\{x(t)\}_{t\in\mathbb{R}_0^+}$ made at time $t = i\Delta t$, they substitute $\mu\left(t\right)$ in Eq. 2.41 using Eq. 2.44 and discretize the process using Euler–Maruyama. They then derive the probability distributions of the observed discrete samples of the process as a function of the constant parameters α, σ, as well as the parameter γ, which is presumed known a priori, the sampling interval Δt, and the unknown function $m(t)$. For $\gamma = 0$ the parameter estimators $\hat{\alpha}$ and $\hat{\sigma}$ are derived from this as

$$\hat{\alpha} = \frac{\sum_{i=1}^{n}\left[\left(x_i - x_{i-1} - \dot{m}_{i-1}\Delta t\right)\left(m_{i-1} - x_{i-1}\right)\right]}{\Delta t\sum_{i=1}^{n}\left[m_{i-1} - x_{i-1}\right]^2} \tag{2.45}$$

and

$$\hat{\sigma} = \sqrt{\frac{1}{n\Delta t}\sum_{i=1}^{n}\left(x_i - x_{i-1} - \left[\hat{\alpha}\left(m_{i-1} - x_{i-1}\right) + \dot{m}_{i-1}\right]\Delta t\right)^2}. \tag{2.46}$$

Note that as $m(t)$ is not known, its values and the values of its derivative instead need to be approximated by $\{m_i\}_{0\leq i<n}$ and $\{\dot{m}_i\}_{0\leq i<n}$ respectively, so that m_i is an approximation of $m(i\Delta t)$ and $\dot{m}_i$ is an approximation of $\dot{m}(i\Delta t)$. m_i is found using a convolution of the sample path, such as an MA, and the derivative $\dot{m}(i\Delta t)$ at these points is then approximated by $\dot{m}_i$, using numerical differentiation. Using Eq. 2.44 and the approximated values $\{m_i\}_{0\leq i<n}$ of $m(t)$ and $\{\dot{m}_i\}_{0\leq i<n}$ of $\dot{m}(t)$, the estimators $\{\hat{\mu}_i\}_{0\leq i<n}$ are then computed

so that $\hat{\mu}_i$ is the estimator of $\mu(i\Delta t)$, and then $\hat{\alpha}$ and $\hat{\sigma}$ are computed using Eqs. 2.45 and 2.46.

They test this parameter estimation method on a simulated data set for $\gamma = 1$ with some parameters α and σ, for the cases of $\mu(t)$ being a sinusoidal and a parabolic function. They find the estimation method to be "working well", although they find that the estimator for α is biased, with the bias depending on the convolution used to approximate $m(t)$. They also find the estimators $\hat{\mu}_i$ to be "not very accurate". They propose, in cases where there is only one sample path available, a second phase to the estimation, where after the initial estimation, the functional structure of $\mu(t)$ is given from a priori knowledge, and new estimates of $\mu(t)$ at the sampling points are then generated from this and the estimators $\{\hat{\mu}_i\}_{0\leq i<n}$ (obtained in the first estimation phase), after which α and σ may then be re-estimated. They find that adding this second phase significantly reduces the bias in the estimate of α, but does not have a significant effect on the estimate of σ.

2.5 Scaling and self-similarity

Considering the importance of the FX market, it is not surprising that much research has been conducted on its behaviour, producing a wealth of stylized facts, which may help us build better models of the market. When it comes to statistical properties of FX rate time series, there is generally a wide consensus that FX rates have fat-tailed, non-stable, mostly symmetric distributions, with first, second and third, but not fourth, moments existing for free-floating pairs [9]. Another thing that has been widely shown is the seasonality of FX rates, which is very closely linked with the opening times of the FX markets in different parts of the world. These intra-day and intra-week patterns are found in a variety of statistics related to FX prices, such as volatility, tick frequency, and many others [9]. A third characteristic feature of the FX market is its scaling properties. Scaling laws can be useful when devising trading strategies, for example as they help in refining models of the FX market, as described by Dupuis and Olsen [76] and as implementing trading strategies on a range of time scales at once can lead to a smoothing of the returns.

The scaling relation, or scaling law, that is at the center of Part 1 (Chapter 4) of this thesis has been reported in many papers, but numerous other scaling laws in FX have also been discovered since. Below, we will describe what self-similarity means for stochastic processes, before reviewing the existing literature on the scaling of mean absolute log returns. We then give an overview of other scaling laws that have been observed in FX, and finally briefly look at scaling outside of FX.

2.5.1 Self-similar stochastic processes

A stochastic process $\{X(t)\}_{t\in\mathbb{R}_0^+}$ is said to be self-similar or self-affine if for any $a > 0$ there exists a $b > 0$ such that

$$X(at) \stackrel{d}{=} bX(t) \tag{2.47}$$

for all $t \geq 0$, where $\stackrel{d}{=}$ denotes equality of distribution [77]. In this case, it can be shown that there exists a unique constant $H \geq 0$ so that

$$b = a^H. \tag{2.48}$$

In the above equation, H is referred to as the scaling exponent. As mentioned previously, an example of a self-similar stochastic process is fractional Brownian motion, of which the Wiener process is a special case with $H = 0.5$.

While the scaling exponent of a stochastic process indicates its memory, with $H \in (0, 0.5)$ indicating a negative autocorrelation, and $H \in (0.5, 1)$ indicating a positive one (in which case H may be referred to as the Hurst exponent [78]), the fractal dimension, or Hausdorff dimension, D measures the roughness of a process, with a higher fractal dimension indicating a rougher process. In the case of self-affine processes the relationship between D and H is

$$D = n + 1 - H, \tag{2.49}$$

where n is the dimension of the space in which the process takes its values. A one-dimensional Wiener process therefore has fractal dimension $D = 1.5$.

As described by Di Matteo [78], the scaling behaviour of a process $\{X(t)\}_{t \in \mathbb{R}_0^+}$ may be measured by determining whether the quantity

$$K_q(\tau) = \frac{\overline{|x(t+\tau) - x(t)|^q}}{\overline{|x(t)|^q}}, \tag{2.50}$$

scales according to

$$K_q(\tau) = c\tau^{qH(q)}, \tag{2.51}$$

where c is a constant, $q \geq 0$ is the order of the moments and τ is the size of the time interval with regard to which the quantity scales, in which case $H(q)$ is the generalized Hurst exponent. If the generalized Hurst exponent is constant, so that $H(q) = H$, the process $\{X(t)\}_{t \in \mathbb{R}_0^+}$ is considered to be uniscaling, and otherwise it is multiscaling.

The oldest method for estimating the Hurst exponent is the rescaled range (R/S) analysis [79]. This method divides series into subseries of equal lengths and then for each subseries computes the range of the series of cumulative sums of deviations from the subseries' mean value, divided by the standard deviation of values in the subseries. The resulting value is the rescaled range, and the mean rescaled range of all subseries is computed for different lengths of subseries to determine its dependence on the length of the subseries.

Related to this method is the detrended fluctuation analysis (DFA), which splits the series of cumulative sums of the series to be analysed into a number of subseries of equal lengths before subtracting the linear trend from each subseries and then computing the standard deviation of each detrended subseries. The mean of the standard deviations computed for all subseries is then found, and the dependence of this value on the size of

subseries is determined [80].

Another method is the detrended moving average analysis (DMA). This method was first proposed by Alessio et al. in 2002 [81] and estimates the Hurst exponent in the following way: for a range of τs, a simple moving average over τ is computed and subtracted from the series. The variance of each thus detrended series is then recorded. The dependence of the variance of the detrended series on τ is expressed as a power law, and the exponent of the power law is the estimate of the Hurst exponent.

2.5.2 Scaling of mean absolute log returns

The law first described in 1990 by Müller et al. [82], and inspired by the work of Mandelbrot [83], relating mean absolute changes of the logarithmic mid price to the length of time over which they occur, is probably the most widely reported scaling law in the FX market, and provides the basis for the first part of this thesis. Müller et al.'s paper is also significant as it was one of the first studies to analyse a large set of intra-day FX data, providing a foundation for determining the statistical properties of high-frequency FX time series. The paper analyses millions of intra-day spot rate quotes for USD/DEM, USD/JPY, USD/CHF and GBP/USD spanning 3 years, as well as daily prices spanning 15 years.

For each currency pair their analysis is based on a time series of n pairs of bid and ask quotes $\{(p_{\text{bid}}(t_i), p_{\text{ask}}(t_i))\}_{1\leq i\leq n}$ for an irregularly spaced series $\{t_i\}_{1\leq i\leq n}$ of points in time, sampled over the observation window $[t_1, t_n]$. For any particular currency pair at time t_i they compute the logarithmic mid price $x(t_i)$ as

$$x(t_i) = \frac{\log p_{\text{ask}}(t_i) + \log p_{\text{bid}}(t_i)}{2}. \tag{2.52}$$

Note that throughout this thesis for the purpose of calculations we will assume prices to be dimensionless. From the irregularly spaced time series $\{x(t_i)\}_{1\leq i\leq n}$, which is treated as an irregular sampling of a continuous stochastic process $\{X(t)\}_{t\in\mathbb{R}_0^+}$, they create a number of regularly spaced time series $\{x_{\Delta t,j}\}$ using linear interpolation for different sizes of time steps Δt, where $x_{\Delta t,j}$ is the interpolated value of the unknown continuous series $\{x(t)\}_{t\in\mathbb{R}_0^+}$ at time $t = j\Delta t$. For each Δt, they compute the mean absolute change of the logarithmic mid price of the series $\{x_{\Delta t,j}\}_{0\leq j\leq m}$ corresponding to that Δt as

$$\overline{|\Delta x|}_{\Delta t} = \frac{1}{m}\sum_{j=1}^{m} |x_{\Delta t,j} - x_{\Delta t,j-1}|. \tag{2.53}$$

We will also refer to the change of the logarithmic mid price as the log return. The relationship they find is the power law

$$\overline{|\Delta x|}_{\Delta t} = c\Delta t^E, \tag{2.54}$$

translating into a linear relationship on a log-log scale as

$$\log\left(\overline{|\Delta x|}_{\Delta t}\right) = \log c + E \log \Delta t, \tag{2.55}$$

where c and E are constants depending on the currency pair analysed and E is called the drift exponent. Note that this law is equivalent to Eq. 2.51 with $q = 1$.

They compute the quantity in Eq. 2.53 for intervals Δt ranging from ten minutes to two years, and they find that allowing the intervals over which the changes of logarithmic mid prices were computed to overlap does not significantly affect the results, with a bigger overlap only leading to smoother distributions. With intervals overlapping by 2/3 they observe correlation coefficients between $\log \Delta t$ and $\log \overline{|\Delta x|}_{\Delta t}$ higher than 0.999 and standard errors of the exponents E smaller than 1.0%.

This law has been widely reported in the literature, for example by Guillaume et al. [9], who observe it in all the spot rate time series they examine and over intervals ranging from ten minutes to two months, using the same definition of the mid price as described in Eq. 2.52. Both papers refer to the quantity defined in Eq. 2.53 as the "volatility" of the series, justified by the fact that "the existence of standard deviations is not proven" for the distribution of price changes [82]. Guillaume et al. find lower drift exponents in the scaling law in Eq. 2.54 for currencies within the European Monetary System (EMS) when EMS bands were narrow compared to free-floating currencies, relating to a smaller average volatility. Glattfelder, Dupuis and Olsen [84], observe the scaling law in five years' worth of tick data for 13 currency pairs.

While Aloud et al. [3] also observe Müller et al.'s [82] scaling law from Eq. 2.54 in 2.25 years' worth of high-frequency bid and ask prices for EUR/USD and EUR/CHF, they use a different definition for the "log returns": If $\{p_i\}$ is a regularly spaced sequence of mid prices, so that p_i is the price at time $t = i\Delta t$ then the "log return" at time $t = i\Delta t$ is defined as

$$\Delta x_i = \frac{p_i - p_{i-1}}{p_{i-1}}. \tag{2.56}$$

This is an approximation of the actual log return [74], as

$$\begin{aligned} \log p_i - \log p_{i-1} &= \log \frac{p_i}{p_{i-1}} = \log\left(\frac{p_i + p_{i-1} - p_{i-1}}{p_{i-1}}\right) = \log\left(\frac{p_i - p_{i-1}}{p_i - 1} + 1\right) \\ &= \frac{p_i - p_{i-1}}{p_{i-1}} - \frac{1}{2}\left(\frac{p_i - p_{i-1}}{p_{i-1}}\right)^2 + \frac{1}{3}\left(\frac{p_i - p_{i-1}}{p_{i-1}}\right)^3 - \ldots \\ &\approx \frac{p_i - p_{i-1}}{p_{i-1}}. \end{aligned} \tag{2.57}$$

A variation of Müller's law has been reported by Galluccio et al. [85], who analysed both bid and ask prices for exchange rates between USD, JPY and DEM from the period of 1 October 1992 to 30 September 1993. Using linear interpolation, they obtain regularly spaced price values with time step 30 seconds, including non-trading times in their time series as periods over which prices did not change. Periods with less activity are assigned

less weight in the analysis. Related to the scaling law in Eq. 2.54 from Müller et al.'s paper [82], they observe the scaling of the square root of the mean of the squared price changes, or the square root of the mean squared displacement, over a time interval as being proportional to a power of this interval, with the slope on a log-log scale being 0.45 for the currency pair DEM/USD over intervals ranging from 30s to 10,000s. Note that this exponent is very different from the one found for Eq. 2.54, indicating a multi-scaling behaviour [85]. Müller et al. also observe scaling of this quantity, with a scaling exponent of about 0.52.

2.5.3 Other scaling laws in foreign exchange

While the scaling of absolute log returns is of the most interest to us, it is only one of many scaling behaviours identified in the FX market. The FX market is very complex, and not only has agents acting in different time zones, but also agents acting on different time scales, which is by many thought to be the cause of the fractal structure the market exhibits. To illustrate this, we will present some of the other scaling behaviours found in FX data.

Guillaume et al.'s [9] 1997 paper is one of the earliest to provide an overview of a large number of statistical properties of FX data of a frequency which was higher than daily. They present a scaling relation for directional changes, which is a change in direction (upward or downward) of the trend of the series. Specifically, they find a scaling law relating the number of directional changes to the threshold above which the changes were registered. They define a directional change d_r as a change in direction of the trend of the time series. The threshold r indicates the "tolerance" to a change in direction, i.e. the threshold above which the size of a movement has to be for the movement to be registered as a change in direction rather than "noise". They then calculate the number $N(d_r)$ of directional changes over the sampling period given a particular time series spaced regularly at intervals Δt, with directional changes registered above a threshold size of r. The law they find is

$$N(d_r) = c' r^{E'} \tag{2.58}$$

with c' being a constant depending on the FX rate, r being the size of the threshold for the directional changes, and E' being the drift exponent.

Guillaume et al. offer what they call a "highly tentative economic interpretation" of this scaling behaviour, which is that it is due to "a mix of risk profiles of agents trading at different time horizons".

They estimate the drift exponents for this scaling law and the one in Eq. 2.54, which they also observed in their data, by least squares. A relation between these two scaling laws is shown, as they find

$$E' \approx -E^{-1}. \tag{2.59}$$

Twelve new scaling laws as well as the one discovered in Müller et al.'s paper [82] are

observed by Glattfelder, Dupuis and Olsen [84] in FX data. Like Guillaume et al. they analyse high-frequency data using a directional change event-based approach, which they use to define an intrinsic time. This intrinsic time scale based on directional change events and its implications are further explored by Aloud et al. [86], who also measure the FX coastline, i.e. the length of the price curve, using this approach. Galluccio et al. [85] also look at scaling laws and intrinsic time as found in FX markets.

More recently, Aloud et al. [3] have published a paper which focuses on observing old and new stylized facts in a large set of FX data, with some of the stylized facts confirmed or established in this paper relating to seasonality but some being scaling laws. In addition to observing Müller et al.'s [82] scaling law from Eq. 2.54, as well as a number of other previously known stylized facts, four new scaling laws and six relationships between them are also found. Aloud et al.'s analysis is based on two sets of 2.25 years' worth of historical high-frequency data. Transaction data for 48 currency pairs is analysed for seasonality, but only bid and ask prices for two currency pairs (EUR/USD and EUR/CHF) are analysed for scaling laws.

Aloud et al. confirm the scaling law from Eq. 2.58 first found by Guillaume et al. [9], with thresholds of sizes between 0.10% and 0.80%. Aloud et al. also observe two of the scaling laws described in Glattfelder, Dupuis and Olsen [84]. All parameters are found by fitting a least squares regression line on a log-log scale, and goodness of fit was assessed with the adjusted R^2 value. In addition to these four, Aloud et al. also observe four new scaling laws in transactions data rather than price data. These show relationships between the threshold size for registering an event and the average number of trades during an event, the average transaction volume during an event, the average number of opened positions, and the average number of closed positions during an event, respectively.

2.5.4 Scaling elsewhere

While we focus on scaling in the FX market, scaling is a universal phenomenon, and similar scaling laws have been observed in a wide range of other fields, in particular in physics. However scaling is also observed in other types of financial markets, and looking at some of these may be helpful in gaining a deeper understanding of the scaling behaviour of the FX market.

For example, Mantegna and Stanley [87] find scaling behaviour in the Standard and Poor's 500, which is a price index of the New York Stock Exchange. For a range of time intervals Δt from 1 min to 1,000 min, they observe the probability $P(\Delta x_{\Delta t} = 0)$ of a price change over the interval Δt being 0. On a log-log scale they conduct a line fit to find the relationship between the size of Δt and $P(\Delta x_{\Delta t} = 0)$, and find that a straight line was a good fit, albeit with the slope being significantly steeper than -0.5, indicating a non-normal scaling behaviour.

Ballocchi et al. [88] provide an analysis of implied forward rate time series constructed from Eurofutures contracts. They find scaling behaviour but also intra-day patterns which

are very similar to those found in FX ones.

Di Matteo, Aste and Dacorogna [89] fit a multiscaling model to a variety of financial markets, including 29 FX rates and show that $H(2)$ is a good indicator of the stage of development of a market.

Chapter 3

Data sets

In this chapter, the data analysed in Parts 1–3 (Chapters 4–6) will be described in detail. For each data set we will describe the source, the type of data, as well as the size and nature of the set. We then describe some of the methodology used for treating the data as well as for generating the simulated time series used throughout the thesis.

3.1 Data set 1: Thomson Reuters

The first data set was obtained from the Thomson Reuters Eikon terminals located at University College London. Historical bid close prices captured at six different frequencies were downloaded, with the time intervals between observations being 24 hours, 60 minutes, 30 minutes, 10 minutes, 5 minutes and 1 minute. This data stemmed from nine different days in August 2014 and reached back about 40 years for daily data and about 40 days for minutely data. The 17 currency pairs downloaded were USD/CAD, USD/GBP, USD/JPY, EUR/AUD, EUR/CAD, EUR/CHF, EUR/GBP, EUR/JPY, EUR/USD, EUR/NOK, EUR/SEK, GBP/AUD, GBP/CAD, GBP/CHF, GBP/EUR, GBP/JPY and CHF/JPY.

The data stemming from the different days was combined and duplicates removed. It was found that in some cases values for the same currency pair with the same time stamp and interval size differed by a small degree depending on the download day. In these cases, we chose the most recently downloaded value. A portion of these cases appeared to be instances of the value being updated in the day or days following the time stamp, and no conflicting values of this type varied by a large degree.

3.1.1 Preparing the data

The raw data as downloaded from Thomson Reuters Eikon contained separate series per pair per download day per observation interval. While a small number of series were missing, there was always at least one series per interval per currency pair. We reduced the set to 102 time series by combining the data downloaded on different days for the same

interval and currency pair into one series with each value consisting of price, time stamp, and date of download.

From here on, all series were treated in the following way: First, each series was sorted by time stamp and duplicate rows (ignoring download day) were removed. The remaining time series were checked for conflicting values. The following types of conflicting values were found:

1. Some values with the same time stamp but downloaded on different days differed within the range of price changes seen between values belonging to consecutive time stamps. These were conflicts between values
   (a) downloaded previous to the day of the time stamp and values downloaded on the day of the time stamp;
   (b) downloaded on the day of the time stamp and values downloaded in the days after the time stamp;
   (c) downloaded on different days but relating to data long before the download dates.
2. For some series it was apparent from the number of conflicting values and/or from the magnitudes of the differences between conflicting values that the time series included values belonging to a different currency pair. If the range of values downloaded on one day was distinct from the range of values downloaded on all other days the values downloaded on that day were presumed to be invalid.

Conflicts of the first type were resolved by always choosing the most recently downloaded value for each time stamp. Conflicts of the second type were identified and resolved by comparing the series from all download days and determining whether, and which, one differed significantly from all the others. Once the data had been treated in this way, we removed the download date from each value, took the logarithm of each rate and interpolated to fill any gaps in the data.

3.1.2 Properties of the data set

The Thomson Reuters time series and their properties after combining the series and resolving conflicting values, but before taking the logarithm and interpolating, are described in more detail in the following tables.

Table 3.1 shows the length of the time range covered by each series in days.

	1d	60min	30min	10min	5min	1min
CAD	15,932	378	378	105	105	41
GBP	14,473	378	378	105	105	40
JPY	15,932	378	378	105	105	40
EURAUD	10,330	352	352	105	105	43
EURCAD	14,473	352	352	105	105	40
EURCHF	14,473	352	352	105	105	40
EURGBP	10,330	352	352	105	105	40
EURJPY	14,473	352	352	105	105	40
EUR	14,473	378	378	105	105	40
EURNOK	14,473	352	352	105	105	40
EURSEK	14,473	352	352	105	105	41
GBPAUD	14,473	352	352	105	105	41
GBPCAD	14,473	351	351	105	105	43
GBPCHF	14,473	352	352	105	105	40
GBPEUR	10,330	352	352	105	105	40
GBPJPY	14,473	352	352	105	105	40
CHFJPY	11,914	352	352	105	105	41

Table 3.1: Time range in days covered by data set

Tables 3.2 and 3.3 contain the mean, standard deviation, number of values, and maximum time step in days for each series. Note the difference in properties between the daily and intra-daily data sets, which is due to the fact that the daily series cover a much larger range of time than the intra-daily series.

		1d	60min	30min	10min	5min	1min
CAD	$\overline{X}$	1.2137	1.0742	1.0742	1.0823	1.0824	1.0826
	σ	0.1711	0.0271	0.0271	0.0095	0.0096	0.0098
	n	11,212	6,735	13,348	10,996	21,932	41,939
	Δt_{max}/d	5.00	1.92	1.90	1.90	1.89	1.84
GBP	$\overline{X}$	1.6993	1.6461	1.6462	1.6922	1.6922	1.6933
	σ	0.2345	0.0438	0.0438	0.0140	0.0140	0.0146
	n	10,227	6,744	13,342	10,971	21,877	40,526
	Δt_{max}/d	5.00	1.96	1.94	1.92	1.92	1.92
JPY	$\overline{X}$	163.94	101.30	101.31	101.92	101.92	101.98
	σ	74.45	2.06	2.06	0.41	0.41	0.50
	n	11,224	6,729	13,343	10,995	21,943	40,527
	Δt_{max}/d	18	1.96	1.94	1.92	1.92	1.91
EURAUD	$\overline{X}$	1.6082	1.4774	1.4773	1.4517	1.4517	1.4395
	σ	0.1605	0.0412	0.0412	0.0153	0.0153	0.0075
	n	7,357	6,059	12,051	10,654	21,192	39,122
	Δt_{max}/d	6.00	2.13	2.10	2.01	2.09	2.09
EURCAD	$\overline{X}$	1.4479	1.4666	1.4667	1.4691	1.4691	1.4568
	σ	0.1852	0.0465	0.0465	0.0170	0.0170	0.0065
	n	10,146	6,185	12,334	10,600	21,702	40,394
	Δt_{max}/d	5.00	1.96	1.96	1.93	1.93	1.92
EURCHF	$\overline{X}$	1.7903	1.2234	1.2234	1.2170	1.2170	1.2145
	σ	0.4707	0.0072	0.0072	0.0030	0.0030	0.0016
	n	10,199	6,192	12,332	10,872	21,726	40,444
	Δt_{max}/d	6.00	1.96	1.94	1.92	1.91	1.91
EURGBP	$\overline{X}$	0.7322	0.8243	0.8244	0.8020	0.8020	0.7941
	σ	0.0815	0.0171	0.0171	0.0091	0.0091	0.0035
	n	7,364	6,269	12,434	10,910	21,772	40,444
	Δt_{max}/d	4.00	1.92	1.92	1.90	1.90	1.90
EURJPY	$\overline{X}$	176.51	138.39	138.39	138.33	138.33	137.17
	σ	74.44	3.44	3.44	1.15	1.15	0.52
	n	10,157	6,233	12,418	10,890	21,749	40,437
	Δt_{max}/d	5.00	1.96	1.96	1.95	1.95	1.95
EUR	$\overline{X}$	1.1870	1.3602	1.3602	1.3572	1.3572	1.3450
	σ	0.1835	0.0172	0.0172	0.0125	0.0125	0.0082
	n	10,234	6,712	13,338	11,002	21,962	40,517
	Δt_{max}/d	5.00	1.92	1.92	1.92	1.91	1.83

Table 3.2: Mean, standard deviation, number of values and maximum time step for Thomson Reuters time series (1/2)

		1d	60min	30min	10min	5min	1min
EURNOK	$\overline{X}$	7.6522	8.2554	8.2552	8.2661	8.2660	8.3533
	σ	0.6946	0.1413	0.1414	0.1206	0.1206	0.0620
	n	10,190	6,225	12,371	10,868	21,643	40,160
	Δt_{max}/d	6.00	1.96	1.96	1.92	1.91	1.91
EURSEK	$\overline{X}$	7.9475	8.9433	8.9426	9.1350	9.1349	9.2144
	σ	1.4373	0.1703	0.1703	0.0959	0.0959	0.0303
	n	10,190	6,169	12,217	10,738	21,400	40,181
	Δt_{max}/d	5.00	2.00	2.00	1.92	1.92	1.92
GBPAUD	$\overline{X}$	2.0858	1.7928	1.7928	1.8098	1.8098	1.8116
	σ	0.3863	0.0566	0.0566	0.0114	0.0114	0.0106
	n	10,144	6,137	12,235	10,732	21,416	39,955
	Δt_{max}/d	5.00	2.08	2.06	2.05	2.05	2.05
GBPCAD	$\overline{X}$	2.0806	1.7800	1.7801	1.8317	1.8317	1.8337
	σ	0.2847	0.0751	0.0751	0.0085	0.0085	0.0077
	n	10,193	5,915	11,751	10,442	20,705	38,579
	Δt_{max}/d	5.00	2.25	2.25	2.26	2.26	2.26
GBPCHF	$\overline{X}$	2.6350	1.4841	1.4841	1.5172	1.5172	1.5289
	σ	0.9053	0.0255	0.0255	0.0146	0.0145	0.0081
	n	10,172	6,158	12,255	10,810	21,564	40,228
	Δt_{max}/d	5.00	2.00	1.98	1.97	1.96	1.96
GBPEUR	$\overline{X}$	1.3811	1.2131	1.2131	1.2467	1.2467	1.2588
	σ	0.1486	0.0255	0.0255	0.0141	0.0141	0.0056
	n	7,363	6,214	12,367	10,880	21,720	40,388
	Δt_{max}/d	4.00	1.96	1.96	1.95	1.95	1.95
GBPJPY	$\overline{X}$	260.30	167.90	167.90	172.46	172.46	172.72
	σ	130.56	5.95	5.96	1.21	1.21	0.96
	n	10,184	6,146	12,242	10,759	21,472	40,133
	Δt_{max}/d	5.00	2.00	2.00	1.98	1.98	1.94
CHFJPY	$\overline{X}$	90.03	113.07	113.06	113.63	113.63	112.94
	σ	12.67	3.13	3.13	0.80	0.80	0.43
	n	8,452	6,080	12,128	10,659	21,194	39,724
	Δt_{max}/d	5.00	2.08	2.06	2.06	2.06	2.02

Table 3.3: Mean, standard deviation, number of values and maximum time step for Thomson Reuters time series (2/2)

Table 3.4 provides more information on the sizes of gaps in the daily series. The number of times that a gap of size n days occurred for each currency pair is given. The frequency of gaps in the data is relevant as we later interpolate and assume a homogeneous time series for our further analysis.

	1d	2d	3d	4d	5d	6d	18d
CAD	8,865	70	2,179	95	2		
GBP	8,132	24	2,002	53	15		
JPY	8,888	61	2,190	81	2		1
EURAUD	5,872	7	1,466	10		1	
EURCAD	8,024	48	1,961	90	22		
EURCHF	8,103	23	1,987	63	21	1	
EURGBP	5,880	5	1,472	6			
EURJPY	8,068	15	1,956	78	39		
EUR	8,149	11	2,010	43	20		
EURNOK	8,092	25	1,980	70	21	1	
EURSEK	8,090	26	1,982	70	21		
GBPAUD	8,055	14	1,948	84	42		
GBPCAD	8,104	15	1,982	62	29		
GBPCHF	8,084	14	1,966	72	35		
GBPEUR	5,878	6	1,472	6			
GBPJPY	8,096	14	1,975	66	32		
CHFJPY	6,727	22	1,667	33	2		

Table 3.4: Gaps in daily Thomson Reuters series

Tables 3.5–3.9 give the number of times that observation steps of different sizes occur in the series.

Table 3.5 shows how many steps in the 60-minute time series are 60 minutes, how many are between 60 minutes and 1 day, and how many are 1 day or larger.

	60min	(60min,1d)	[1d,$\Delta t_{\max}$]
CAD	6,651	29	54
GBP	6,646	44	53
JPY	6,626	48	54
EURAUD	5,988	20	50
EURCAD	6,129	5	50
EURCHF	6,135	6	50
EURGBP	6,203	15	50
EURJPY	6,174	8	50
EUR	6,624	33	54
EURNOK	6,156	18	50
EURSEK	6,081	37	50
GBPAUD	6,080	6	50
GBPCAD	5,841	23	50
GBPCHF	6,090	17	50
GBPEUR	6,155	8	50
GBPJPY	6,088	7	50
CHFJPY	6,023	5	51

Table 3.5: Occurrences of time steps in 60-minute data

Table 3.6 shows how many steps in the 30-minute time series are 30 minutes, how many are between 30 minutes and 1 day, and how many are 1 day or larger.

	30min	(30min,1d)	[1d,$\Delta t_{\max}$]
CAD	13,249	44	54
GBP	13,220	68	53
JPY	13,233	55	54
EURAUD	11,959	41	50
EURCAD	12,265	18	50
EURCHF	12,267	14	50
EURGBP	12,358	25	50
EURJPY	12,358	9	50
EUR	13,242	41	54
EURNOK	12,289	31	50
EURSEK	12,089	77	50
GBPAUD	12,161	23	50
GBPCAD	11,645	55	50
GBPCHF	12,178	26	50
GBPEUR	12,300	16	50
GBPJPY	12,168	23	50
CHFJPY	12,059	17	51

Table 3.6: Occurrences of time steps in 30-minute data

Table 3.7 shows how many steps in the 10-minute time series are 10 minutes, how many are between 10 minutes and 1 day, and how many are 1 day or larger.

	10min	(10min,1d)	[1d,$\Delta t_{\max}$]
CAD	10,957	23	15
GBP	10,937	18	15
JPY	10,964	15	15
EURAUD	10,620	18	15
EURCAD	10,322	262	15
EURCHF	10,851	5	15
EURGBP	10,880	14	15
EURJPY	10,863	11	15
EUR	10,973	13	15
EURNOK	10,820	32	15
EURSEK	10,678	44	15
GBPAUD	10,704	12	15
GBPCAD	10,399	27	15
GBPCHF	10,771	23	15
GBPEUR	10,855	9	15
GBPJPY	10,721	22	15
CHFJPY	10,628	15	15

Table 3.7: Occurrences of time steps in 10-minute data

Table 3.8 shows how many steps in the 5-minute time series are 5 minutes, how many are between 5 minutes and 1 day, and how many are 1 day or larger.

	5min	(5min,1d)	[1d,$\Delta t_{\max}$]
CAD	21,870	46	15
GBP	21,816	45	15
JPY	21,896	31	15
EURAUD	21,073	103	15
EURCAD	21,680	6	15
EURCHF	21,701	9	15
EURGBP	21,730	26	15
EURJPY	21,711	22	15
EUR	21,915	31	15
EURNOK	21,553	74	15
EURSEK	21,320	64	15
GBPAUD	21,355	45	15
GBPCAD	20,506	183	15
GBPCHF	21,496	52	15
GBPEUR	21,682	22	15
GBPJPY	21,414	42	15
CHFJPY	21,077	101	15

Table 3.8: Occurrences of time steps in 5-minute data

Table 3.9 shows how many steps in the 1-minute time series are 1 minute, how many are between 1 minute and 1 day, and how many are 1 day or larger.

	1min	(1min,1d)	[1d,$\Delta t_{\max}$]
CAD	41,821	111	6
GBP	40,425	94	6
JPY	40,402	118	6
EURAUD	36,972	2,143	6
EURCAD	40,353	34	6
EURCHF	40,424	13	6
EURGBP	40,412	25	6
EURJPY	40,405	25	6
EUR	40,383	127	6
EURNOK	39,997	156	6
EURSEK	40,104	70	6
GBPAUD	39,716	232	6
GBPCAD	36,374	2,198	6
GBPCHF	40,078	143	6
GBPEUR	40,365	16	6
GBPJPY	39,998	128	6
CHFJPY	39,518	199	6

Table 3.9: Occurrences of time steps in 1-minute data

It is apparent from these tables that most gaps in the data are weekends and there are few other holes of missing data.

3.2 Data set 2: Commerzbank

The second data set was a proprietary data set obtained from Commerzbank. It contained high-frequency data for the time period between 1 January 2015 and 15 December 2016. Quotes for 63 currency pairs were included in the data. Each quote came from either London or New York, and for each source the median tick size of the data could be as small as 0.01 seconds for the most liquid currency pairs.

Quotes consisted of a bid and ask price, along with a time stamp as well as the name of the source and the currency pair. The values in this data set were the core prices upon which the bank based its quotes given to clients. Before clients were quoted these prices they would be adjusted based on the individual client's credit parameters. Not all of these prices were dealt on. The prices were algorithmically generated in response to new real-time information becoming available. This information could be in the form of things such as trades or changing market making prices. The exact algorithm used for generating the prices is not known to us.

3.2.1 Preparing the data

The data was provided with all rates from a particular day for all pairs, prices and sources combined into one file. We read these files in, computed the mid price as the mean between ask and bid price, and sorted each time stamp/mid price pair into one of 126 time series, one for each currency pair and source. We then chose from these series those that were suitable for our analysis, based on number and frequency of data points. For these series we removed outliers, took the natural logarithm, and then interpolated the series to make them homogeneous in time.

3.2.2 Properties of the data set

See Tables 3.10–3.13 for the properties of the raw data before taking the logarithm and interpolating. Tables 3.10 and 3.11 refer to data with the source London and Tables 3.11 and 3.12 refer to data with the source New York. The tables list all currency pairs along with the size n_{days} of the date range covered by each series in days, the number n_{dwv} of days in this range for which values were provided, the number n_{vals} of values contained in the series, as well as the median tick size Δt_{med} in seconds and the mean and standard deviation σ of prices for each series.

	n_{days}	n_{dwv}	n_{vals}	$\Delta t_{med}/\text{s}$	mean	σ
AUDJPY	286	233	32,292,397	0.0810	92.07	3.6554
AUDUSD	714	583	82,150,097	0.0580	0.7487	0.0302
CNYJPY	1	1	2	15.0250	19.56	0.0001
EURBRL	31	6	9,175	4.7785	3.0781	0.1379
EURCHF	710	141	4,336,996	0.0570	1.0827	0.0868
EURCNY	1	1	3	11.0190	7.4141	0.0001
EURCZK	710	109	62,973	0.2690	27.1774	0.2047
EURDKK	710	108	134,412	0.0370	7.4451	0.0097
EURGBP	710	108	2,309,001	0.0540	0.7767	0.0598
EURHRK	710	105	22,228	6.8460	7.5625	0.0789
EURHUF	710	104	476,199	0.0250	309.6101	4.2601
EURINR	1	1	2	25.0450	76.5014	0.0006
EURJPY	710	105	3,095,779	0.0410	128.04	8.3851
EURKRW	1	1	3	14.2570	1,322.99	0.0114
EURMYR	31	5	166	15.0300	4.1233	0.0794
EURNOK	710	102	861,675	0.0230	9.1457	0.3249
EURPEN	52	9	5,248	15.0300	3.4824	0.0713
EURPLN	710	103	405,171	0.2400	4.3296	0.1094
EURRON	710	101	1,170	21.7500	4.4615	0.0453
EURSEK	710	102	836,696	0.0170	9.4998	0.2411
EURUSD	712	217	9,787,663	0.0930	1.1145	0.0167
GBPJPY	283	41	926,984	0.0540	184.64	5.4213
GBPPEN	52	9	4,613	15.0300	4.6090	0.0812
GBPUSD	710	103	1,308,044	0.0580	1.4556	0.1006
INRJPY	1	1	3	10.5180	1.8952	0.0000
KRWJPY	1	1	1		0.1096	
NOKSEK	710	100	1,061,868	0.0290	1.0382	0.0452
NZDUSD	710	99	763,977	0.0820	0.6949	0.0390
USDCAD	714	427	28,248,571	0.1020	1.3136	0.0415
USDCHF	714	336	18,642,597	0.0750	0.9817	0.0463
USDCNH	712	255	6,429,952	0.0310	6.6897	0.1375
USDCZK	52	8	13,936	2.9740	23.9546	0.6597

Table 3.10: Statistical properties of LN Commerzbank data (1/2)

	n_{days}	n_{dwv}	n_{vals}	Δt_{med}/s	mean	σ
USDDKK	52	8	94,697	0.0530	6.4350	0.1967
USDDZD	712	220	1,085,446	6.0480	109.5853	1.5188
USDETB	712	217	2,295	2,107.1000	21.9471	0.3796
USDHKD	710	102	45,933	0.5030	7.7696	0.0141
USDHUF	52	8	30,100	0.3390	269.7378	5.9378
USDILS	710	103	2,470	22.7500	3.8577	0.0548
USDISK	52	9	7,565	15.0300	172.3583	9.3267
USDJPY	710	103	1,532,168	0.0550	114.99	7.2626
USDKWD	710	102	6,978	56.2790	0.3008	0.0035
USDLKR	710	101	153	6.048E+05	139.5344	6.3216
USDMAD	710	101	14,172	30.0600	9.7193	0.2598
USDMXN	710	101	488,741	0.0100	18.8468	1.8129
USDMYR	710	61	121	2.715E+05	4.0857	0.1997
USDNOK	52	8	27,396	0.2500	7.6284	0.1052
USDOMR	710	98	290	23,491.0000	0.3850	0.0000
USDPLN	52	8	22,863	0.5500	3.6653	0.0776
USDRON	52	7	5,209	10,541.0000	3.8637	0.1068
USDSAR	365	6	9	1.193E+06	3.7547	0.0017
USDSGD	710	98	285,757	0.0500	1.3664	0.0274
USDTHB	710	98	26,186	40.3130	34.5219	1.2306
USDTND	710	98	64,122	3.6930	2.0702	0.1390
USDTRY	710	96	246,265	0.0480	2.9038	0.2585
USDZAR	710	96	476,990	0.0230	14.3528	0.9266
XAGUSD	710	95	30,770	4.7910	17.1134	1.7742
XAUUSD	710	95	81,334	2.1020	1,238.32	80.5793
XPDUSD	710	95	13,760	7.7170	652.12	95.9262
XPTUSD	710	95	25,921	4.9450	1,037.45	107.4882
ZARJPY	269	37	43,231	12.5240	9.8920	0.4511
USDBRL	713	379	10,610,770	0.3700	3.5222	0.2776
USDBHD	709	199	30,268	40.4800	0.3771	0.0001
USDARS	713	481	580,497	5.0680	11.0182	2.1223

Table 3.11: Statistical properties of LN Commerzbank data (2/2)

	n_{days}	n_{dwv}	n_{vals}	Δt_{med}/s	mean	σ
AUDJPY	286	233	35,597,659	0.0720	92.06	3.6523
AUDUSD	714	582	78,892,426	0.0610	0.7484	0.0303
CNYJPY	1	1	5	4.2745	19.56	0.0001
EURBRL	31	6	9,352	4.1260	3.0821	0.1378
EURCHF	710	140	4,104,510	0.0610	1.0827	0.0891
EURCNY	1	1	1		7.4141	
EURCZK	710	108	61,548	0.2610	27.1794	0.2057
EURDKK	710	107	133,810	0.0360	7.4450	0.0096
EURGBP	710	107	2,155,131	0.0590	0.7785	0.0599
EURHRK	710	104	21,906	6.4560	7.5628	0.0795
EURHUF	710	103	455,123	0.0250	309.60	4.3073
EURINR	1	1	1		76.5017	
EURJPY	710	104	2,846,614	0.0470	127.81	8.3990
EURKRW	1	1	2	16.0620	1,322.98	0.0301
EURMYR	31	5	162	15.0300	4.1230	0.0790
EURNOK	710	101	823,062	0.0230	9.1509	0.3316
EURPEN	52	9	5,242	15.0300	3.4836	0.0717
EURPLN	710	102	378,304	0.0230	4.3245	0.1107
EURRON	710	100	1,174	21.2500	4.4617	0.0452
EURSEK	710	101	792,253	0.0190	9.4804	0.2339
EURUSD	712	216	9,015,303	0.1040	1.1143	0.0167
GBPJPY	283	41	805,220	0.0570	184.73	5.4101
GBPPEN	52	9	4,546	15.0300	4.6090	0.0815
GBPUSD	710	102	1,110,752	0.0630	1.4496	0.1016
INRJPY	1	1	3	11.5380	1.8952	0.0000
KRWJPY	1	1	3	11.7880	0.1096	0.0000
NOKSEK	710	99	1,026,313	0.0300	1.0365	0.0453
NZDUSD	710	97	766,963	0.0820	0.6943	0.0387
USDCAD	714	426	28,445,045	0.1090	1.3131	0.0416
USDCHF	714	335	18,152,352	0.0800	0.9817	0.0957
USDCNH	712	255	6,126,171	0.0370	6.6837	0.1417
USDCZK	52	8	14,490	2.4620	23.9380	0.6679

Table 3.12: Statistical properties of NY Commerzbank data (1/2)

	n_{days}	n_{dwv}	n_{vals}	Δt_{med}/s	mean	σ
USDDKK	52	8	86,130	0.0580	6.4330	0.1996
USDDZD	712	219	1,089,556	6.0100	109.5841	1.5170
USDETB	712	216	2,295	2,107.1000	21.9461	0.3812
USDHKD	710	101	44,277	0.5030	7.7698	0.0141
USDHUF	52	8	31,516	0.2840	269.69	5.9449
USDILS	710	102	2,281	30.0010	3.8586	0.0570
USDISK	52	9	7,623	15.0300	172.3985	9.3342
USDJPY	710	102	1,395,648	0.0600	114.78	7.2474
USDKWD	710	101	6,975	56.0440	0.3008	0.0035
USDLKR	710	100	154	6.048E+05	139.46	6.3418
USDMAD	710	100	13,766	30.0600	9.7208	0.2634
USDMXN	710	100	448,904	0.0120	18.7913	1.8436
USDMYR	710	61	120	5.791E+05	4.0847	0.2002
USDNOK	52	8	28,142	0.2250	7.6258	0.1067
USDOMR	710	97	289	20,544.0000	0.3850	0.0000
USDPLN	52	8	24,150	0.4180	3.6637	0.0780
USDRON	52	7	5,301	9.4975	3.8647	0.1066
USDSAR	365	6	9	1.193E+06	3.7547	0.0017
USDSGD	710	97	276,884	0.0450	1.3656	0.0271
USDTHB	710	97	26,009	40.3130	34.5106	1.2279
USDTND	710	97	63,295	3.6240	2.0717	0.1392
USDTRY	710	95	228,063	0.0470	2.8699	0.2315
USDZAR	710	95	462,985	0.0230	14.3653	0.9309
XAGUSD	710	94	30,636	4.7720	17.1244	1.7699
XAUUSD	710	94	80,966	2.0950	1,238.95	80.2558
XPDUSD	710	94	13,641	7.6980	652.69	96.2154
XPTUSD	710	94	25,731	4.9280	1,037.98	107.7299
ZARJPY	269	36	42,528	10.7100	9.92	0.4203
USDBRL	713	377	10,707,368	0.3650	3.5244	0.2777
USDBHD	709	204	30,254	40.4260	0.3771	0.0001
USDARS	713	478	579,544	5.0690	11.0240	2.1245

Table 3.13: Statistical properties of NY Commerzbank data (2/2)

The statistics in Tables 3.10–3.13 formed the basis for our decision on which of the 126 series were suitable for further analysis. We excluded series with recurring gaps of more than 3 days, series with a median tick size larger than 1 second, as well as any series with fewer than 10,000 values. For some series the local mean tick size varied so significantly that we decided to only use the values from the series within the date range of higher frequency. We were left with 14 series belonging to seven currency pairs in our final data set. The pairs, the time range covered by each series in days, the number of values, and the median tick sizes after cropping where necessary and after removing outliers, that we used in our further analysis are listed in Table 3.14. The table describes the data before interpolation.

	src	n_{days}	n_{vals}	$\Delta t_{\text{med}}/\text{s}$
AUDJPY	LN	287	32,291,141	0.08100
	NY	287	35,596,420	0.07201
AUDUSD	LN	715	82,150,097	0.05800
	NY	715	78,892,426	0.06100
EURUSD	LN	96	4,672,259	0.10900
	NY	110	4,669,929	0.11799
USDBRL	LN	395	10,609,771	0.36999
	NY	395	10,706,374	0.36500
USDCAD	LN	235	14,007,041	0.13299
	NY	239	14,394,267	0.14100
USDCHF	LN	165	9,242,949	0.09401
	NY	165	8,889,466	0.10301
USDCNH	LN	147	3,542,507	0.03699
	NY	142	3,457,391	0.04100

Table 3.14: Size of date range, number of values, median tick size of Commerzbank data used in further analysis

We next took the logarithm, and used linear interpolation to obtain series with observation steps 0.2 seconds. These series are what we will from here on refer to as the Commerzbank data set.

3.3 Treating the data

In this section we will present some of the methodology we employed in treating the data used for the experiments.

3.3.1 Cleaning the data

Before analysing the data, it was cleaned by removing outliers and errors. While the errors in the Thomson Reuters series were eliminated by consolidating the values from different download dates as the data was pre-cleaned, the Commerzbank data contained some outliers that required manual removal. We took a conservative approach to removing outliers, only removing those values whose deviation from the mean differed from that of surrounding values by an order of magnitude.

3.3.2 Mid prices and log returns

While the Thomson Reuters series only contained one price per time stamp, the Commerzbank data set included both ask and bid prices, from which we computed the mid price that was used in our further analysis. There are a number of ways in which the mid price between ask and bid prices may be determined. For the purpose of this thesis we define the mid price as the arithmetic mean of the ask and bid price. Therefore, with regard to the Commerzbank series, by "log price" we mean the logarithm of the arithmetic

mean of the ask and bid prices. An alternative quantity would be the the arithmetic mean of the logarithms of the ask and bid price.

Our "log returns" are the differences between two log prices with different time stamps. An alternative quantity that may be used to approximate this value in the case of small time steps is the difference between the two prices divided by one of the prices.

3.3.3 Interpolation

As the data downloaded from Thomson Reuters Eikon contained gaps as described above, and as the tick data from Commerzbank analysed in this thesis is unevenly spaced in time, but the analysis we conducted was with regard to evenly distributed data, we had to interpolate data points to make them evenly spaced in time. We used linear interpolation, but Müller et al. [82] found that there was no significant difference in their results between linearly interpolated and last point interpolated data. We used linear interpolation on the logarithms of the mid prices rather than on the raw mid prices or on the raw bid and ask prices.

Like Müller et al. [82] we worked on a physical time scale rather than in business time. We therefore interpolated values to span weekends as well as any gaps in the data.

Of course interpolation introduces a bias into the data and it was therefore necessary to find an appropriate level of interpolation. For the Thomson Reuters data the purpose of the interpolation was to fill in the gaps, and we therefore chose as the interpolation interval the interval of the series. However for the Commerzbank data the purpose of interpolation was to make the data evenly spaced in time. We therefore chose interpolation intervals of 0.2 seconds for the Commerzbank series, but elected to consider the frequency of the raw series when deciding which intervals should in fact be used in our research.

3.4 Simulation

The simulated Ornstein–Uhlenbeck processes that we analysed were generated using Matlab. The processes were discretized as described in Section 2.2.3 and the Gaussian noise was generated by Matlab's *randn* function.

Given a mean value μ, a mean reversion strength α, and a noise coefficient σ, as well as a starting value X_0, a size of time steps Δt, and a number of steps n_{steps}, a standard Ornstein–Uhlenbeck process was generated in the following way: The standard deviation was calculated as $s = \sigma\sqrt{\frac{1-e^{-2\alpha\Delta t}}{2\alpha}}$. With X_0 being the first value in the process, the remaining values of the process were then computed iteratively as $X_i = \mu + (X_{i-1} - \mu)e^{-\alpha\Delta t} + s \times N_i$ for $i = 1, 2, ..., n_{\text{steps}}$, where N_i for $i = 1, 2, ..., n_{\text{steps}}$ were independent random numbers drawn from $N(0, 1)$ by Matlab's *randn* function. $\{X_i\}_{0\leq i\leq n_{\text{steps}}}$ was then a discretized Ornstein–Uhlenbeck process with the input parameters.

In order to simulate Ornstein–Uhlenbeck processes with time-dependent reversion levels, instead of a constant μ as an input parameter, a series $\{\mu_i\}_{0\leq i\leq n_{\text{steps}}}$ was given as input.

Starting from X_0, the remaining values of the process were then generated according to $X_i = \mu_i + (X_{i-1} - \mu_i)e^{-\frac{\alpha}{\Delta t}} + s \times N_i$ for $i = 1, 2, ..., n_{\text{steps}}$.

3.5 Summary

The two data sets we used had different strengths and weaknesses, with the Thomson Reuters data set covering a much larger range of time and more currency pairs, and the Commerzbank data set providing much higher frequency.

Throughout this thesis we are working with the following data sets:

1. The Thomson Reuters data set:
   These are the series relating to one currency pair and one time interval, after combining all data downloaded on different days, cleaning the data, taking the logarithm, and then interpolating.

2. The Commerzbank data set:
   These are the series relating to one currency pair and after taking the logarithm and interpolating to the smallest appropriate time interval.

3. The synthetic data:
   These are simulated Ornstein–Uhlenbeck processes which we have generated as described above, according to the specified parameters.

Chapter 4

Scaling of log returns

In this chapter we present Part 1 of our research, where we examine the dependence of mean absolute log returns of FX rates on the time intervals over which they are measured, as well as the effect that detrending of the data has on this relationship. We also compare our findings to two different models, which we simulate before analysing them in the same way.

4.1 Research question

The scaling law first reported by Müller et al. [82] with respect to FX data has been observed in numerous data sets and widely reported in the literature [3, 9, 84]. As described in Section 2.5.2, it gives the relationship between the mean of the absolute values of the log price returns $\Delta x_{\Delta t}$ measured over a certain time interval Δt and the size of the time interval as

$$\overline{|\Delta x|}_{\Delta t} = c\Delta t^E \tag{4.1}$$

for some constants c and E, where E is the scaling exponent. This is the law from Eq. 2.54.

However, this has so far been reported purely as an empirical scaling law, and it is not known whether it holds for time intervals outside of the ranges that have been tested. Additionally, while it has been proposed that the law is a result of the spectrum of time horizons at which agents in the market operate [9], the law appears to be inconsistent with models of exchange rates being mean reverting around an underlying rate. Our motivation for this first part of our research was twofold. Firstly, we wanted to test for the scaling property in a novel data set and over intervals for which it had not been previously observed. Secondly, we wanted to examine the scaling law in light of two different stochastic models of the time series.

The research of this chapter is therefore divided into two parts. In the first part we will analyse our real-world data sets with regard to the scaling law. In the second part we will compare our findings for the scaling law in our data before and after detrending to a simulated Brownian motion and a simulated OU process with a time-dependent reversion

level.

4.2 Scaling in FX data

In order to test for the scaling law in our FX data we computed the mean absolute returns $\overline{|\Delta x|}_{\Delta t}$ of the logarithmic FX rates for different time intervals Δt. We then conducted a line fit to the relationship between the logarithms of these two quantities. This was done by creating a series sampled at observation steps Δt from the original log data for each Δt, and then computing the mean absolute increments for each of these series.

4.2.1 Methodology

Due to the differences between the two data sets, we sampled the series from the two sets in different ways, leading to the same analysis done on different ranges of time scales.

Thomson Reuters

We computed the mean absolute log returns for each currency pair in the Thomson Reuters data set over the intervals 1, 2, 5, 10 and 30 minutes, 1, 2, 6 and 12 hours, 1, 2, 7, 14, 30, 60 and 180 days, and 1, 2 and 4 years. We then conducted a line fit to the log mean absolute log returns as a function of the log time intervals.

As described in Section 3.1, the Thomson Reuters data set already consisted of six differently sampled series of logarithmic nominal exchange rates for each currency pair, with observation steps Δt of sizes 1 minute, 5 minutes, 10 minutes, 30 minutes, 1 hour and 1 day. Let $\{X_{i;\Delta t}\}$ be the series of log prices sampled with the observation step Δt. In addition to these series, we created a series with observation step 2 minutes by sampling every other value from $\{X_{i;1\text{min}}\}$, series with observation steps 2, 6 and 12 hours by sampling every 2nd, 6th and 12th value respectively from $\{X_{i;1\text{hour}}\}$, and series for the observation steps 2, 7, 14, 30, 60 and 180 days by sampling $\{X_{i;1\text{day}}\}$ accordingly. (For all of these we started sampling with the first data point available in the sampled series.) For each of these series, we computed the mean absolute value of all increments, and this is what we shall denote as $\overline{|\Delta x|}_{\Delta t}$. See below for some example graphs: Figures 4.1 and 4.2 show the increments of our Thomson Reuters CAD/USD time series observed at frequencies 1/minute and 1/hour, respectively. See Appendix A for plots of the log prices of these series. Note that the increments for both frequencies appear to fluctuate around 0, however the increments of the series with minutely frequency in Figure 4.1 have a significantly narrower distribution than the hourly ones in Figure 4.2.

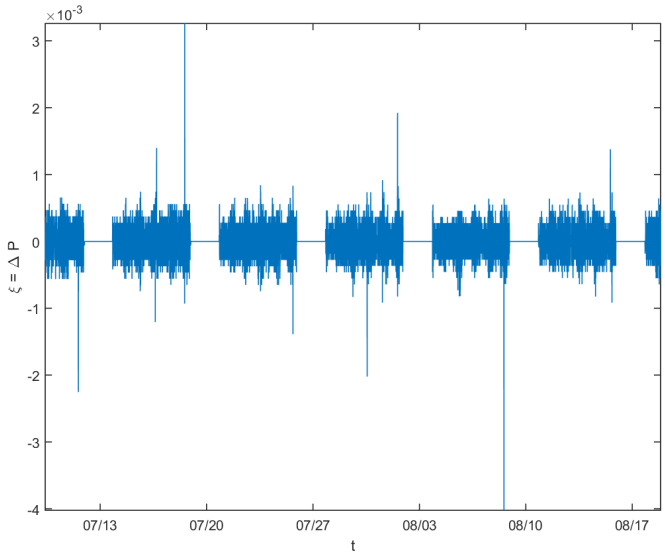

Figure 4.1: Minutely CAD/USD increments from Thomson Reuters for July–August 2014

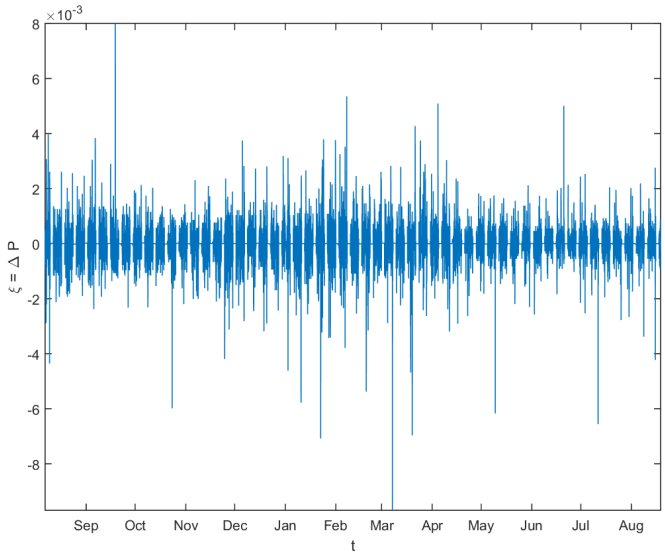

Figure 4.2: Hourly CAD/USD increments from Thomson Reuters for 2013–2014

Finally we computed $\overline{|\Delta x|}_{\Delta t}$ for Δt of sizes one, two and four years (365 days, 2×365 days, and 4×365+1 days) by sampling the daily series with an overlap of 2/3, as done by Müller et al. [82], to increase the number of data points in each sample. We chose (4×365+1) days as the largest interval to account for leap years and as this number would allow for an overlap of 2/3. The overlap sampling was done in the following way: For each $\Delta t = n\text{d}$, we sampled $\{X_{i;1\text{d}}\}$ three times, giving us $\{X_{i;n\text{days},1}\}$, $\{X_{i;n\text{days},2}\}$ and $\{X_{i;n\text{days},3}\}$, where $\{X_{i;n\text{days},j}\}$ is the series of every n-th value sampled from $\{X_{i;1\text{day}}\}$, starting at value $X_{k;1\text{day}}$ where $k = 1 + n\left(\frac{j-1}{3}\right)$. $\overline{|\Delta x|}_{n\text{d}}$ was then found by finding the

mean of the absolute increments of $\{X_{i;\mathrm{nd},1}\}$, $\{X_{i;\mathrm{nd},2}\}$ and $\{X_{i;\mathrm{nd},3}\}$. We then found the correlation coefficient R between $\log \Delta t$ and $\log \overline{|\Delta x|}_{\Delta t}$, and fitted a line using simple linear regression to

$$\log \overline{|\Delta x|}_{\Delta t} = a + E \log \Delta t, \tag{4.2}$$

so that E is the estimator of the scaling exponent. The correlation coefficients and scaling exponents for all currency pairs in the Thomson Reuters data set are presented in Section 4.2.2. An example of the different log mean absolute log returns measured over the different log intervals, along with a line fit, for the currency pair GBP/CHF can be found in Figure 4.3. See Appendix A for another example graph.

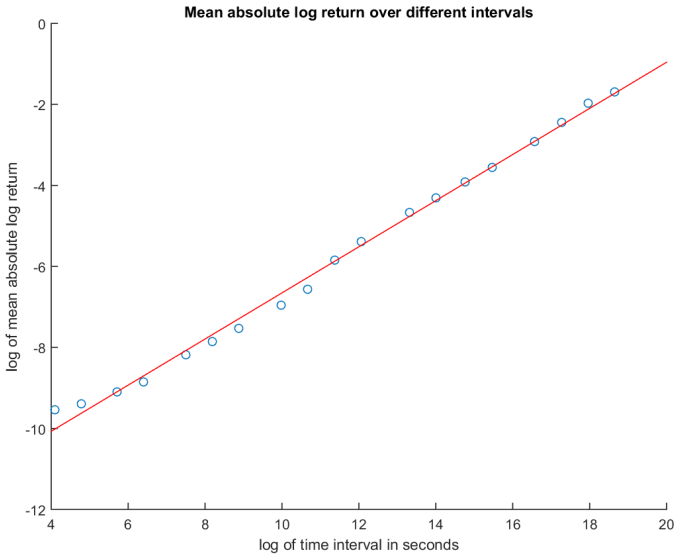

Figure 4.3: Scaling for Thomson Reuters data GBP/CHF

Commerzbank data

For the series in the Commerzbank data set, we computed the mean absolute log returns over intervals ranging from 0.2 seconds to seven days. We then again conducted a line fit to find the relationship between the log mean absolute log returns and the log time intervals.

For the Commerzbank data we only had one series per currency pair per source, and we did not use any overlap in our sampling as there were sufficient data points available for smaller time intervals, and larger intervals were analysed as part of the Thomson Reuters series. As described in Section 3.2, as part of our pre-processing of the data, all series of logarithmic NERs were interpolated to a time grid with observation step 0.2 seconds. We chose as observation steps Δt the intervals 0.2 seconds, 0.4 seconds, 1, 2, 5, 10 and 30 seconds, 1, 2, 5, 10 and 30 minutes, 1, 2, 6 and 12 hours, and 1, 2 and 7 days. However, to reduce the bias introduced by interpolation, for the currency pairs EUR/USD, USD/CAD and USD/CHF we only used observation steps of 0.4 seconds and larger, and for USD/BRL

we only used observation steps of 1 second and larger, due to the lower frequency in the raw data for these pairs, as shown in Table 3.14. Like with the Thomson Reuters data, for each pair and source, we sampled the series at each observation step Δt to obtain the series $\{X_{i;\Delta t}\}$, then computed the mean absolute increments $\overline{|\Delta x|}_{\Delta t}$ thereof, and then found the correlation coefficient as well as the slope of the linear relationship between the logarithms of Δt and $\overline{|\Delta x|}_{\Delta t}$. See Figure 4.4 for the graph of this relationship as found for the currency pair USD/CHF for the London source data. See Appendix A for another example graph.

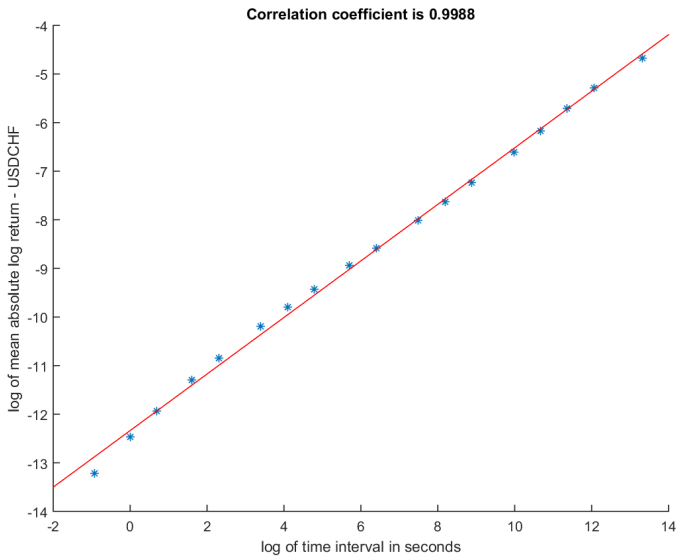

Figure 4.4: Scaling for LN source Commerzbank data USD/CHF

4.2.2 Results

We have observed Müller et al.'s [82] scaling law for slightly different range of intervals than previously reported in the literature. The scaling relationship appears to hold for this widened range, although the data points for either end of the spectrum of observation intervals are less reliable for a variety of reasons, such as interpolation bias, fewer data points being available or overlapping intervals being used, and different time ranges being covered by the original data.

For the Thomson Reuters data we found a good linear fit over intervals ranging from one minute to four years, with a median scaling exponent of 0.567, a mean scaling exponent of 0.559, and correlation coefficients of 0.99478 and larger, although the data points for the smallest and largest intervals tended to deviate slightly from the linear fit. However, this may be due to the fact that for smaller time intervals the interpolation has a larger effect, and for the larger time intervals we used overlapping sampling. Additionally, data for different observation intervals spanned different date ranges, as described in Section 3.1, which may be the cause of the slight curvatures of the line. We found the scaling exponents of all but one pair (EUR/NOK) to lie above 0.5.

The correlation coefficients and scaling exponents for the Thomson Reuters data are presented in Table 4.1.

Pair	R	E
CAD	0.99832	0.518
GBP	0.99810	0.603
JPY	0.99846	0.585
EURAUD	0.99587	0.531
EURCAD	0.99729	0.555
EURCHF	0.99478	0.589
EURGBP	0.99685	0.532
EURJPY	0.99855	0.578
EUR	0.99774	0.609
EURNOK	0.99796	0.476
EURSEK	0.99871	0.509
GBPAUD	0.99930	0.564
GBPCAD	0.99830	0.567
GBPCHF	0.99756	0.568
GBPEUR	0.99792	0.549
GBPJPY	0.99910	0.590
CHFJPY	0.99851	0.584

Table 4.1: Correlation coefficients R and scaling exponents E for Thomson Reuters data

For the Commerzbank data we analysed intervals ranging from 0.2 seconds to seven days and found a median scaling exponent of 0.574 and a mean scaling exponent of 0.585, with correlation coefficients larger than 0.99536. We found larger scaling exponents in the Commerzbank data set than we did in the Thomson Reuters data, with the lowest Commerzbank exponent still exceeding 0.53. Like the results for the Thomson Reuters data set, our results are in line with those reported in the literature. The correlation coefficients and scaling exponents for each pair and source of the Commerzbank data set are presented in Table 4.2.

Pair	Source	R	E
AUDJPY	LN	0.99844	0.557
	NY	0.99872	0.556
AUDUSD	LN	0.99797	0.572
	NY	0.99823	0.570
EURUSD	LN	0.99940	0.599
	NY	0.99948	0.605
USDBRL	LN	0.99539	0.546
	NY	0.99536	0.546
USDCAD	LN	0.99888	0.576
	NY	0.99896	0.571
USDCHF	LN	0.99880	0.582
	NY	0.99871	0.579
USDCNH	LN	0.99699	0.665
	NY	0.99702	0.666

Table 4.2: Correlation coefficients R and scaling exponents E for Commerzbank data

4.3 Scaling of detrended data

While there is overwhelming evidence of nominal exchange rates scaling as described in Section 2.5.2, there is no conclusive evidence of the underlying processes producing this behaviour. As noted by others [82, 84], while nominal exchange rates following a geometric Brownian motion as in Eq. 2.6 would lead to a linear relationship between $\log \Delta t$ and $\log \overline{|\Delta x|}_{\Delta t}$, the fact that the slope found is systematically larger than 0.5, and, for example, the multiscaling property described in Section 2.5, all suggest that a simple geometric Brownian motion is not sufficient as a model to explain the scaling behaviour of FX rates.

Since a common assumption of FX rate determination models is that exchange rates are mean-reverting around an underlying rate, and similarly many trading strategies assume a mean reversion to some underlying trend, we will in the following compare the scaling behaviour of two different models to that of the real data. Our first model (Model 1) proposes that logarithmic nominal exchange rates follow an OU process around a time-dependent underlying value, which in turn is modelled as a smoothed Brownian motion. The second model (Model 2) is of nominal exchange rates following geometric Brownian motion.

A distinctive feature of mean reverting processes with constant reversion level is that we would not expect to see increments growing indefinitely with increasing time intervals over which they are measured, and therefore we would under Model 1 interpret the scaling behaviour for larger time intervals to be a result of the movements of the underlying value itself, rather than the fluctuations of the NER around the underlying value. In order to distinguish between these two merged stochastic processes we therefore attempt to approximate the movements of the underlying value by a moving average, and thus to detrend the NER, after which we would expect to see a dependence of $\log \overline{|\Delta x|}_{\Delta t}$ on $\log \Delta t$ which is similar to that seen in an OU processes. For a process following an OUP according to Eq. 2.7 with reversion strength α, reversion level μ, and diffusion coefficient σ, the expected value of the absolute return over Δt is

$$\mathrm{E}\left(|X_{t+\Delta t} - X_t|\right) = \mathrm{E}\left(|\Delta X|_{\Delta t}\right) = \sigma\sqrt{\frac{2 - 2e^{-\alpha \Delta t}}{\pi \alpha}}, \tag{4.3}$$

and its limits as $\Delta t \to 0$ and $\Delta t \to \infty$ are

$$\lim_{\Delta t \to 0} \mathrm{E}\left(|X_{t+\Delta t} - X_t|\right) = \sigma\sqrt{\frac{2\Delta t}{\pi}} \tag{4.4}$$

and

$$\lim_{\Delta t \to \infty} \mathrm{E}\left(|X_{t+\Delta t} - X_t|\right) = \sigma\sqrt{\frac{2}{\pi \alpha}}. \tag{4.5}$$

To test our two models, we thus simulated first an OU process with a smoothed Wiener process as reversion level and then a simple Wiener process, to model minutely log nominal exchange rate data spanning one year. We then analysed both of these models for their scaling behaviour of $\overline{|\Delta x|}_{\Delta t}$ as a function of Δt and compared this to the scaling

behaviour found in Section 4.2. We then detrended both simulated series as well as some of the FX series by subtracting a range of moving averages, and compared the dependence of $\log \overline{|\Delta x|}_{\Delta t}$ on $\log \Delta t$ in the detrended simulated series with that found in the detrended FX data as well as in a standard OUP.

4.3.1 Methodology

We shall now go into more detail regarding the exact methodology employed to conduct the comparison between the two models and the real data.

FX data

We chose to compare our models with the daily Thomson Reuters series spanning 40 years, as the half-life of shocks to RERs reported in the literature is around 3-7 years [19] and these longer series allowed for a larger range of time intervals to be analysed without interpolation introducing too much bias into the analysis.

Model 1

For Model 1 we simulated a series of values following an OU process mean reverting to a smoothed Wiener process, to represent one year's worth of minutely data fluctuating around a random walk underlying value.

This was done by generating $(n+s-1)$ normal random values $\{N_i\}_{1\leq i\leq n+s-1}$ so that $N_i \sim N(0,1)$ for $1 \leq i \leq n+s-1$, where $n = 365 \times 24 \times 60 + 1$ is the number of values we want the OUP to have and $s = 2 \times 24 \times 60$ is the smoothing interval for the reversion level, and then computing $W_i = \sum_{j=1}^{i} N_j$ for $1 \leq i \leq n+s-1$ so that $\{W_i\}_{1\leq i\leq n+s-1}$ was a discretized Wiener process with $(n+s-1)$ values. We then smoothed this process using its SMA over $s = 2 \times 24 \times 60$ values by computing

$$\mu'_i = \frac{1}{s}\sum_{j=0}^{s-1} W_{i+j} \tag{4.6}$$

for $1 \leq i \leq n$. We then computed $\{\mu_i\}_{1\leq i\leq n}$ with $\mu_i = 0.001 \times (\mu'_i - \mu'_0)$ to represent the minutely underlying value of the log exchange rate over one year.

We next simulated minutely samples of an OUP $\{X_i\}_{1\leq i\leq n}$ over one year with starting value $X_0 = \mu_0 = 0$, reversion strength $\alpha = \frac{1}{12\times 60}$, diffusion coefficient $\sigma = 0.001$, and $\{\mu_i\}_{1\leq i\leq n}$ as reversion level, as described in Section 3.4, by generating $(n-1)$ i.i.d. standard normal random values $N'_i \sim N(0,1)$ for $1 \leq i \leq (n-1)$ and then computing

$$X_{i+1} = \mu_i + e^{-\alpha}(X_i - \mu_i) + \sigma\sqrt{\frac{1-e^{-2\alpha}}{2\alpha}}N'_i \tag{4.7}$$

for $1 \leq i \leq (n-1)$ as per the discretization equation 2.16 in Section 2.2.3. Note in this case our time unit is one minute, and therefore Δt=1 and α corresponds to a mean reversion

strength with time constant 12 hours.

See Figure 4.5 for a sample path simulated according to Model 1 along with the underlying reversion level.

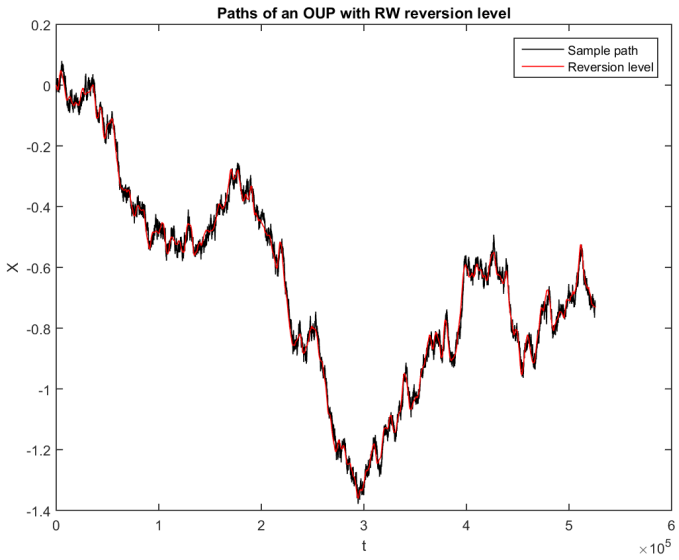

Figure 4.5: Simulated path according to Model 1 with underlying reversion level

Model 2

For Model 2 we simulated a Wiener process intended to represent one year's worth of log NERs, where NERs follow a geometric Brownian motion.

This was done by generating $(n-1) = 60 \times 24 \times 365$ i.i.d. random values N_i with $N_i \sim N(0,1)$ for $1 \leq i \leq (n-1)$ and then computing $X_i = 0.005 \times \sum_{j=1}^{i} N_j$ for $1 \leq i \leq (n-1)$ so that $\{X_i\}_{0 \leq i \leq n-1}$ with $X_0 = 0$ was the simulated series representing one year's worth of hourly logarithmic nominal exchange rates starting at 0. See Figure 4.6 for a sample path of the simulated Model 2.

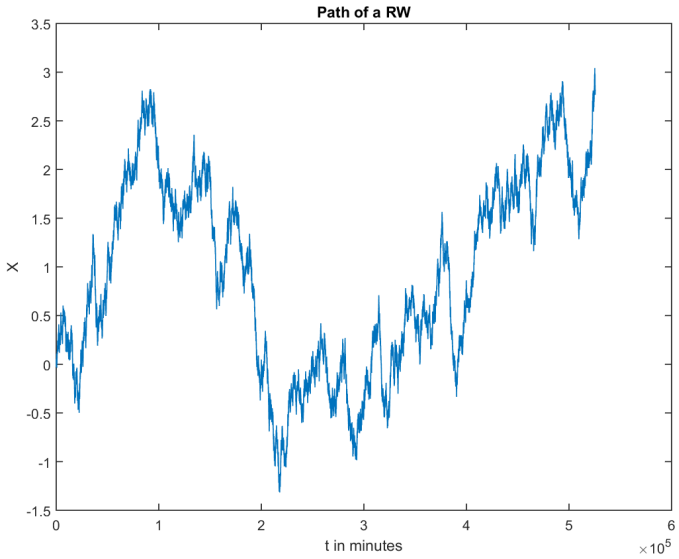

Figure 4.6: Simulated path of Model 2

Standard OUP

Additionally, for comparison, we simulated a standard OU process with $\Delta t = 60 \times 60 \times 24$, $T = 60 \times 60 \times 24 \times 365 \times 20{,}000$ with parameters $\alpha = \frac{1}{60 \times 60 \times 24 \times 365}$, $\sigma = 10^{-5}$ and $X_0 = \mu = 1$. With time unit 1 second this corresponds to daily observations of an OUP with reversion constant 1 year, observed over 20,000 years, on which to conduct the same analysis as on the detrended models and FX data. We chose such a large observation window so as to have a greater number of data points even for large observation steps, in order to reduce the effect of X_0 on the mean absolute return, and thus better approximate the expected absolute return. Alternatively this could be achieved by producing multiple paths and allowing X_0 to be a random variable.

Detrending

The next step was to detrend the series from Models 1 and 2 as well as the FX data by subtracting a moving average.

For each of these series we generated a range of detrended series $\{X_{i,\mathrm{SMA}(\tau)}\}$ and $\{X_{i,\mathrm{EMA}(\tau)}\}$ by subtracting the τ-period SMA $\{\overline{X}_{i,\mathrm{SMA}(\tau)}\}$ and the τ-period EMA $\{\overline{X}_{i,\mathrm{EMA}(\tau)}\}$ respectively, where τ is the detrending time constant divided by Δt. For the series $\{X_i\}_{1 \leq i \leq n}$, we computed $\{\overline{X}_{i,\mathrm{SMA}(\tau)}\}$ as

$$\overline{X}_{i,\mathrm{SMA}(\tau)} = \frac{1}{\tau} \sum_{j=1}^{\tau} X_{i-\tau+j} \tag{4.8}$$

for $\tau \leq i \leq n$. Note that $\{\overline{X}_{i,\mathrm{SMA}(\tau)}\}$ is not defined for $i < \tau$, meaning that the detrended series $\{X_{i,\mathrm{SMA}(\tau)}\}$ was also only defined for $i \geq \tau$. Furthermore, note that this is the

lagging SMA, computed only from the data points leading up to the current point in time. We have chosen this over the symmetrical SMA as it is computable in real time and therefore any methods built on the lagging SMA can be applied to analysis or trading strategies done in real time.

We computed the EMA $\{\overline{X}_{i,\mathrm{EMA}(\tau)}\}$ of $\{X_i\}_{1\leq i\leq n}$ as

$$\begin{aligned}\overline{X}_{0,\mathrm{EMA}(\tau)} &= X_0 \\ \overline{X}_{i,\mathrm{EMA}(\tau)} &= \overline{X}_{i-1,\mathrm{EMA}(\tau)} + a_\tau(X_i - \overline{X}_{i-1,\mathrm{EMA}(\tau)})\end{aligned} \tag{4.9}$$

for $1 \leq i \leq n$, where

$$a_\tau = \frac{2}{\tau + 1}. \tag{4.10}$$

We chose to define a_τ in this way as it leads to SMA(τ) and EMA(τ) having the same centre of mass when using the same τ. EMA(τ) of course is only an approximation of the "real" exponentially weighted moving average, as in order to calculate an EMA exactly, $\{X_i\}$ would have to be available infinitely far into the past. However, for larger is, the approximation becomes more accurate. This is why we only use $\{X_{i,\mathrm{EMA}(\tau)}\}$ for $i \geq \tau$ in our later analysis of the data.

From the computed MAs we generated the detrended series $\{X_{i,\mathrm{SMA}(\tau)}\}$ as

$$X_{i,\mathrm{SMA}(\tau)} = X_i - \overline{X}_{i,\mathrm{SMA}(\tau)} \tag{4.11}$$

for $\tau \leq i \leq n$ and $\{X_{i,\mathrm{EMA}(\tau)}\}$ as

$$X_{i,\mathrm{EMA}(\tau)} = X_i - \overline{X}_{i,\mathrm{EMA}(\tau)} \tag{4.12}$$

for $0 \leq i \leq n$.

See Figure 4.7 for the Thomson Reuters daily log FX series CAD/USD with its 100-day and 1000-day EMA, and Figures 4.8 and 4.9 for simulated paths from Model 1 and Model 2, with their 5-day and 50-day EMAs.

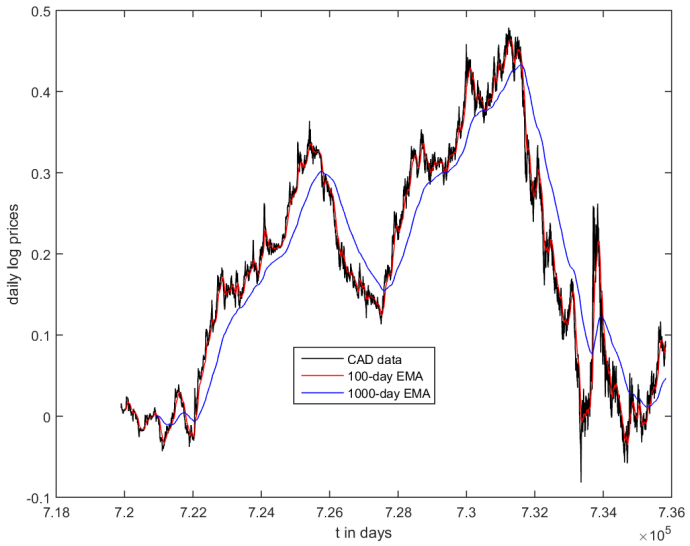

Figure 4.7: Daily Thomson Reuters CAD/USD data with 100-day and 1000-day EMA

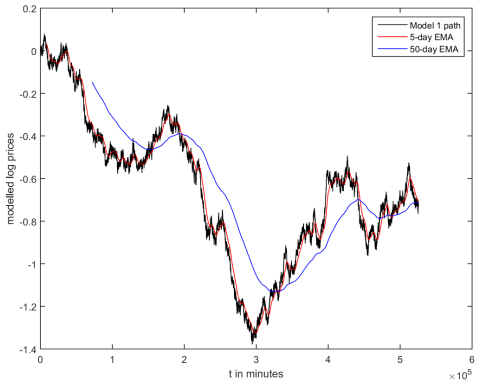

Figure 4.8: Daily simulated Model 1 data with 5-day and 50-day EMA

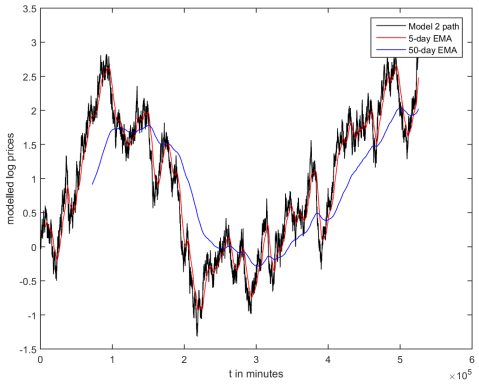

Figure 4.9: Daily simulated Model 2 data with 5-day and 50-day EMA

Log mean absolute returns

For all of the modelled series, as well as the daily Thomson Reuters FX series, all first in their non-detrended and then in several detrended forms, we computed the log mean absolute returns over a range of time intervals.

This was done in the following way: We set $t_0 = \tau_{\max}$ to be the starting point for sampling in all series, where $\tau_{\max}$ is the largest of the time intervals we choose to include in our analysis, as $\{X_{i,\mathrm{SMA}(\tau)}\}$ was only defined for $\tau \leq i$, $\{\overline{X}_{i,\mathrm{EMA}(\tau)}\}$ had a larger approximation error for smaller is, and we wanted the series for all detrending time constants to cover the same date range. For each sampling interval Δt, we then sampled each series at point t_0 and then every Δt-th value to produce $\{X_{i;\Delta t}\}$, as well as $\{X_{i,\mathrm{SMA}(\tau);\Delta t}\}$ and $\{X_{i,\mathrm{EMA}(\tau);\Delta t}\}$ for a range of τs and for each of these series we then found the logarithm

$\log \overline{|\Delta x|}_{\Delta t}$ of the mean of all absolute increments. Finally, we fitted a curve of the shape of Eq. 4.3, i.e. the dependence of the expected absolute return of an OUP on the time interval over which it is measured, to the dependence of $\log \overline{|\Delta x|}_{\Delta t}$ on $\log \Delta t$ and found the coefficient of determination R^2.

See Figure 4.10 for a graph of the log MARs as a function of the log time intervals for the daily Thomson Reuters CAD/USD series after subtracting a 100-day SMA. See Figures 4.11 and 4.12 for the same graph for Models 1 and 2, after subtracting a 5-day SMA.

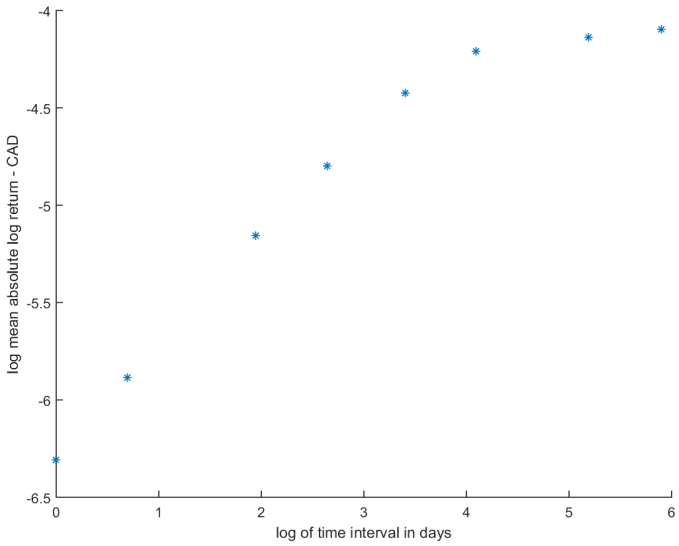

Figure 4.10: Scaling for daily Thomson Reuters CAD/USD data after subtracting 100-day SMA

The coefficient of determination for the fit of the values in Figure 4.10 to the shape of the MAR of an OUP was $R^2 = 0.9856$.

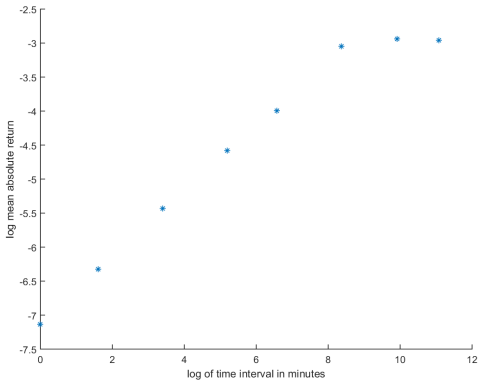

Figure 4.11: Scaling for daily simulated OUP around Wiener process after subtracting 5-day SMA (Model 1)

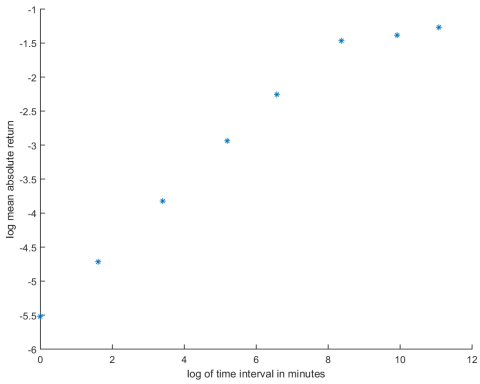

Figure 4.12: Scaling for daily simulated Wiener process after subtracting 5-day SMA (Model 2)

The coefficients of determination for the fit of the log mean absolute returns of Models 1 and 2 after detrending using a 2-day SMA as a function of the time interval over which they are measured to the shape of the MAR of an OUP were $R^2 = 0.9964$ and $R^2 = 0.9879$ respectively.

Additionally, for the non-detrended simulated series, we conducted a line fit using simple linear regression to the relationship between $\log \Delta t$ and $\log \overline{|\Delta x|}_{\Delta t}$ like we did for the real-world FX data in Section 4.2. See Figures 4.13 and 4.14 for the dependence of the log mean absolute returns in the non-detrended series of both models on the logarithm of the time interval over which they are measured.

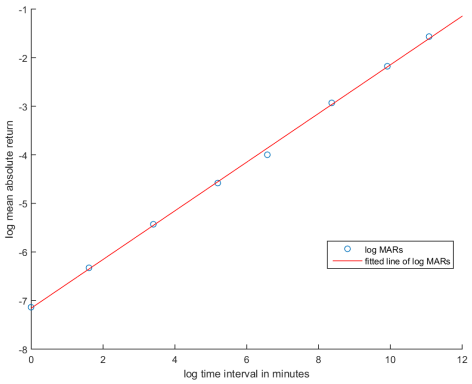

Figure 4.13: Standard scaling in simulated Model 1

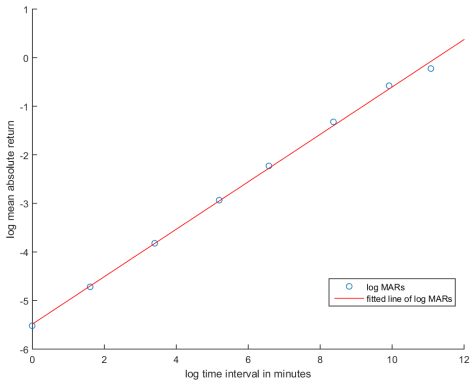

Figure 4.14: Standard scaling in simulated Model 2

The correlation coefficients for Figures 4.13 and 4.14 were $R = 0.9988$ and $R = 0.9994$ and the scaling exponents were $E = 0.5102$ and $E = 0.4869$ respectively.

Finally, we produced a plot of the log mean absolute return of the simulated standard OUP to compare against the behaviour of the same quantity in the detrended series. See Figure 4.15 for the log mean absolute returns measured in a simulated standard OUP with parameters $X_0 = \mu = 1$, $\alpha = \frac{1}{60\times60\times24\times365}$, $\Delta t = 60 \times 60 \times 24$, $\sigma = 10^{-5}$, and $n = 365 \times 20{,}000$ simulated values over different time intervals, along with the expected absolute return as $\Delta t \to \infty$ in red.

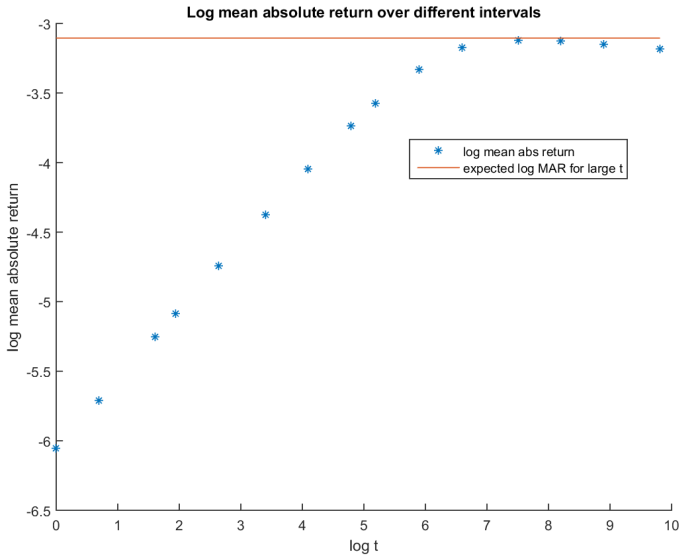

Figure 4.15: MAR for simulated standard OUP

The time intervals we analysed were the equivalent of 1, 5 and 30 minutes, 3 and 12 hours and 3, 14 and 45 days for Models 1 and 2. They were 1, 2, 7, 14, 30, 60, 180 and 365 days for the FX data, and the equivalent of 1, 2, 5, 7, 14, 30, 60, 120, 180 days and 1, 2, 5, 10, 20 and 50 years for the simulated standard OUP.

4.3.2 Results

We found that both models in their non-detrended form produced a linear relationship between $\log \Delta t$ and $\log \overline{|\Delta x|}_{\Delta t}$, mimicking the relationship found in the real-world data sets.

However, for both simulated data sets, as expected, the expected scaling exponent appeared to be around 0.5. This is unlike the scaling exponent found in FX data, which is found to be systematically larger. For the detrended series we found a good fit of the shape of log MARs to the dependence of expected absolute returns of the OUP on the time intervals over which they are measured, with what looked like a limiting of $\log \overline{|\Delta x|}_{\Delta t}$ to a constant value for larger $\log \Delta t$, with this constant depending on the τ used in the detrending method of the data.

See Figures 4.16–4.18 for graphs of the dependence of the log MARs on $\log \Delta t$ in daily log CAD/USD data as well as in the sample paths from Models 1 and 2 before detrending, and after subtracting different MAs.

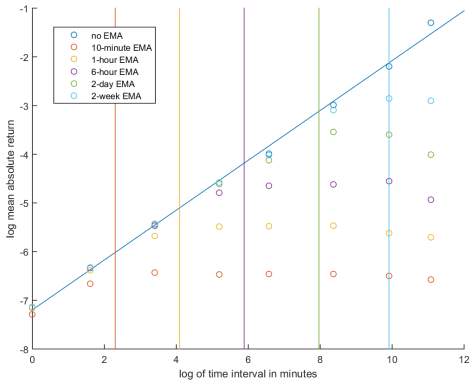

Figure 4.17: MARs for simulated path of Model 1 before and after subtracting different MAs

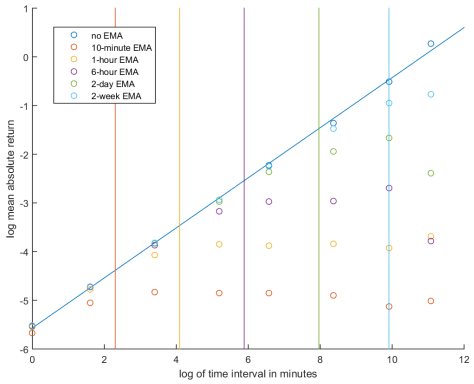

Figure 4.18: MARs for simulated path of Model 2 before and after subtracting different MAs

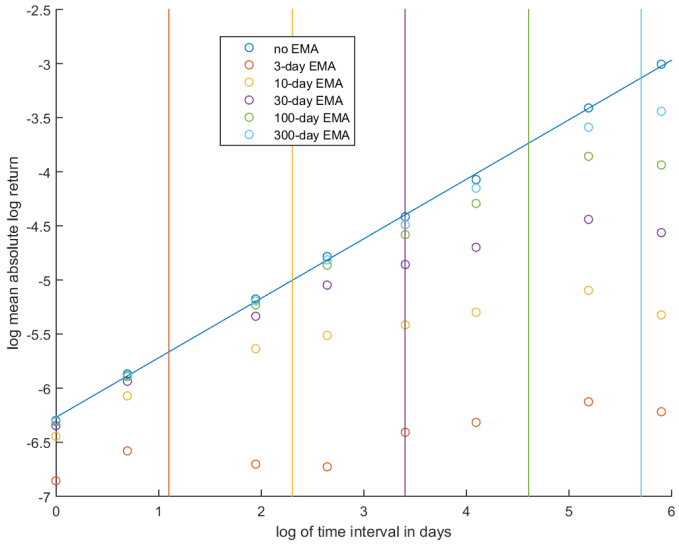

Figure 4.16: MARs for CAD/USD before and after subtracting different MAs

The shape of $\log \overline{|\Delta x|}_{\Delta t}$ as a function of $\log \Delta t$ for the detrended series from Model 1, like that for detrended FX data, appears to mimic that found in a series following an OU process, however without any additional knowledge it appears impossible to determine purely from the series itself the detrending method that, when applied to Model 1, causes the shape of $\log \overline{|\Delta x|}_{\Delta t}$ as a function of $\log \Delta t$ to most closely match the true underlying OUP. Additionally, as seen in Model 2, Brownian motion, too, displays this behaviour, rendering our results inconclusive.

4.4 Discussion

We shall now discuss the results of Part 1 of our research in more detail.

The scaling law

We have observed Müller et al.'s [82] scaling law in our data, and with a widened range of intervals. With scaling exponents of about 0.56 for the Thomson Reuters data and 0.58 for the Commerzbank data, and correlation coefficients of 0.995 and larger, our results are in line with those previously reported in the literature, and equally convincing. This adds to the existing evidence in the literature of this scaling law holding, but more importantly, expands our knowledge of the range in which we know the law to be true. Therefore, while we still cannot say, and may never be able to say, whether the law holds for indefinitely large time intervals, we can confirm that, based on the empirical evidence, this is still currently the indication. While we will never have access to FX data spanning an infinite range of time, this range will of course increase, and may one day show evidence of a flattening of the log mean absolute log returns as a function of log time intervals. So far, however, there is no way of saying whether there is a very slow mean reversion at work in the logarithmic nominal exchange rates, since, as we have shown, the scaling law approximates the behaviour of log mean absolute log returns as a function of log time intervals as found in an OUP for smaller intervals.

For now, while it would be possible to analyse larger intervals than the ones we did, this leads to fewer data points being available, or a larger overlap in the intervals becoming necessary, and there is therefore a trade-off between the novelty and the reliability of the results which can be achieved.

An alternative approach may be to conduct an inter-pair analysis, where in lieu of more consecutive increments from one currency pair, we instead look for a pattern of an overall reduction in volatility as measured over larger time intervals, although this would have various disadvantages, including the fact that currency rates of course are not independent of each other, and therefore any effect seen across currency pairs may be due to the same random cause rather than a statistical property of exchange rates. Alternatively, it may be possible to use a different fitting method to see if the dependence of the log mean absolute log returns on the log time intervals is better described by a very slightly concave slope than by a straight line, however in this case we run the risk of overfitting.

Other things to be considered are that, as noted by Müller et al. [82], the linear regression conducted on our data points is an approximation due to the dependence of larger increments on smaller ones, as well as some optional adjustments that could be made to our method. For example, the same analysis could be conducted with an alternative definition of the mid price. Additionally for the Thomson Reuters data an alternative would be to fit separate line segments to those intervals covering different date ranges. Also, for homogeneity purposes it may be preferable to use the same overlap on all intervals. However, we observed high correlation coefficients nonetheless, and therefore adjusting these methods may not achieve significantly stronger results.

There is a question of whether it may be possible to avoid interpolation altogether, and instead use a method such as binning all intervals in a certain range and applying a

linear regression to this instead, or even sampling the increment from each raw log data point to all other ones along with the time increment individually, and then conducting a statistical analysis of dependence on this whole set, although the computational cost of this would be large.

Mean absolute returns in detrended data

We have shown that an Ornstein–Uhlenbeck process with a Brownian motion reversion level displays the same scaling behaviour as that found in the real-world data. However, like the geometric Brownian motion model, which also follows this scaling law, this model leads to a scaling exponent of 0.5, while the scaling exponents found in foreign exchange rates, as mentioned above, are systematically larger than this. Therefore both of our models are simplifications, and a better fit might be achieved with a fractal Brownian motion, and an even more complex model would be needed to incorporate the multi-scaling behaviour of FX rates. Both the detrended log FX data and the detrended simulated data following an OUP with Brownian motion reversion level displayed a dependence of log mean absolute returns on log time intervals that mimicked that found in standard Ornstein–Uhlenbeck processes. However, it is not clear how to determine the optimal moving average to use for detrending in order to retrieve the OUP from the simulated path of Model 1.

Furthermore, the data simulated according to Model 2, too, displays this behaviour after detrending, ultimately rendering our results inconclusive, since this model does not contain a mean "reversion" as such, and instead the distribution of the fluctuation of the detrended value around the MA is purely an artifact of the detrending method. A mean reversion test, such as the Dickey–Fuller test, applied to the detrended series of Model 1 and Model 2 may shed light on whether it is possible to distinguish between a mean reverting series and a "detrended" random walk.

The effect that different choices of MA have on the shape of the curve may also be explored further, and differently weighted MAs, such as a symmetrical SMA might be tried to more accurately approximate the reversion level.

We may conclude that a different way of interpreting these results is that the underlying trend, if existent, is as much a vital part of the self-similarity of FX rate time series as the rates' fluctuations around this trend.

Chapter 5

OUP parameter estimation under various conditions

In this chapter we focus on OUP parameter estimation in order to better understand the reliability of our estimators, as well as to gain some insight into parameter estimation of OUPs with time-dependent reversion level. We test parameter estimation methods on simulated processes with a variety of parameters and constant and time-dependent reversion levels under a variety of conditions and propose a new method for estimating the parameters of an OUP with unknown time-dependent reversion level.

5.1 Research question

As we presented in Section 2.3.4, there is much literature on the various parameter estimation methods that may be applied to various forms of the OUP. Many of these are used to allow for the parameter estimation of generalizations and variations of the OUP, but even for the standard OUP following Eq. 2.7 parameter estimation is not straightforward. This is due to the bias of the estimators for finite samples of the process, and many of the techniques that may reduce some of this bias lead to a larger variance of the estimator, as seen in the jackknife technique [47], require observation of multiple paths, a priori knowledge of some of the properties of the process, or come at a computational cost.

Additionally, in this thesis, as is the case with most real-world applications, we are dealing with imperfect data, meaning in our case that our data is not only observed discretely, but also at irregular intervals, and contains some substantial gaps in the observations for market closing times and sometimes due to technical issues. This means that we cannot directly infer the reliability of our calibration methods from papers such as that by Tang and Chen [46], which gives expansions for the expected values and variances of the estimators, but is based on discrete but regular observations over an observation window tending to infinity.

Secondly, in this thesis we model OUPs with time-dependent reversion level, as in Eq. 2.42. While it is a common problem to estimate the parameters of such processes based

on an external knowledge of the reversion level, such as in the Hull–White model, there are very few papers dedicated to the parameter estimation where the reversion level is unknown. One method that has been proposed is that by Sanchez et al. [75]. However while their method is intended for a class of processes including the OUP with time-dependent reversion level, they do not test it on an OUP and to the best of our knowledge no study of the performance of this method on an OUP has been published.

In this chapter we therefore aim to do two things: Firstly, we will conduct a detailed numerical exploration of the parameter estimation accuracy of the standard OUP with finite samples and imperfect observations. By simulating an OUP and then applying standard parameter estimation techniques to the generated data, we test the parameter estimation accuracy for a range of process parameters, observation frequencies and observation windows, before exploring the effect of gaps and irregularity in the observations in the same way. We then explore the parameter estimation of the OU process with time-dependent reversion level by simulating such a process and testing Sanchez et al.'s [75] calibration method against an alternative proposed by us.

5.2 Standard OUP estimation

In Section 2.3 we presented the standard estimation methods of the standard OUP observed at regular discrete intervals. Throughout this section we will be using the maximum likelihood method as described in Section 2.3.1 to explore the effect that different process parameters and observation frequencies and windows have on the parameter estimation of a discretely but regularly observed simulated OUP. It has already been shown that the bias of the reversion strength estimator in particular increases for smaller reversion strengths, while a larger observation window reduces the bias [46]. In this section, we test these and other properties of the estimators numerically, as a basis for our further analysis in the following sections.

5.2.1 Methodology

We simulated several paths for each process for a range of parameters, simulation frequencies, observation frequencies and observation windows, giving us discrete regular observations of a standard OUP following Eq. 2.7. To each of these we then applied the standard maximum likelihood estimation method as described in Section 2.3.1. We chose parameters α and σ in the ranges observed in the financial world (when assuming seconds as our unit of time) and simulated in the literature [46, 47, 75]. In particular, this meant we worked with a near-unit-root situation. From our default parameters we then varied one value at a time to find the effect of this on the accuracy of the estimators of the reversion level μ, reversion strength α, and diffusion coefficient σ. The reversion level μ and the starting value X_0 remained the same throughout the simulations. For the parameters we tested, this meant that we were mostly examining the non-stationary part of the process.

We determined the mean square error (MSE) as well as the mean error (ME), which is an estimator of the bias, of the estimators $\hat{\alpha}$, $\hat{\sigma}$ and $\hat{\mu}$ for each parameter configuration over the simulated paths.

Effect of reversion strength

We first explored the effect of the reversion strength parameter on the ME and MSE of the estimators. We explored this by simulating a standard OUP as described in Section 3.4 for the process parameters $\sigma = 10^{-5}$, $X_0 = 0.5$ and $\mu = 1$, with an observation step of $\Delta t = 60 \times 60$ over an observation period of $T = 60 \times 60 \times 24 \times 365 \times 5$. With time unit 1 second, this would correspond to hourly observations of a process over 5 years. Of course the individual values of reversion level and starting value are irrelevant to the outcomes of the study and purely a cosmetic choice, since any results are only affected by the magnitude of the initial displacement. We varied α in the range $10^{-9} \leq \alpha \leq 6.5 \times 10^{-8}$, corresponding to a reversion time constant ranging roughly from 180 days to 30 years, which contains the reversion time constants found in real exchange rates, and found the MEs and MSEs of the three parameters over 1000 paths for each value of α. While a larger number of paths would lead to a smoothing of our results, this number enabled us to vary the observation period and observation step in most later simulations while keeping the number of paths constant for comparison purposes. We simulated the process at the observation rate since we used the exact discretization method, as described in Section 2.2.3. See Figure 5.1 for a graph of the arithmetic mean taken over all paths of the errors $\hat{\alpha} - \alpha$ of $\hat{\alpha}$ as a function of α.

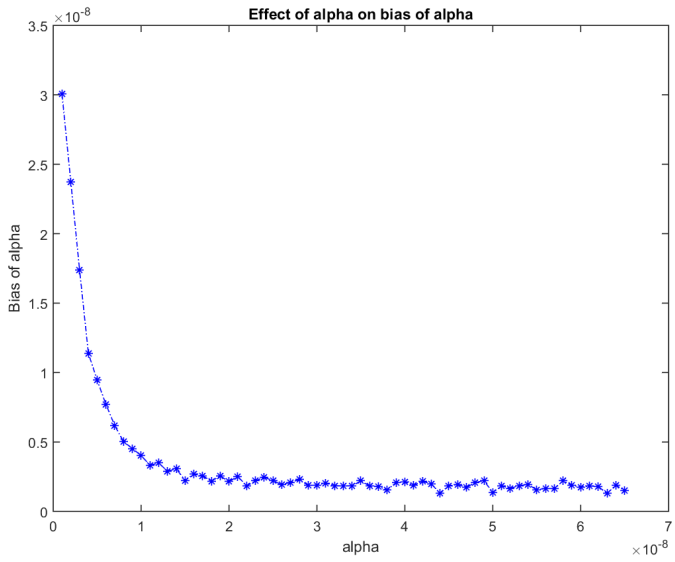

Figure 5.1: Mean error of $\hat{\alpha}$ as a function of α in a standard OUP

The MSEs and mean errors for all parameter estimators for a selection of the values of α tested are presented in Table 5.1. As described in the literature [46], we found the

estimator of the reversion strength parameter to be positively biased, with the bias being larger in the near-unit-root case and tending to zero for larger αs. We found that, as is to be expected, a small α leads to a large variability in $\hat{\mu}$, as $\hat{\alpha}$ is more heavily biased and as the unconditional variance of the process increases. We found that α had no significant effect on $\hat{\sigma}$ in the ranges we observed.

α	MSE($\hat{\mu}$)	MSE($\hat{\alpha}$)	MSE($\hat{\sigma}$)	ME($\hat{\mu}$)	ME($\hat{\alpha}$)	ME($\hat{\sigma}$)
1.00E-09	2.04497	1.63E-15	1.19E-15	-0.37933	3.01E-08	1.16E-09
6.00E-09	39.65148	2.19E-16	1.07E-15	0.07869	7.71E-09	-2.51E-10
1.10E-08	12.11843	6.82E-17	1.19E-15	-0.08140	3.33E-09	4.81E-10
1.60E-08	0.00956	4.95E-17	1.18E-15	-0.00192	2.68E-09	-6.53E-10
2.10E-08	0.00410	5.26E-17	1.13E-15	-0.00092	2.52E-09	-7.91E-10
2.60E-08	0.00180	4.61E-17	1.13E-15	-0.00019	1.93E-09	-1.17E-09
3.10E-08	0.00105	4.73E-17	1.19E-15	-0.00125	2.04E-09	1.80E-10
3.60E-08	0.00070	4.71E-17	1.20E-15	-0.00123	1.83E-09	-5.58E-10
4.10E-08	0.00054	5.16E-17	1.23E-15	-0.00073	1.87E-09	-1.15E-09
4.60E-08	0.00044	5.29E-17	1.07E-15	-0.00100	1.93E-09	-1.63E-09
5.10E-08	0.00031	6.05E-17	1.15E-15	-0.00040	1.84E-09	-3.71E-10
5.60E-08	0.00024	6.27E-17	1.18E-15	-0.00050	1.66E-09	-8.96E-10
6.10E-08	0.00021	6.36E-17	1.16E-15	-0.00046	1.83E-09	1.72E-09

Table 5.1: Mean errors and MSEs of estimators for varying αs in a standard OUP with μ = 1, σ = 1.00E-05, $X_0 = 0.5$, Δt_{sim} = 3,600, Δt_{obs} = 3,600, n_{obs} = 43,801, 1,000 paths

Effect of observation period

We next explored the effect of the size of the observation period on the ME and MSE of the estimators. For this purpose we simulated a standard OUP with process parameters $\sigma = 10^{-5}$, $X_0 = 0.5$, $\mu = 1$, and $\alpha = \frac{1}{60\times60\times24\times365\times5}$, corresponding to a reversion time constant of 5 years for a time unit of 1 second, with an observation step of $\Delta t = 60\times60$. We varied the observation window in the range $60\times60\times24\times365 \leq T \leq 60\times60\times24\times365\times30$, corresponding to a period between 1 and 30 years, which is a similar range to that of the time periods spanned by our data sets. Note that by varying T we also varied the number of observed points of the process, keeping the size of the observation step constant. For each value of T we generated 1000 paths, over which we computed the ME and MSE of the three estimators.

See Figure 5.2 for the bias of $\hat{\alpha}$ as a function of T.

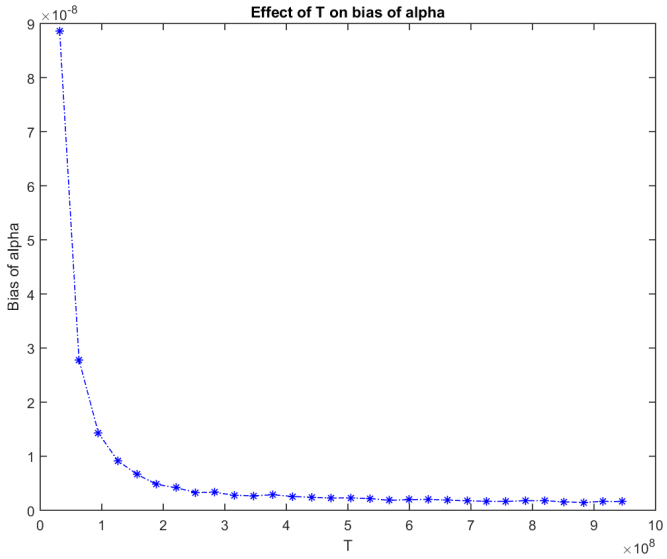

Figure 5.2: Mean error of $\hat{\alpha}$ as a function of T in a standard OUP

See Table 5.2 for the MSEs and mean errors of all parameter estimators for some of the values of T tested. Our results were consistent with the literature, finding the mean error of $\hat{\alpha}$ to tend to zero for large Ts, while we observe a positive mean error of $\hat{\alpha}$ of nearly 1400% for our smallest observation period. While we observe no significant bias of $\hat{\sigma}$ in the parameter ranges examined, we observe that T has a similar effect on the MSE of $\hat{\sigma}$ as on the mean error of $\hat{\alpha}$, with the MSE decreasing for larger observation periods and growing steeply as $T \to 0$, albeit with the errors observed in $\hat{\sigma}$ being of a much smaller order. We observe a great variability in $\hat{\mu}$ for smaller observation periods, which is related to the large bias of $\hat{\alpha}$ and may also be due to the fact that some of the observation periods tested are smaller than the reversion time constant.

T	MSE($\hat{\mu}$)	MSE($\hat{\alpha}$)	MSE($\hat{\sigma}$)	ME($\hat{\mu}$)	ME($\hat{\alpha}$)	ME($\hat{\sigma}$)
31,536,000	9.63409	2.06E-14	5.79E-15	-0.24287	8.86E-08	-2.95E-09
189,216,000	47.03482	1.04E-16	9.04E-16	0.17295	4.80E-09	2.98E-10
346,896,000	1.19102	3.01E-17	5.26E-16	0.04080	2.69E-09	4.93E-10
504,576,000	6.61115	2.19E-17	3.58E-16	-0.08339	2.29E-09	-1.18E-10
662,256,000	0.01088	1.48E-17	2.55E-16	0.00236	1.89E-09	-5.52E-10
819,936,000	0.00484	1.22E-17	2.24E-16	-0.00616	1.78E-09	1.80E-10

Table 5.2: Mean errors and MSEs of estimators for varying Ts in a standard OUP with μ = 1, σ = 1.00E-05, α = 6.34E-09, $X_0 = 0.5$, Δt_{sim} = 3,600, Δt_{obs} = 3,600, 1,000 paths

Effect of observation step

We next tested the effect that the sampling rate would have on the parameter estimation by varying Δt. In doing so, we also varied the number of observed points of the process. This was done by simulating the process hourly, with the fixed parameters being $\sigma = 10^{-5}$, $X_0 = 0.5$, $\mu = 1$, $T = 60 \times 60 \times 24 \times 365 \times 5$ and $\alpha = \frac{1}{60 \times 60 \times 24 \times 365 \times 5}$. We varied our

observation step in the range $60 \times 60 \leq \Delta t \leq 60 \times 60 \times 48$, simulating a new set of 1000 sample paths for each size of observation step. By keeping the observation period constant, we reduced the number of observed points by increasing the observation step. In the ranges we tested there seemed to be no discernible bias of $\hat{\mu}$, with a large variability in the estimator.

See Figure 5.3 for a graph of the MSE of $\hat{\sigma}$ as a function of Δt.

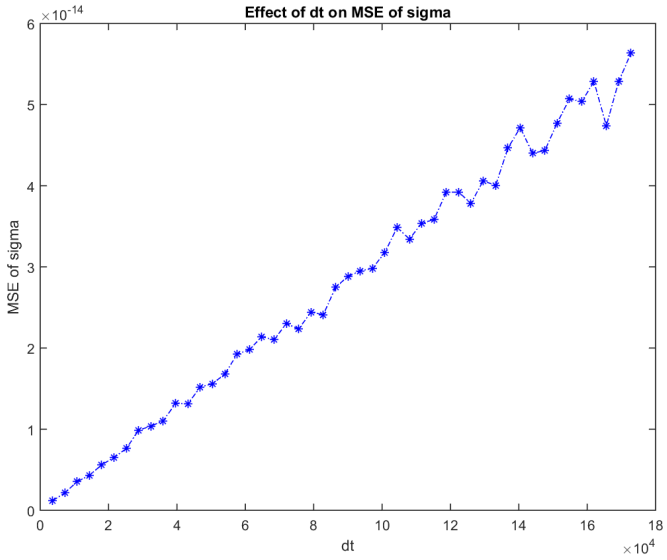

Figure 5.3: MSE of $\hat{\sigma}$ as a function of Δt in a standard OUP

In Table 5.3 we present the effect that the observation step had on the estimators by giving the MSE and mean errors for a selection of Δts. We found no significant effect of Δt on the ME or MSE of $\hat{\alpha}$ in the ranges we tested, but we found what looks like a very strong positive linear relationship between the size of Δt and the MSE of $\hat{\sigma}$. Again, this is to be expected as the number of observed points decreases.

n_{obs}	Δt_{obs}	MSE($\hat{\mu}$)	MSE($\hat{\alpha}$)	MSE($\hat{\sigma}$)	ME($\hat{\mu}$)	ME($\hat{\alpha}$)	ME($\hat{\sigma}$)
43,801	3,600	29.74	1.64E-16	1.19E-15	-0.05777	6.12E-09	8.91E-10
8,760	18,000	7969.22	1.56E-16	5.62E-15	-3.03377	6.74E-09	1.22E-10
4,867	32,400	112.24	1.79E-16	1.04E-14	-0.11581	7.06E-09	-6.13E-09
3,369	46,800	10.97	1.60E-16	1.52E-14	-0.17916	6.32E-09	-2.53E-11
2,577	61,200	12.24	1.84E-16	1.98E-14	-0.26120	6.82E-09	-1.20E-08
2,086	75,600	11.56	1.87E-16	2.23E-14	-0.24003	7.18E-09	-6.77E-10
1,752	90,000	25.34	1.89E-16	2.88E-14	0.08619	6.85E-09	-1.69E-08
1,510	104,400	1017.76	1.88E-16	3.49E-14	1.07145	6.71E-09	-1.14E-08
1,327	118,800	104.06	1.60E-16	3.92E-14	-0.14963	6.37E-09	-6.28E-09
1,184	133,200	864.54	1.75E-16	4.00E-14	-0.83052	6.63E-09	-6.66E-09
1,068	147,600	1410.49	1.64E-16	4.43E-14	1.14115	6.51E-09	-1.00E-08
973	162,000	14.97	1.66E-16	5.28E-14	-0.17288	6.56E-09	-2.92E-09

Table 5.3: Mean errors and MSEs of estimators for varying Δts in a standard OUP. $\mu = 1$, $\sigma =$ 1.00E-05, $\alpha =$ 6.34E-09, $X_0 = 0.5$, $\Delta t_{\text{sim}} =$ 3,600, 1,000 paths.

Effect of diffusion coefficient

Finally, we tested the effect of σ on the parameter estimation accuracy of the standard OUP. We tested this on an OUP with parameters $X_0 = 0.5$, $\mu = 1$, $T = 60{\times}60{\times}24{\times}365{\times}5$, $\Delta t = 60 \times 60$ and $\alpha = \frac{1}{60{\times}60{\times}24{\times}365}$, varying σ in the range $10^{-7} \leq \sigma \leq 0.99 \times 10^{-5}$. We produced 1000 paths for each set of parameters. Note that we employed a larger α in our simulation than we did for testing the other three parameters, so as to allow us to observe the effect of σ more clearly. See Figure 5.4 for a graph of the MSE of $\hat{\mu}$ as a function of σ.

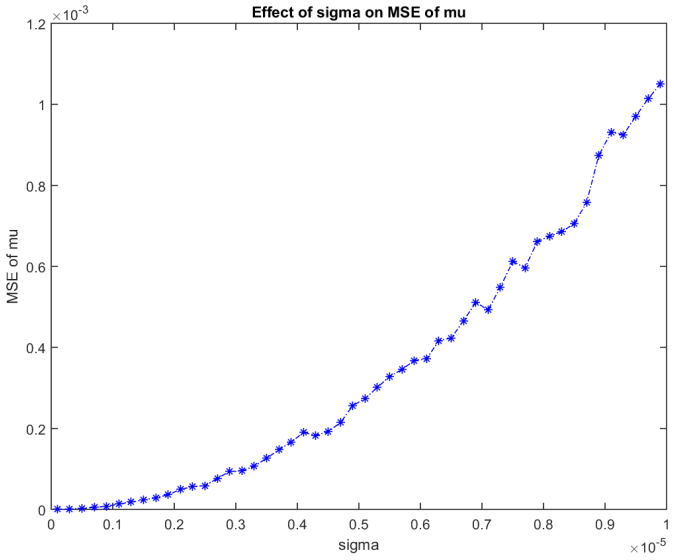

Figure 5.4: MSE of $\hat{\mu}$ as a function of σ in a standard OUP

The MEs and MSEs of all estimators for a selection of values of σ is presented in Table 5.4. As is to be expected, we found a very clear increase in the MSEs of all estimators for larger σs. Additionally, we found a significant increase in the positive mean error of $\hat{\alpha}$ as σ increased.

σ	MSE($\hat{\mu}$)	MSE($\hat{\alpha}$)	MSE($\hat{\sigma}$)	ME($\hat{\mu}$)	ME($\hat{\alpha}$)	ME($\hat{\sigma}$)
1.00E-07	1.05E-07	4.58E-21	1.19E-19	0.00002	-4.15E-12	9.01E-12
1.10E-06	1.32E-05	5.18E-19	1.29E-17	-0.00015	4.23E-11	-3.74E-11
2.10E-06	4.93E-05	1.85E-18	5.24E-17	0.00011	6.38E-11	9.22E-11
3.10E-06	9.49E-05	3.93E-18	1.14E-16	-0.00069	2.22E-10	-2.12E-10
4.10E-06	1.90E-04	8.09E-18	1.89E-16	-0.00037	4.07E-10	-3.36E-10
5.10E-06	2.74E-04	1.13E-17	2.93E-16	0.00021	4.32E-10	-6.09E-10
6.10E-06	3.72E-04	1.64E-17	4.44E-16	-0.00040	7.91E-10	9.81E-11
7.10E-06	4.93E-04	2.18E-17	6.04E-16	-0.00070	9.64E-10	-4.06E-10
8.10E-06	6.75E-04	3.01E-17	8.08E-16	-0.00066	1.33E-09	-9.40E-10
9.10E-06	9.31E-04	3.78E-17	8.85E-16	-0.00149	1.77E-09	-1.49E-09

Table 5.4: Mean errors and MSEs of estimators for varying σs in a standard OUP with μ = 1, α = 3.17E-08, $X_0 = 0.5$, Δt_{sim} = 3,600, Δt_{obs} = 3,600, n_{obs} = 43,801, 1,000 paths

5.2.2 Results

We have observed a positive bias of $\hat{\alpha}$, which is reduced by an increase in α and by an increase in T. Similarly, the MSE of $\hat{\mu}$ is much larger for smaller α and T. The MSE of $\hat{\sigma}$ is much smaller than that of $\hat{\alpha}$ and $\hat{\mu}$, but increases for smaller T and for larger Δt. Finally, and not surprisingly, an increase in σ leads to an increase in the MSEs of all estimators. These results are in line with what has been reported in the literature.

5.3 Effect of gaps in the data

The next step was to explore the effect of gaps in the data on estimation accuracy. For simplicity, we simulated 5 years' worth of hourly data with gaps for weekends but not nights.

5.3.1 Methodology

In order to test for the effect of gaps in the data on estimation accuracy, we again simulated multiple paths each for a number of parameter sets. Each path was then analysed in three ways: As a benchmark, our standard estimation method was applied to the full path. Then, we inserted gaps into the simulated paths to represent weekends, producing incomplete paths. Each incomplete path was then analysed in two ways: First, we used linear interpolation to "fix" the gaps in the data, and conducted parameter estimation on these interpolated series. Second, we applied our estimation method to the incomplete paths as if they were spanning a shorter period of time, where the last value before the "weekend" was directly followed by the first value after the "weekend", with no "time" passing during periods without observations, thus mimicking a "business time scale".

Based on our real-world data sets, we chose to simulate 1000 paths of a standard OUP with parameters $\sigma = 10^{-5}$, $X_0 = 0.5$, $\mu = 1$, $\Delta t = 60 \times 60$, $T = 60 \times 60 \times 24 \times 365 \times 5$ and $\alpha = \frac{1}{60 \times 60 \times 24 \times 365 \times 5}$, which with time unit 1 second would correspond to hourly data spanning 5 years. Into these we then inserted gaps of weekends by removing $\{x_i\}_{i \in W}$, where W is the set of indices of the "weekend values", defined as

$$W = \left\{ wj | 4.5 \times 24 \leq w \leq 7 \times 24 \cap 1 \leq j \leq \left\lfloor \frac{365 \times 5}{7} \right\rfloor \right\}. \tag{5.1}$$

We then estimated the parameters of these incomplete observations in two different ways: First, we treated any periods of time for which we did not have observations as non-existent, thereby analysing the data on what may be interpreted as a "business time scale". (Note that of course this interpretation of incomplete series only applies where data is missing due to the market being closed, rather than for other reasons such as technical errors.) We then generated a second series by replacing the "weekend values" with values found by linear interpolation. We applied our standard parameter estimation to both the interpolated series and the "business time" series. Additionally, we conducted

the parameter estimation on the complete data set, without gaps, as a benchmark.

Each path for each set of parameters was therefore estimated three times, and we computed the mean error and MSE for each of the three methods over all paths, to compare their accuracy. To gain further insight, we varied some of the parameters like we did in Section 5.2, to see how this would affect the three methods.

The parameter sets and sample sizes used to test the three sampling methods were the same as presented in Section 5.2, with the exception of the set-up for testing the methods under varying observation steps. This is because we had to use different observation steps in order to allow for the weekends to be removed. In this case, we therefore simulated the process with simulation step Δt_{sim} 1 minute, and varied the observation steps in the range $60 \leq \Delta t_{\text{obs}} \leq 12 \times 60 \times 60$. For computational reasons, for the minutely simulations we only produced 100 paths for each parameter set. All other parameters tested were the same as in Section 5.2.

5.3.2 Results

See Figure 5.5 for a graph of the mean error of $\hat{\alpha}$ as a function of α in the three different cases. We found that for the parameters examined by us, the reversion strength estimator based on the interpolated series, while following a similar shape, lies consistently below that from the completely observed series. However, the ME and MSE of the reversion strength appears to be less affected by interpolation than it is by the true value of α. The estimator based on the business time, however, appears to have a significantly larger positive bias, with this difference further increasing as α does. In fact, it appears that on the business time, while for small αs the MSE of $\hat{\alpha}$ follows a similar shape to that in the standard case, above a certain value of α, the mean error of $\hat{\alpha}$ appears to grow proportionally with α, while the mean error in the standard observation scenario tends to zero. This difference between the three observation types may be due to the fact that in the non-stationary part of the process, business time leads to regular jumps towards the reversion level, while linear interpolation slows what should be an exponential approach towards the reversion level to a linear one. In particular, a larger reversion strength would lead to business time introducing larger jumps, leading to greater inaccuracy in the estimation in this case.

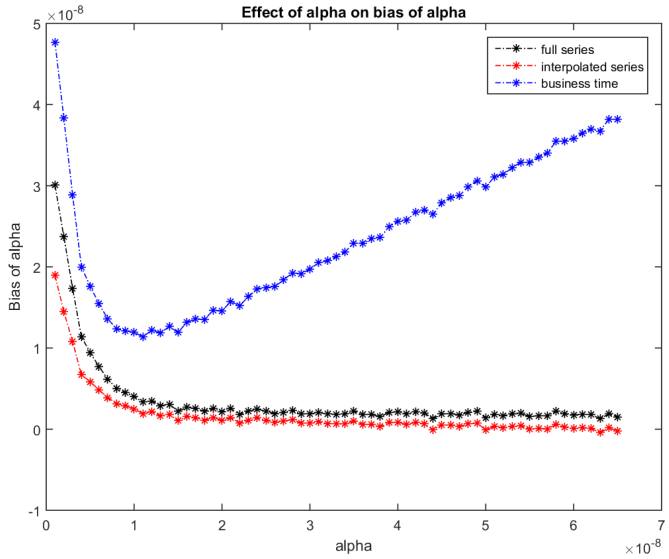

Figure 5.5: Mean error of $\hat{\alpha}$ as a function of α for complete observation, interpolated weekends and business time

The mean errors and MSEs of all estimators for the complete estimation, the interpolated series and the business time series for some of the values of α are presented in Table 5.5. See Appendix B for a more comprehensive table.

α	method	MSE($\hat{\mu}$)	MSE($\hat{\alpha}$)	MSE($\hat{\sigma}$)	ME($\hat{\mu}$)	ME($\hat{\alpha}$)	ME($\hat{\sigma}$)
1.00E-09	stnd	2.04497	1.63E-15	1.19E-15	-0.37933	3.01E-08	1.16E-09
	intp	4,013.27653	7.24E-16	4.05E-12	2.15519	1.90E-08	-2.01E-06
	b-time	4.52535	4.05E-15	6.46E-12	-0.51016	4.77E-08	2.53E-06
1.10E-08	stnd	12.11843	6.82E-17	1.19E-15	-0.08140	3.33E-09	4.81E-10
	intp	30.98837	5.53E-17	4.05E-12	-0.10019	1.93E-09	-2.01E-06
	b-time	416.08171	2.68E-16	6.56E-12	-0.61133	1.14E-08	2.55E-06
2.10E-08	stnd	0.00410	5.26E-17	1.13E-15	-0.00092	2.52E-09	-7.91E-10
	intp	0.00461	4.53E-17	4.05E-12	0.00667	1.43E-09	-2.01E-06
	b-time	0.00411	3.59E-16	6.80E-12	-0.00054	1.57E-08	2.60E-06
3.10E-08	stnd	0.00105	4.73E-17	1.19E-15	-0.00125	2.04E-09	1.80E-10
	intp	0.00109	4.15E-17	4.05E-12	0.00243	8.89E-10	-2.01E-06
	b-time	0.00105	5.24E-16	6.97E-12	-0.00093	2.05E-08	2.63E-06
4.10E-08	stnd	0.00054	5.16E-17	1.23E-15	-0.00073	1.87E-09	-1.15E-09
	intp	0.00055	4.59E-17	4.06E-12	0.00167	5.68E-10	-2.01E-06
	b-time	0.00054	7.77E-16	7.13E-12	-0.00044	2.57E-08	2.66E-06
5.10E-08	stnd	0.00031	6.05E-17	1.15E-15	-0.00040	1.84E-09	-3.71E-10
	intp	0.00032	5.43E-17	4.06E-12	0.00138	3.53E-10	-2.01E-06
	b-time	0.00031	1.10E-15	7.33E-12	-0.00013	3.11E-08	2.70E-06
6.10E-08	stnd	0.00021	6.36E-17	1.16E-15	-0.00046	1.83E-09	1.72E-09
	intp	0.00021	5.72E-17	4.05E-12	0.00095	1.54E-10	-2.01E-06
	b-time	0.00021	1.47E-15	7.54E-12	-0.00021	3.65E-08	2.74E-06

Table 5.5: Mean errors and MSEs of estimators for varying αs in case of observation gaps in a standard OUP with $\mu = 1$, $\sigma =$ 1.00E-05, $X_0 = 0.5$, $\Delta t_{\text{sim}} =$ 3,600, $\Delta t_{\text{obs}} =$ 3,600, $n_{\text{obs}} =$ 43,801, 1,000 paths

See Figure 5.6 for a graph of the MSE of $\hat{\sigma}$ for different observation steps for complete observation, linear interpolation, and business time. We see that like the estimator for the complete series, the MSEs of $\hat{\sigma}$ for the interpolated series and business time, too, increase for larger Δts. The MSEs of the estimators for the interpolated series and the business time series are several orders of magnitude larger than the MSE of the estimator based on the full series, with the error of the business time estimator being about 1.5 times that of the interpolated series in our simulations.

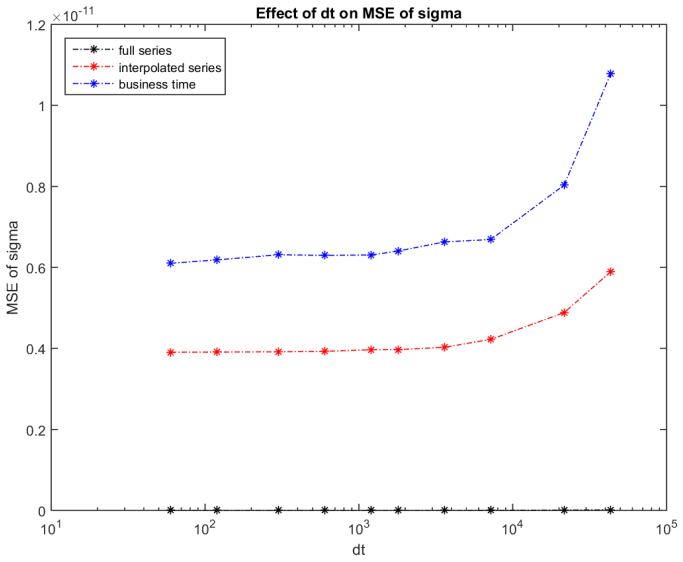

Figure 5.6: MSE of $\hat{\sigma}$ as a function of Δt for complete observation, interpolated weekends and business time

The mean errors and MSEs of all estimators for some of the observation steps in the case of complete observation, interpolation and business time are presented in Table 5.6. See Appendix B for a more comprehensive list.

n_{obs}	Δt_{obs}	method	MSE($\hat{\mu}$)	MSE($\hat{\alpha}$)	MSE($\hat{\sigma}$)	ME($\hat{\mu}$)	ME($\hat{\alpha}$)	ME($\hat{\sigma}$)
2,628,001	60	stnd	37.0273	1.72E-16	2.15E-17	-0.12549	6.98E-09	4.09E-10
		intp	38.1845	1.18E-16	3.91E-12	-0.87597	4.49E-09	-1.98E-06
		b-time	10.0698	4.95E-16	6.10E-12	-0.07397	1.43E-08	2.46E-06
525,600	300	stnd	2.2204	2.30E-16	8.20E-17	0.09888	8.35E-09	3.48E-10
		intp	2.2045	1.40E-16	3.92E-12	-0.28491	5.12E-09	-1.98E-06
		b-time	3.3647	6.62E-16	6.31E-12	0.13648	1.65E-08	2.50E-06
131,400	1,200	stnd	1.7782	2.01E-16	4.12E-16	-0.08256	6.18E-09	-2.55E-09
		intp	2.5683	1.39E-16	3.97E-12	-0.05571	3.47E-09	-1.99E-06
		b-time	2.7938	5.70E-16	6.31E-12	-0.05366	1.32E-08	2.51E-06
43,800	3,600	stnd	1.7117	1.53E-16	1.11E-15	0.06823	5.72E-09	3.36E-09
		intp	14.1926	1.12E-16	4.03E-12	-0.28331	3.39E-09	-2.01E-06
		b-time	2.9223	4.46E-16	6.63E-12	0.13343	1.25E-08	2.57E-06
7,300	21,600	stnd	1.4454	1.82E-16	7.63E-15	-0.25518	7.56E-09	-7.77E-09
		intp	216.3876	1.19E-16	4.88E-12	-1.50011	4.70E-09	-2.21E-06
		b-time	5.4700	6.05E-16	8.03E-12	-0.21633	1.64E-08	2.82E-06

Table 5.6: Mean errors and MSEs of estimators for varying Δts in case of observation gaps in a standard OUP with $\mu = 1$, $\sigma =$ 1.00E-05, $\alpha =$6.34E-09, $X_0 = 0.5$, $\Delta t_{\text{sim}} = 60$, 100 paths

See Figure 5.7 for the mean error of $\hat{\sigma}$ as a function of the observation period for the three different observation types. We see a large positive bias for the business time series, and a large negative bias for the interpolated series, both of which appear to be unaffected by the observation period. This may be explained by the fact that the business time series contain regular jumps, while the interpolated series contain regular periods without noise.

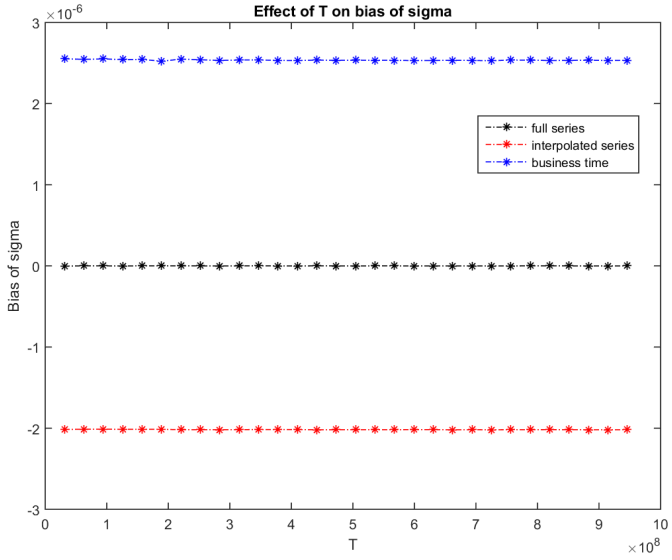

Figure 5.7: Mean error of $\hat{\sigma}$ as a function of T for complete observation, interpolated weekends and business time

The mean errors and MSEs of all estimators for different observation periods in the case of complete observation, interpolation and business time are presented in Table 5.7.

n_{obs}	method	MSE($\hat{\mu}$)	MSE($\hat{\alpha}$)	MSE($\hat{\sigma}$)	ME($\hat{\mu}$)	ME($\hat{\alpha}$)	ME($\hat{\sigma}$)
8,761	stnd	9.63409	2.06E-14	5.79E-15	-0.24287	8.86E-08	-2.95E-09
	intp	4.16409	1.01E-14	4.07E-12	-0.46528	5.58E-08	-2.02E-06
	b-time	3.96658	4.88E-14	6.72E-12	-0.40354	1.39E-07	2.55E-06
52,561	stnd	47.03482	1.04E-16	9.04E-16	0.17295	4.80E-09	2.98E-10
	intp	19.01773	7.63E-17	4.06E-12	0.05097	2.87E-09	-2.01E-06
	b-time	10.03111	3.19E-16	6.4E-12	0.03549	1.11E-08	2.52E-06
96,361	stnd	1.19102	3.01E-17	5.26E-16	0.04080	2.69E-09	4.93E-10
	intp	1.31234	2.17E-17	4.07E-12	0.04572	1.49E-09	-2.02E-06
	b-time	0.52864	1.17E-16	6.46E-12	0.02491	7.80E-09	2.54E-06
140,161	stnd	6.61115	2.19E-17	3.58E-16	-0.08339	2.29E-09	-1.18E-10
	intp	0.11362	1.51E-17	4.08E-12	0.01173	1.22E-09	-2.02E-06
	b-time	4.40744	9.25E-17	6.44E-12	-0.06839	7.18E-09	2.53E-06
183,961	stnd	0.01088	1.48E-17	2.55E-16	0.00236	1.89E-09	-5.52E-10
	intp	0.04703	9.87E-18	4.08E-12	0.02944	8.70E-10	-2.02E-06
	b-time	0.01086	7.06E-17	6.43E-12	0.00239	6.56E-09	2.53E-06
227,761	stnd	0.00484	1.22E-17	2.24E-16	-0.00616	1.78E-09	1.80E-10
	intp	0.00685	7.51E-18	4.07E-12	0.00868	7.18E-10	-2.02E-06
	b-time	0.00484	6.29E-17	6.41E-12	-0.00611	6.39E-09	2.53E-06

Table 5.7: Mean errors and MSEs of estimators for varying Ts in case of observation gaps in a standard OUP with $\mu = 1$, $\sigma =$ 1.00E-05, $\alpha =$ 6.34E-09, $X_0 = 0.5$, $\Delta t_{\text{sim}} =$ 3,600, 1,000 paths

See Figure 5.8 for the MSE of $\hat{\mu}$ as a function of σ for the three different observation types. We see that interpolation leads to an increase in the MSE of $\hat{\mu}$. However, this effect is negligible compared to the effect that σ has on the MSE of the estimator in the parameter ranges tested by us, meaning that process parameters should be taken into account before considering the effects of observation inaccuracies. This is not surprising as we have seen previously that business time leads to an increase and interpolation to a decrease in the mean error of $\hat{\alpha}$, and furthermore we know that inaccuracies of $\hat{\alpha}$ affect the estimation of μ, and that a larger σ leads to an increase in the mean error of $\hat{\alpha}$.

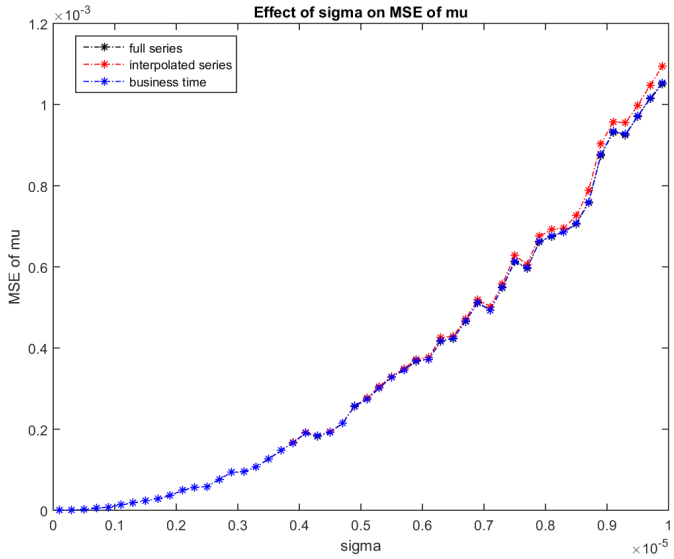

Figure 5.8: MSE of $\hat{\mu}$ as a function of σ for complete observation, interpolated weekends and business time

In Table 5.8 we show the mean errors and MSEs of all estimators for three different observation types for a number of σ values. See Appendix B for a more comprehensive table.

σ	method	MSE($\hat{\mu}$)	MSE($\hat{\alpha}$)	MSE($\hat{\sigma}$)	ME($\hat{\mu}$)	ME($\hat{\alpha}$)	ME($\hat{\sigma}$)
1.00E-07	stnd	1.05E-07	4.58E-21	1.19E-19	0.00002	-4.15E-12	9.01E-12
	intp	1.05E-07	4.58E-21	4.05E-16	0.00002	-4.41E-12	-2.01E-08
	b-time	2.43E-07	3.14E-16	2.75E-12	0.00037	1.77E-08	1.66E-06
1.10E-06	stnd	1.32E-05	5.18E-19	1.29E-17	-0.00015	4.23E-11	-3.74E-11
	intp	1.32E-05	5.17E-19	4.90E-14	-0.00010	2.77E-11	-2.21E-07
	b-time	1.32E-05	3.18E-16	1.28E-12	0.00020	1.78E-08	1.13E-06
3.10E-06	stnd	9.49E-05	3.93E-18	1.14E-16	-0.00069	2.22E-10	-2.12E-10
	intp	9.49E-05	3.87E-18	3.90E-13	-0.00034	1.07E-10	-6.24E-07
	b-time	9.48E-05	3.36E-16	1.35E-12	-0.00035	1.81E-08	1.16E-06
5.10E-06	stnd	2.74E-04	1.13E-17	2.93E-16	0.00021	4.32E-10	-6.09E-10
	intp	2.77E-04	1.09E-17	1.06E-12	0.00117	1.25E-10	-1.03E-06
	b-time	2.75E-04	3.65E-16	2.31E-12	0.00055	1.84E-08	1.51E-06
7.10E-06	stnd	4.93E-04	2.18E-17	6.04E-16	-0.00070	9.64E-10	-4.06E-10
	intp	5.01E-04	2.04E-17	2.05E-12	0.00115	3.71E-10	-1.43E-06
	b-time	4.94E-04	4.20E-16	3.80E-12	-0.00035	1.92E-08	1.94E-06
9.10E-06	stnd	9.31E-04	3.78E-17	8.85E-16	-0.00149	1.77E-09	-1.49E-09
	intp	9.57E-04	3.36E-17	3.36E-12	0.00146	7.96E-10	-1.83E-06
	b-time	9.34E-04	5.03E-16	5.87E-12	-0.00116	2.05E-08	2.42E-06

Table 5.8: Mean errors and MSEs of estimators for varying σs in case of observation gaps in a standard OUP with $\mu = 1$, $\alpha = 3.17\text{E-}08$, $X_0 = 0.5$, $\Delta t_{\text{sim}} = 3{,}600$, $\Delta t_{\text{obs}} = 3{,}600$, $n_{\text{obs}} = 43{,}801$, 1,000 paths

We generally find that business time leads to a large positive, and interpolation to a large negative, bias in $\hat{\sigma}$. This effect may be explained by the fact that in the business

time series we have multiple large jumps in the values, whereas in the interpolated series we have significant stretches where the data follows a linear course without noise. We also generally observe that the business time leads to a significant increase in the positive bias of $\hat{\alpha}$, while the estimator based on interpolation experiences a smaller bias. This might be due to the fact that without noise, the process approaches μ exponentially, while with linear interpolation it approaches μ linearly during this time, thus effectively slowing the mean reversion. With business time, on the other hand, the process appears to jump towards the reversion level. On the whole it is apparent that gaps in the observations tend to have a significant effect on the estimators, which could possibly outweigh any biases or MSEs that the estimators have naturally for regular observations.

5.4 Effect of irregular sampling

We next explored the effect on the accuracy of parameter estimation caused by irregularly spaced observations, as often observations made at regular intervals are not available. For example, this is the form in which tick data is provided. When applying a standard estimation technique to irregularly sampled data we have a choice between interpolating, which introduces a bias as shown in Section 5.3, and treating the data as if it were sampled at regular intervals, the effect of which we will study in this section. We explored two different types of irregularity, first sampling the process at a random point within a defined closed interval around the "regular" sampling point, and then picking all observation points at random, with only the number of observations being defined. In all cases, we treated the data as if it were regularly sampled.

5.4.1 Methodology

We tested these methods by first simulating 1000 paths of a standard OUP with a discretization step of 1 hour, with parameters $\alpha = 10^{-5}$, $\sigma = 10^{-5}$, $X_0 = 0.5$ and $\mu = 1$ over an observation window of size $T = 60 \times 60 \times 24 \times 365 \times 5$, which, with time unit 1 second, would correspond to $l = 24 \times 365 \times 5$ hourly simulated points over 5 years. As a benchmark, we first sampled each path regularly with an observation step of size 10 hours by sampling the first and every 10th simulated value. (While irregularly observed data is maybe most common in high-frequency data, as we wanted to keep our parameters in the ranges tested so far, we chose a Δt_{obs} of 10 hours. Of course any time scale is purely hypothetical and these results are easily translated to high-frequency data.) We then sampled each path three more times, but this time irregularly, first with two different degrees of "tolerance" around the "regular" sampling point, and then completely randomly. Like in Section 5.3, we computed the mean error and the MSE over all sample paths for each observation type, and in order to gain further insight did so for a number of parameter sets.

Variation of parameters

We tested the effect of irregular sampling under a variety of reversion strengths in the range $10^{-9} \leq \alpha \leq 6.5 \times 10^{-8}$, and under a variety of diffusion coefficients in the range $10^{-7} \leq \sigma \leq 10^{-5}$. Additionally, to explore the effects of the two observation types on other scales, we picked another set of parameters, varying the reversion strength in the range $10^{-8} \leq \alpha \leq 0.7 \times 10^{-4}$ and the diffusion coefficient in the range $10^{-6} \leq \sigma \leq 10^{-1}$.

Irregular sampling

We tested two different intervals for the irregular sampling. These were $[-1, 1]$ and $[-4, 4]$. For each maximum offset size n, we sampled each path $\{X_t\}_{1 \leq t \leq l}$ of the process $m = 24 \times 365 \times 5/10$ times, with the samples being $\{X_{t'_i}\}_{1 \leq i \leq m}$, where t'_i for each $1 \leq i \leq m$ was an integer chosen at random from $\{t_i - n, t_i - n + 1, ..., t_i + n\}$, where t_i is the regular sampling point. Therefore, with a time unit of one second, this would correspond to sampling the process within an interval of 2 and 8 hours respectively, centred around each regular sampling point. We set $X_{t'_0} = X_{t_0}$ and $X_{t'_m} = X_{t_m}$. We then estimated the parameters of this process using our standard estimation method, as if each $X_{t'_i}$ had been sampled at time t_i.

Random sampling

In order to increase the range of irregularity further, we next sampled the process at random time points. We did this for each path of the process by picking m points from $\{t | 1 \leq t \leq l\}$ at random. These were sorted so the time stamps would be ascending, giving us the points $\{t'_i\}_{1 \leq i \leq m}$ at which we then sampled the path. The sampled values of the process were then treated as if they had been sampled regularly, i.e. each $X_{t'_i}$ was treated as if it had been sampled at t_i for the purpose of our parameter estimation.

5.4.2 Results

See Figure 5.9 for a graph of the mean error of $\hat{\sigma}$ as a function of α for the different sampling types. We can see that irregular sampling introduces a significant bias in $\hat{\sigma}$. Figure 5.10 shows the same relationship for larger αs. We see that in the case of irregular sampling, while $\hat{\sigma}$ is positively biased for small αs, it is in fact negatively biased for larger αs, with the bias apparently tending to zero for very small αs, and the bias being larger for greater irregularity in the sampling.

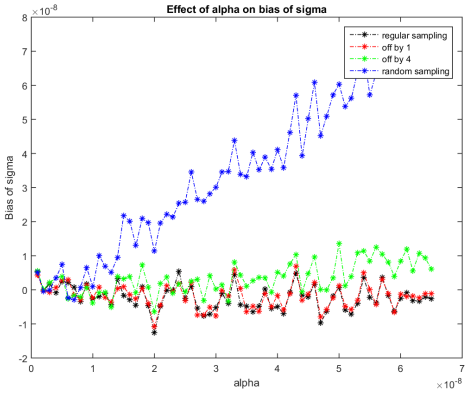

Figure 5.9: Mean error of $\hat{\sigma}$ as a function of α for small αs for regular, irregular and random observation with $\mu = 1$, $\sigma = 0.00001$, $\Delta t_{\text{sim}} = 3600$

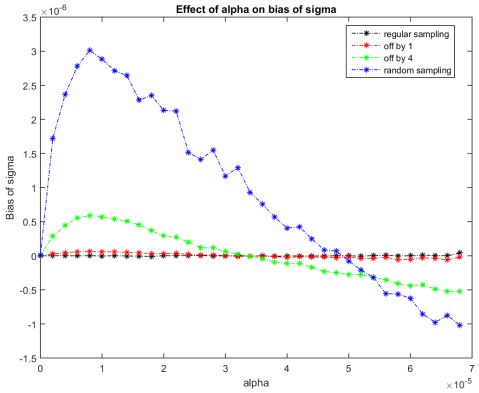

Figure 5.10: Mean error of $\hat{\sigma}$ as a function of α for greater range of αs for regular, irregular and random observation

Figure 5.11 shows the mean error of $\hat{\alpha}$ for different αs for regular and irregular observations. When compared to the effect of α, regularity of sampling appears to have no significant effect on the bias of $\hat{\alpha}$ in the parameter ranges examined for the near-unit-root case. However, in Figure 5.12 we see the same relationship for larger αs. We find that $\hat{\alpha}$ incurs a significant negative bias from irregularity in the observations, with this bias being larger for larger αs and greater irregularity.

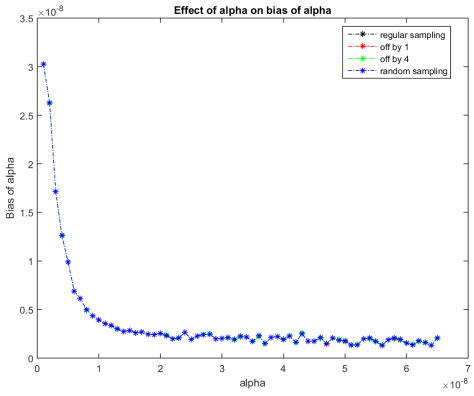

Figure 5.11: Mean error of $\hat{\alpha}$ as a function of α for small αs for regular, irregular and random observation

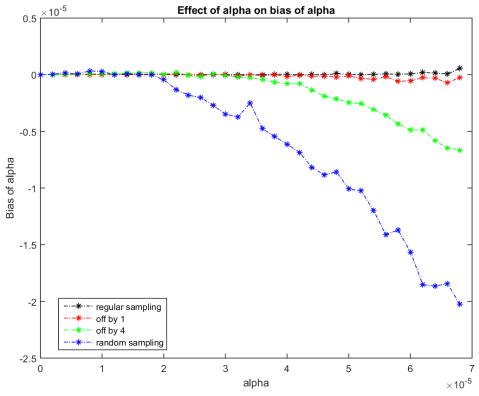

Figure 5.12: Mean error of $\hat{\alpha}$ as a function of α for greater range of αs for regular, irregular and random observation

Figure 5.13 shows the mean error of $\hat{\alpha}$ as a function of σ. We see that in the ranges observed in this graph, irregularity appears to introduce a significant positive bias of $\hat{\alpha}$. However, Figure 5.14 shows the same relationship for larger σs for regular and irregular sampling. We see that for larger σs, greater irregularity in the sampling leads to a greater negative bias of $\hat{\alpha}$. Note that for the parameter ranges examined, the positive bias of $\hat{\alpha}$ for regular sampling is insignificant compared to the bias introduced by irregular sampling at

the levels of irregularity we have tested.

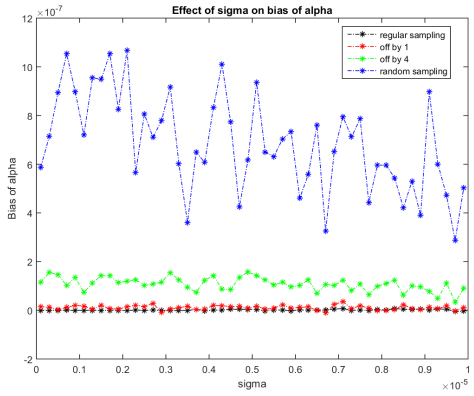

Figure 5.13: Mean error of $\hat{\alpha}$ as a function of σ for smaller σs for regular, irregular and random observation

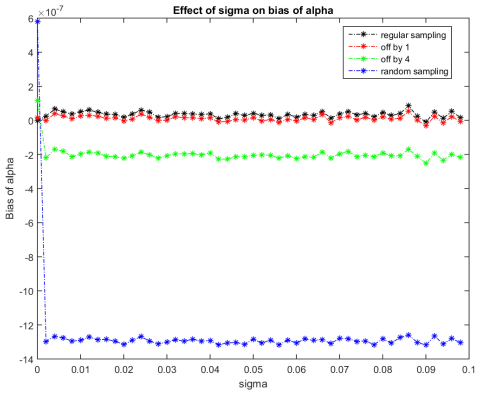

Figure 5.14: Mean error of $\hat{\alpha}$ as a function of σ for greater range of σs for regular, irregular and random observation

See Figure 5.15 for the mean error of $\hat{\sigma}$ as a function of σ in the different sampling scenarios, and Figure 5.16 for the same relationship for larger σs. We see that irregular sampling leads to a positive bias for smaller σs but to a negative bias for larger σs, which appears to be proportional to σ.

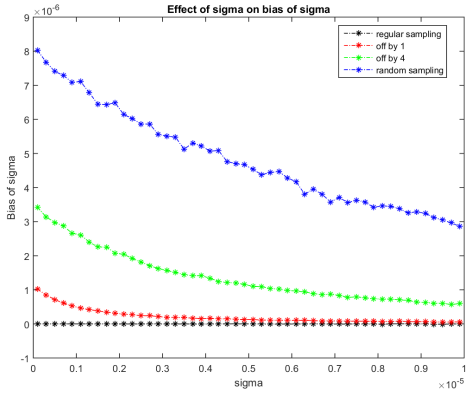

Figure 5.15: Mean error of $\hat{\sigma}$ as a function of σ for smaller σs for regular, irregular and random observation

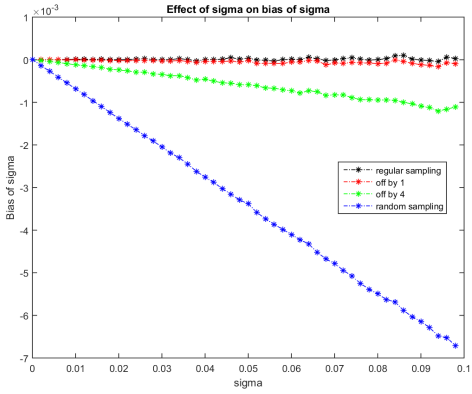

Figure 5.16: Mean error of $\hat{\sigma}$ as a function of σ for greater range of σs for regular, irregular and random observation

Finally, in Figure 5.17 we show the MSE of $\hat{\mu}$ as a function of σ for the different sampling scenarios, and in Figure 5.18 the same relationship for larger σs. We find that the MSE is larger in the case of irregular sampling, with this effect being more significant for larger σs.

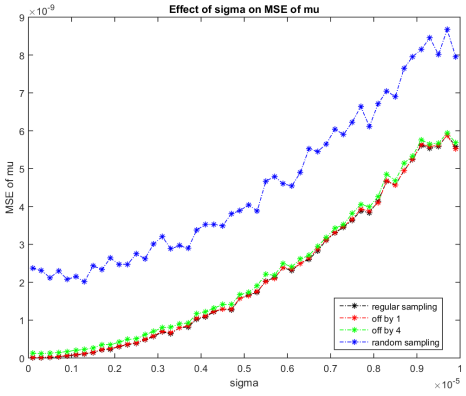

Figure 5.17: MSE of $\hat{\mu}$ as a function of σ for smaller σs for regular, irregular and random observation

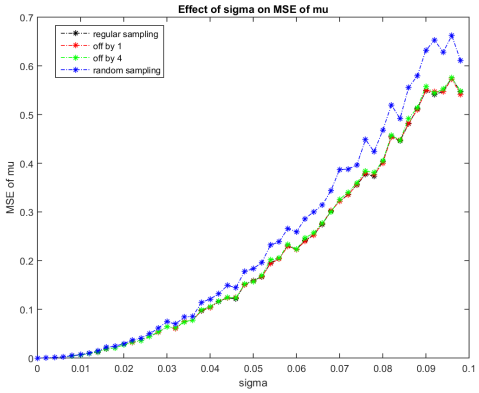

Figure 5.18: MSE of $\hat{\mu}$ as a function of σ for greater range of σs for regular, irregular and random observation

See Table 5.9 for the mean errors and MSEs of all estimators for some of the αs in the three sampling scenarios. Table 5.10 gives the same data for some larger αs. See Appendix B for more comprehensive tables.

Tables 5.11 and 5.12 give the MSEs and mean errors of all parameters for some of the smaller and larger values of σ respectively under the different sampling scenarios. See Appendix B for more comprehensive tables.

α	method	MSE($\hat{\mu}$)	MSE($\hat{\alpha}$)	MSE($\hat{\sigma}$)	ME($\hat{\mu}$)	ME($\hat{\alpha}$)	ME($\hat{\sigma}$)
1.00E-09	regular	0.81363	1.64E-15	1.25E-14	-0.40359	3.03E-08	5.36E-09
	off 1	1.01554	1.63E-15	1.26E-14	-0.44035	3.03E-08	4.37E-09
	off 4	231.35356	1.63E-15	1.38E-14	0.07411	3.03E-08	5.52E-09
	random	2.69461	1.64E-15	2.43E-14	-0.36794	3.02E-08	5.16E-09
1.60E-08	regular	0.27435	5.54E-17	1.13E-14	0.02786	2.60E-09	-2.93E-09
	off 1	0.29228	5.54E-17	1.13E-14	0.02842	2.60E-09	-1.41E-09
	off 4	0.30288	5.54E-17	1.26E-14	0.02869	2.61E-09	3.91E-09
	random	0.76016	5.63E-17	2.17E-14	0.03870	2.62E-09	2.02E-08
3.10E-08	regular	0.00110	4.81E-17	1.14E-14	-0.00085	2.07E-09	-1.09E-09
	off 1	0.00110	4.81E-17	1.16E-14	-0.00086	2.07E-09	-1.21E-10
	off 4	0.00110	4.81E-17	1.27E-14	-0.00086	2.07E-09	1.39E-09
	random	0.00109	4.92E-17	2.36E-14	-0.00089	2.11E-09	3.46E-08
4.60E-08	regular	0.00044	5.51E-17	1.12E-14	-0.00199	2.03E-09	1.61E-09
	off 1	0.00044	5.52E-17	1.15E-14	-0.00200	2.03E-09	2.08E-09
	off 4	0.00044	5.52E-17	1.26E-14	-0.00201	2.04E-09	9.69E-09
	random	0.00044	5.99E-17	2.70E-14	-0.00201	2.14E-09	6.08E-08
6.10E-08	regular	0.00021	6.38E-17	1.22E-14	-0.00047	1.38E-09	-8.06E-10
	off 1	0.00021	6.38E-17	1.24E-14	-0.00046	1.38E-09	-1.97E-09
	off 4	0.00021	6.39E-17	1.37E-14	-0.00048	1.39E-09	1.19E-08
	random	0.00022	7.24E-17	2.66E-14	-0.00047	1.38E-09	7.13E-08

Table 5.9: Mean errors and MSEs of estimators for varying αs in case of irregular observations in a standard OUP with $\mu = 1$, $\sigma =$ 1.00E-05, $X_0 = 0.5$, $\Delta t_{\text{sim}} =$ 3,600, $\Delta t_{\text{obs}} =$ 36,000, $n_{\text{obs}} =$ 4,380, 1,000 paths

α	method	MSE($\hat{\mu}$)	MSE($\hat{\alpha}$)	MSE($\hat{\sigma}$)	ME($\hat{\mu}$)	ME($\hat{\alpha}$)	ME($\hat{\sigma}$)
1.00E-08	regular	3.11E+00	7.38E-17	1.16E-14	6.72E-02	4.08E-09	-5.54E-09
	off 1	1.90E+00	7.38E-17	1.23E-14	5.41E-02	4.09E-09	-3.84E-09
	off 4	9.59E-01	7.38E-17	1.33E-14	2.83E-02	4.09E-09	1.97E-09
	random	1.69E+00	7.43E-17	2.28E-14	3.69E-03	4.11E-09	9.67E-09
1.80E-05	regular	2.07E-09	4.59E-14	1.24E-14	-7.81E-07	7.57E-09	-9.70E-09
	off 1	2.08E-09	5.50E-13	2.27E-14	-6.39E-07	2.38E-08	2.90E-08
	off 4	2.21E-09	5.16E-12	3.76E-13	-1.62E-06	1.69E-07	3.67E-07
	random	3.25E-09	1.32E-10	1.58E-11	6.56E-06	-2.58E-08	2.35E-06
3.60E-05	regular	5.7E-10	4.38E-13	1.69E-14	-5.08E-07	-6.97E-09	-1.25E-09
	off 1	5.59E-10	4.55E-12	6.75E-14	-2.19E-07	-9.88E-08	-6.56E-09
	off 4	5.78E-10	4.02E-11	4.62E-13	6.57E-07	-4.34E-07	-4.27E-08
	random	9.1E-10	4.02E-10	1.05E-11	3.41E-06	-4.77E-06	7.55E-07
5.40E-05	regular	2.87E-10	2.92E-12	3.17E-14	4.65E-07	3.52E-08	3.33E-09
	off 1	2.89E-10	1.00E-11	8.32E-14	4.28E-07	-4.03E-07	-3.77E-08
	off 4	2.8E-10	7.43E-11	5.97E-13	2.87E-07	-3.09E-06	-3.22E-07
	random	4.47E-10	7.97E-10	8.46E-12	1.87E-06	-1.20E-05	-3.16E-07

Table 5.10: Mean errors and MSEs of estimators for bigger αs in case of irregular observations in a standard OUP with $\mu = 1$, $\sigma =$ 1.00E-05, $X_0 = 0.5$, $\Delta t_{\text{sim}} =$ 3,600, $\Delta t_{\text{obs}} =$ 36,000, $n_{\text{obs}} =$ 4,380, 1,000 paths

σ	method	MSE($\hat{\mu}$)	MSE($\hat{\alpha}$)	MSE($\hat{\sigma}$)	ME($\hat{\mu}$)	ME($\hat{\alpha}$)	ME($\hat{\sigma}$)
1.00E-07	regular	6.33E-13	1.61E-18	1.25E-18	2.56E-08	-4.65E-11	1.43E-11
	off 1	1.25E-11	6.29E-14	1.17E-12	-2.14E-07	1.47E-08	1.02E-06
	off 4	1.23E-10	6.43E-13	1.31E-11	-2.10E-06	1.16E-07	3.42E-06
	random	2.37E-09	5.16E-11	7.84E-11	1.11E-05	5.88E-07	8.02E-06
1.10E-06	regular	7.60E-11	1.87E-16	1.38E-16	4.71E-08	-3.00E-10	2.09E-10
	off 1	8.84E-11	6.15E-14	2.71E-13	-2.45E-07	1.74E-08	4.61E-07
	off 4	2.05E-10	6.15E-13	8.20E-12	-1.49E-06	7.36E-08	2.61E-06
	random	2.15E-09	4.58E-11	6.49E-11	7.48E-06	7.20E-07	7.11E-06
3.10E-06	regular	6.88E-10	1.59E-15	1.09E-15	1.09E-06	-1.48E-09	-8.87E-10
	off 1	7.04E-10	6.29E-14	5.14E-14	1.09E-06	5.43E-09	1.92E-07
	off 4	8.01E-10	6.51E-13	3.25E-12	-1.27E-06	1.54E-07	1.57E-06
	random	3.20E-09	4.62E-11	4.24E-11	8.54E-06	9.17E-07	5.51E-06
6.10E-06	regular	2.31E-09	5.30E-15	4.30E-15	1.75E-06	1.59E-09	-8.05E-10
	off 1	2.34E-09	6.08E-14	2.06E-14	1.54E-06	1.18E-08	1.05E-07
	off 4	2.41E-09	5.91E-13	1.34E-12	-2.73E-07	1.02E-07	9.66E-07
	random	4.54E-09	3.72E-11	2.61E-11	9.65E-06	4.61E-07	4.17E-06
9.10E-06	regular	5.61E-09	1.23E-14	9.51E-15	-3.03E-06	4.08E-10	9.79E-10
	off 1	5.64E-09	6.34E-14	1.77E-14	-3.30E-06	1.35E-08	6.74E-08
	off 4	5.76E-09	5.37E-13	6.16E-13	-4.93E-06	7.71E-08	6.29E-07
	random	8.14E-09	4.15E-11	1.92E-11	4.04E-06	8.97E-07	3.24E-06

Table 5.11: Mean errors and MSEs of estimators for varying σs in case of irregular observations in a standard OUP. $\mu = 1$, $\alpha =$ 1.00E-5, $X_0 = 0.5$, $\Delta t_{\text{sim}} =$ 3,600, $\Delta t_{\text{obs}} =$ 36,000, $n_{\text{obs}} =$ 4,380, 1,000 paths.

σ	method	MSE($\hat{\mu}$)	MSE($\hat{\alpha}$)	MSE($\hat{\sigma}$)	ME($\hat{\mu}$)	ME($\hat{\alpha}$)	ME($\hat{\sigma}$)
0.000001	regular	6.33E-11	1.61E-16	1.25E-16	2.56E-07	-4.43E-10	1.37E-10
	off 1	7.38E-11	6.27E-14	3.39E-13	1.76E-08	1.44E-08	5.19E-07
	off 4	1.85E-10	6.42E-13	8.40E-12	-1.88E-06	1.16E-07	2.67E-06
	random	2.38E-09	5.12E-11	6.56E-11	1.14E-05	5.79E-07	7.20E-06
0.030001	regular	0.06436	1.97E-13	1.47E-07	0.01015	2.23E-08	2.83E-06
	off 1	0.06425	1.96E-13	1.47E-07	0.01147	1.11E-09	-2.89E-05
	off 4	0.06406	2.34E-13	2.73E-07	0.01048	-2.07E-07	-3.44E-04
	random	0.07462	1.87E-12	4.37E-06	0.00803	-1.30E-06	-2.05E-03
0.060001	regular	0.22293	1.83E-13	5.58E-07	0.01748	1.95E-08	8.74E-06
	off 1	0.22280	1.80E-13	5.66E-07	0.01741	-2.33E-09	-5.54E-05
	off 4	0.22318	2.27E-13	1.14E-06	0.01467	-2.24E-07	-7.30E-04
	random	0.25915	1.86E-12	1.76E-05	0.01411	-1.31E-06	-4.10E-03
0.090001	regular	0.54887	1.89E-13	1.25E-06	-0.03016	-9.39E-09	-4.51E-06
	off 1	0.54937	1.90E-13	1.29E-06	-0.03040	-3.12E-08	-1.15E-04
	off 4	0.55731	2.39E-13	2.51E-06	-0.03456	-2.51E-07	-1.09E-03
	random	0.63207	1.90E-12	3.95E-05	-0.01673	-1.32E-06	-6.14E-03

Table 5.12: Mean errors and MSEs of estimators for bigger σs in case of irregular observations in a standard OUP with $\mu = 1$, $\alpha =$ 1.00E-5, $X_0 = 0.5$, $\Delta t_{\text{sim}} =$ 3,600, $\Delta t_{\text{obs}} =$ 36,000, $n_{\text{obs}} =$ 4,380, 1,000 paths

It is clear that irregularity of observations has a non-negligible effect on the parameter estimation of the OUP. We find there to be a large difference in the effect of irregularity of sampling on different scales of parameters. Generally, we find that when dealing with irregular samples, changes in the true values of the parameters appear to have an even greater effect on the mean error and MSE of the estimators than in the regular case.

5.5 Estimation with time-dependent reversion level

We next set out to examine the parameter estimation of the OUP with time-dependent reversion level. We implement Sanchez et al.'s [75] method, as described in Section 2.4.2, since Sanchez et al. only present an analysis of their performance for a process where the diffusion coefficient is scaled by the value of the process. We also propose an alternative method of conducting the parameter estimation of the OUP with time-dependent reversion level.

5.5.1 Methodology

We compared the two methods by simulating 100 paths of an OUP with time-dependent reversion level for a number of parameter sets and then producing two sets of estimators for each sample path, one based on Sanchez et al.'s method and one based on our method. Additionally, we applied the standard estimation method for OUPs with constant reversion level to the paths as a benchmark. We compare the MEs and MSEs over 100 paths of the three estimation methods for each parameter set. We shall now describe both of the methods in detail.

Sanchez et al. method

We will now remind ourselves of the first phase of the method proposed by Sanchez et al., as described in Section 2.4.2, and describe it in some more detail. The method is based on the relationship

$$\mu\left(t\right) = m(t) + \frac{\dot{m}(t)}{\alpha}, \tag{5.2}$$

between the expected value $m(t)$ of the process and the underlying reversion level $\mu(t)$. A moving average is used to approximate the expected value of the process at the sampling points, and a numerical derivation method is used to find its derivative at these points in order to estimate the reversion level. As proposed by Sanchez et al., we employ a three-point derivation where the derivative of the expected path is defined as

$$\begin{aligned} \dot{m}_0 &= \frac{m_1 - m_0}{\Delta t} \\ \dot{m}_N &= \frac{m_N - m_{N-1}}{\Delta t} \\ \dot{m}_i &= \frac{2m_{i+1} - 3m_i + m_{i-1}}{\Delta t} \text{ for } 0 < i < N. \end{aligned} \tag{5.3}$$

Note that in this case $[0, T]$, where $T = N\Delta t$, is the interval over which we are able to compute the moving average, rather than the full interval over which the process was observed. Furthermore note that while this approximation of the derivative involves a time shift, we chose to follow it in order to test the method exactly. However, we found no significant effect of the approximation method used. Based on Sanchez et al.'s method we then computed the estimators as

$$\hat{\alpha} = \frac{\sum_{i=1}^{N} \left(X_i m_{i-1} - X_i X_{i-1} - X_{i-1} m_{i-1} + X_{i-1}^2 - \dot{m}_{i-1} m_{i-1} \Delta t + X_{i-1} \dot{m}_{i-1} \Delta t\right)}{\sum_{i=1}^{N} \left(m_{i-1}^2 - 2m_{i-1} X_{i-1} + X_{i-1}^2\right) \Delta t} \tag{5.4}$$

and

$$\hat{\sigma} = \sqrt{\frac{1}{N\Delta t} \sum_{i=1}^{N} s_i}\,, \tag{5.5}$$

where

$$\begin{aligned} s_i = {} & X_i^2 - 2X_i X_{i-1} + X_{i-1}^2 - \Delta t 2X_i \hat{\alpha} m_{i-1} + 2X_i \Delta t \hat{\alpha} X_{i-1} - 2X_i \dot{m}_{i-1} \Delta t \\ & + 2X_{i-1} \Delta t \hat{\alpha} m_{i-1} - 2X_{i-1}^2 \Delta t \hat{\alpha} + 2X_{i-1} \Delta \dot{m}_{i-1} \\ & + \hat{\alpha}^2 m_{i-1}^2 (\Delta t)^2 - \hat{\alpha}^2 m_{i-1} X_{i-1} (\Delta t)^2 + \hat{\alpha} m_{i-1} \dot{m}_{i-1} (\Delta t)^2 \\ & - \hat{\alpha}^2 m_{i-1} X_{i-1} (\Delta t)^2 + \hat{\alpha}^2 X_{i-1}^2 (\Delta t)^2 - \hat{\alpha} X_{i-1} \dot{m}_{i-1} (\Delta t)^2 \,. \end{aligned} \tag{5.6}$$

See Sanchez et al.'s paper [75] for more details on this method.

Our method

We propose an alternative method, where we use the moving average to approximate the reversion level itself rather than the expected path. While we expect that the moving average is a worse approximation of the reversion level than it is of the expected path, this method allows us to find parameter estimators from the exact discretization as described in Section 2.2.3, rather than the Euler–Maruyama discretization. From the series $\{X_i\}$ we compute the moving average $\{\mathrm{MA}_i\}_{0\leq i\leq N}$, where $[0,T]$ with $T = N\Delta t$ is the interval over which we can compute the moving average, and then from this generate a detrended series $\{X'_i\}_{0\leq i\leq N}$ by

$$X'_i = X_i - \mathrm{MA}_i \tag{5.7}$$

for $0 \leq i \leq N$. We now treat X'_t as an OUP with reversion level 0, applying standard estimation techniques for OUPs with known reversion level to the detrended series.

Our estimators are therefore

$$\hat{\alpha} = -\frac{1}{\Delta t}\log\frac{\sum_{i=1}^{N}(X_{i-1}X_i)}{\sum_{i=1}^{N}(X_{i-1}^2)} \tag{5.8}$$

and

$$\hat{\sigma} = \sqrt{\frac{\sum_{i=1}^{N}(X_i^2) - 2e^{-\hat{\alpha}\Delta t}\sum_{i=1}^{N}(X_{i-1}X_i) + e^{-2\hat{\alpha}\Delta t}\sum_{i=1}^{N}(X_{i-1}^2)2\hat{\alpha}}{N(1-e^{-2\hat{\alpha}\Delta t})}}. \tag{5.9}$$

These are the ML estimators for a standard OUP with known reversion level, based on those described in Section 2.3.1.

Moving averages

Like Sanchez et al., we employed a symmetrical moving average, rather than a lagging MA, so as to better approximate the underlying value of the process. This of course is not possible to do in real time, and the same method could instead be followed using a lagging MA.

We tested a simple moving average of the sampled series $\{X_{i,\Delta t}\}_{0\leq i\leq n}$ by

$$\mathrm{MA}_{i,\Delta t} = \frac{1}{2m+1}\sum_{j=i-m}^{i+m} X_{i,\Delta t} \tag{5.10}$$

for $m \leq i \leq n-m$, where $m = \frac{\tau}{\Delta t}$ with time period $\tau = 60\times 60\times 24\times 7\times 5$, which means with time unit 1 second the total period over which the moving average was computed corresponds to roughly 10 weeks, centred around the current point in time. Therefore, for m sampled values per path, after computing the MA we only had $n-2m$ values per path to base the parameter estimation with Sanchez et al.'s and our method on.

Simulation

We tested both methods on a simulated data set. We tested the methods on an OUP with a sine function as reversion level, with $\mu(t) = \sin \frac{2\times\pi\times t}{T} + 1.5$, based on Sanchez et al.'s simulations in order to facilitate the comparison of results. Like the standard OUP, we simulated the OUP with time-dependent reversion level iteratively, by setting X_0 and then computing

$$X_{i+1} = \mu_i + (X_i - \mu_i)e^{-\alpha\Delta t} + \sigma\sqrt{\frac{1 - e^{-2\alpha\Delta t}}{2\alpha}}\,, \tag{5.11}$$

where

$$\mu_i = \mu(i\Delta t), \tag{5.12}$$

in other words we discretized the reversion level, turning it into a step function. In order to reduce the error introduced by this discretization, we simulated the process with a discretization step of one minute and sampled it with observation steps 30 minutes and larger. Due to this smaller simulation step, we simulated 100 paths for each parameter set. We simulated a discretization of the process $\{X_t\}_{t\geq 0}$ with

$$dX(t) = \alpha(\mu(t) - X(t))dt + \sigma dW(t) \tag{5.13}$$

with $X(0) = 1.5$ and parameters $\sigma = 10^{-4}$ and $\alpha = \frac{1}{60\times 60\times 24\times 4}$ over a period of $T = 60 \times 60 \times 24 \times 7 \times 50 \times 5$, i.e. with a time unit of 1 second the reversion time constant corresponded to roughly 4 days and the observation period to roughly 5 years. These parameters as well as the SMA windows we used are in the ranges of those tested by Sanchez et al. on a different CKLS generalization. We tested Δts of 30 minutes, 1 hour, 6 hours, 12 hours and 1 day. For each size of observation step we generated a new set of 100 minutely sample paths, over which we computed the MEs and MSEs for each method. Note that by increasing Δt, we reduced the number of sampled points.

5.5.2 Results

See Figures 5.19 and 5.20 for example graphs of the mean error of $\hat{\alpha}$ as a function of Δt and the MSE of $\hat{\sigma}$ as a function of Δt for our method, the Sanchez et al. method, and a standard estimation method respectively.

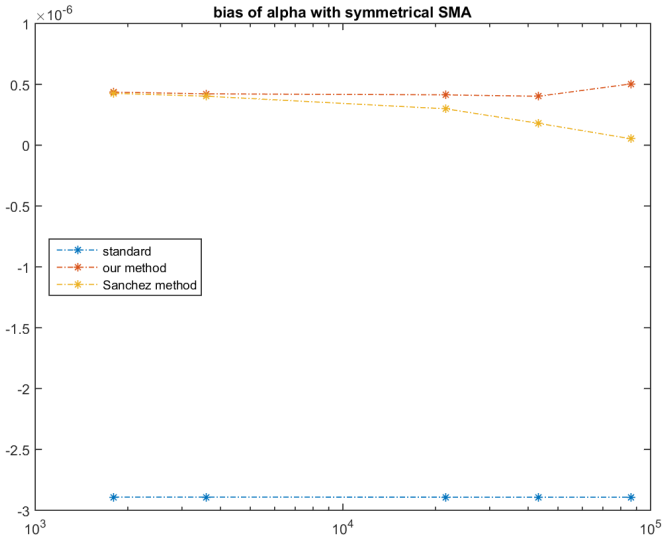

Figure 5.19: Mean error of $\hat{\alpha}$ as a function of Δt for the standard and two alternative methods

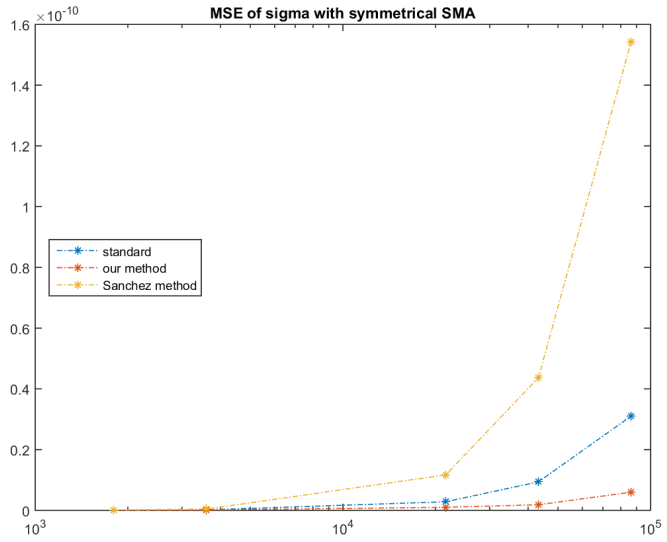

Figure 5.20: MSE of $\hat{\sigma}$ as a function of Δt for the standard and two alternative methods

In our simulations, both methods show a significant positive bias of $\hat{\alpha}$, which is much larger than what would be expected for the values of σ, α and T simulated in the case of constant reversion level and standard estimators. However, for the ranges tested, both methods perform similarly in the estimation of $\hat{\alpha}$ when compared to the estimation with no MA subtracted. We found that Sanchez et al.'s method was better at estimating α while ours was better at estimating σ. Despite Sanchez et al.'s method being based on the Euler–Maruyama discretization, Sanchez et al.'s estimators are in acceptable ranges even for large Δts. Note that in Figure 5.19 we see a negative mean error of $\hat{\alpha}$ for the

standard method, however this is due to the bias induced by the unknown time-dependent reversion level. In the estimation of σ both methods, as well as the standard estimation, perform similarly, and sufficiently accurately.

See Table 5.13 for the MSEs and mean errors for the two methods for the different observation steps.

n_{obs}	Δt_{obs}	Calibration method	MSE($\hat{\alpha}$)	MSE($\hat{\sigma}$)	ME($\hat{\alpha}$)	ME($\hat{\sigma}$)
84,000	1,800	our method	2.46E-13	5.82E-14	4.36E-07	-2.10E-09
		Sanchez	2.37E-13	1.54E-13	4.26E-07	-3.09E-07
42,000	3,600	our method	2.39E-13	1.16E-13	4.22E-07	1.66E-08
		Sanchez	2.22E-13	4.59E-13	4.02E-07	-5.94E-07
7,000	21,600	our method	2.27E-13	1.05E-12	4.13E-07	2.94E-07
		Sanchez	1.38E-13	1.17E-11	2.99E-07	-3.29E-06
3,500	43,200	our method	2.30E-13	1.88E-12	4.02E-07	4.45E-07
		Sanchez	8.34E-14	4.37E-11	1.79E-07	-6.51E-06
1,750	86,400	our method	3.37E-13	5.99E-12	5.03E-07	1.32E-06
		Sanchez	4.90E-14	1.54E-10	5.26E-08	-1.23E-05

Table 5.13: Mean errors and MSEs of estimators for different estimation methods of OUP with time-dependent reversion level with α = 2.89E-06, σ = 1.00E-04

5.6 Discussion

It is apparent that the parameter estimation of the OUP in practice is a very complex matter. It is clearly not sufficient to find theoretical properties of the estimators based on finite but perfectly regular samples. Instead, we propose there is much scope for a detailed analysis of how different types of errors or irregularities in the observation process affect estimator accuracy. While the bias in OUP parameter estimation caused by finite samples is to be taken seriously, in some cases this can in fact become negligible when dealing with the potentially much larger errors introduced by imperfect observations. This means that further research is required in order to better understand the reliability of estimators. Furthermore, we have seen that in the case of imperfect observations the behaviours of the estimators vary qualitatively depending on the orders of magnitude of the parameters of the process and observation. While we have tested the behaviour of the estimators for a range of parameters, there is of course a great number of interactions at play between the process parameters and the observation parameters such as the observation period, the observation steps and the number of observations. For example, in this study we have examined the interaction between parameters mostly in the non-stationary part of the process and in the near-unit root case. Similarly, we have varied the observation step while keeping the observation time constant, and thus varying the observation step along with the number of observations. An alternative would be to vary the observation step along with the observation period, and thus keeping the number of observations constant. Furthermore, our study could also be extended to a scenario where the reversion level is known a priori. Alternatively, these interactions could be determined by finding analytical

descriptions of the MEs and MSEs of the three estimators as a function of the process parameters and observation parameters.

We have shown that the performance of a new method proposed by us for the parameter estimation of an OUP with time-dependent reversion level is similar to the only other existing method. However, much more research is required on this topic, and an improvement to both methods would be desirable. In particular, both methods' accuracy is very dependent on the choice of MA.

Gaps in the data

The first issue to consider when confronted with major gaps in the data is whether these gaps are due to errors in the observation or due to market opening hours. If the gaps are due to market hours, an assumption has to be made regarding whether processes continue during market closing times, or whether they are halted outside of business hours. As pointed out by Müller et al. in FX this decision is further complicated by the fact that the FX market has different opening hours around the world, and therefore there is no absolute business time. Where it is assumed that processes continue during market closing times, or where gaps are due to errors in observation, we have found that when estimating the parameters of an OUP generally linear interpolation appears to be preferable to business time, especially when it comes to the estimation of the mean reversion strength. However, as we have shown, interpolation has different effects on the different estimators, and all of these need to be taken into account when deciding how to proceed.

Due to the FX market having different opening hours around the world we only simulated weekend gaps and not night gaps, but the results should not differ qualitatively. Still, the effect of different sizes and numbers of gaps in the data may be worth exploring.

Irregular observations

It should be noted that in the case where the time stamps of irregular observations are known, it is possible to use the exact transition density function to find the ML estimators of the parameters. However, when we are dealing with inaccuracies in the recording of the time stamps, the irregularities in recording times may be unknown, and therefore we cannot correct for them by adjusting the estimators. In other cases, such as in our Thomson Reuters data set, we are presented with data which is already interpolated. In both scenarios it is important to know how the reliability of estimators may be affected. Additionally, using exact estimators in the case of irregular observations would be more complex than applying the standard estimation method to irregular or interpolated data. For this reason, it is worth exploring whether these computations yield a significant improvement in the results.

In the case of irregular but known observation times, of course an alternative to treating values as if they had been regularly sampled or using exact estimators would be to use interpolation to approximate the values at the desired sampling points. However, as we

have seen in Section 5.3, linear interpolation, too, introduces a significant bias into the data.

Both for irregular observations and for gaps in the observations, an interesting study would be to find the MSEs and MEs of the estimators as functions of some measure of the irregularity, either analytically or numerically. A further area of exploration would be the parameter estimation using methods such as the jackknife technique or the bootstrap technique under the circumstances we have explored.

We conclude from our study that caution should be applied when estimating the parameters of the OUP in practice, and properties of the estimators in the case of perfectly regular observations are not to be transferred to the case of irregular data.

Time-dependent mean

We have tested Sanchez et al.'s method of estimating the parameters of an OUP with time-dependent mean, and have proposed an alternative method. To the best of our knowledge, both of these are novel contributions to the literature. In the parameter ranges and with the reversion level we tested, which were based on Sanchez et al.'s paper, both methods perform similarly, however further study is required to determine the exact difference in performance between the two methods under different circumstances. For example, clearly both methods are significantly affected by the MA used, including which time constant is used in the MA, although the nature of this dependence is not clear. For example, in the case of a sine function as underlying reversion level, the relation between the period of the sine function and the time constant of the MA is relevant. The effect of the time constant used for the MA on the parameter estimation is what we shall explore further in the following chapter.

Chapter 6

Time-dependent OUP reversion levels and the Hurst exponent

This chapter presents Part 3 of the research, which is concerned with the application of the calibration methods from Part 2 (Chapter 5) of the research for a mean-reverting model with time-dependent reversion level to foreign exchange data in order to find out how the calibrated parameters depend on how the mean reversion level is determined. This also relates to trading strategies where an underlying trend is determined through moving averages, and a reversion to this trend is assumed. We show that the dependence of the OUP parameters on the definition of the reversion level is directly related to the Hurst exponent of the process, using a detrended moving average analysis.

6.1 Research question

In this experiment, we assumed that log nominal exchange rates followed an Ornstein–Uhlenbeck process fluctuating around a time-dependent "intrinsic" value. The goal of this part of the research was to calibrate the parameters of this Ornstein–Uhlenbeck process in order to determine their dependence on the way the underlying value was defined. In order to do this, we assumed that the "intrinsic" value could be approximated as a moving average of the data. We therefore applied the calibration methods introduced in Part 2 to high-frequency FX data by calculating a number of different types of moving averages, subtracting these from the data, and then fitting the resulting time series to an Ornstein–Uhlenbeck process with reversion level 0.

We first of all found the dependence of the calibrated reversion strength α on the time constant τ. Then, we hypothesized that the dependence of the estimated parameters was related to the Hurst exponent of the data. This hypothesis arose from the fact that methods for estimating the Hurst exponent of a series, such as the DFA or R/S analysis, introduce a time scale into a series and then measure the variability of the series as a function of this time scale. This is effectively what we are doing when fitting an OU process to FX time series after subtracting a moving average. Due to the self-similarity

of FX time series they are scale-free, and by subtracting a moving average a time scale is introduced via the time constant of the moving average. An OU process has a scale, and its long-term variance is a function of its parameters.

We therefore conducted a detrending moving average analysis, finding the Hurst exponent of the data, and then computed the scaling exponent of the estimated long-term variance of the OUP as a function of the time constant used to define the underlying reversion level in order to compare the two.

6.2 Calibrating the OUP with time-dependent reversion level

In this part of our research, our aim was to find how the calibrated parameters of an OUP with time-dependent reversion level as described in Part 2 (Chapter 5) depend on the time constant used to detrend the process.

Two types of moving average were tested as approximation of the underlying value of the FX rate: a simple and an exponential lagging moving average. We did not consider symmetrical moving averages, as these are not suitable for real-time application. For each of these types of moving average we then varied the time constant of the moving average to find the effect this would have on the calibrated mean reversion strength and diffusion coefficient. We did this by subtracting the computed moving average from the time series and then estimating the reversion strength and volatility coefficient with the reversion level fixed to zero.

We then attempted to find functions to express the calibrated reversion strength as well as the long-term variance of the OUP as a function of the time constant.

6.2.1 Methodology

We chose as the time constants τ for the moving averages for the daily Thomson Reuters data 10, 20, 30, 60, 120 and 200 days and one and two years. We increased the observation step of the Commerzbank data to 1 minute and the time constants we chose for the moving averages for Commerzbank were 2, 5 and 10 hours and 1, 5, 10, 14 and 30 days. For each series we computed the moving averages, subtracted them, and then estimated the parameters of the process, as described below. Thus, for each series, eight SMAs and eight EMAs were computed, and we generated one $\hat{\alpha}$ and one $\hat{\sigma}$ per pair per MA.

Simple moving average

The simple moving average (SMA) with a time window of size τ for a point at time t was calculated as the arithmetic mean of the values of the process with timestamps within the interval $[t-\tau, t]$. The formula for the SMA of the process $\{X_i\}_{0\leq i\leq n}$ was

$$\mathrm{SMA}_i = \frac{X_{i-\tau+1} + X_{i-\tau+2} + ... + X_i}{\tau} \tag{6.1}$$

for $\tau \leq i$. This lagging SMA cannot be calculated for the entire length of the original process but only from the τ-th value onwards, losing $\tau - 1$ values from the beginning of the process. The detrended processes therefore can also only be computed for these periods. In order to make all detrended processes cover the same period of time, we cropped all of them to the length of the shortest detrended process, $n - \tau_{\max} + 1$.

An example of the daily log prices and the SMA over 365 days for daily Thomson Reuters CHF/JPY is presented in Figure 6.1. Both the daily log price and the SMA series were cropped to be the length of the shortest SMA series, i.e. $n - \tau_{\max} + 1$.

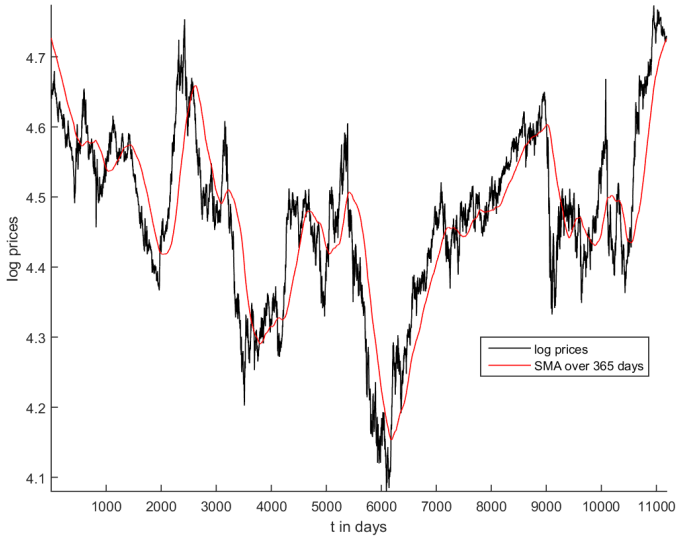

Figure 6.1: Daily CHF/JPY prices and moving average calculated over previous 365 days

Figure 6.1 shows the cropped series of interpolated daily log prices for CHF/JPY from Thomson Reuters in black, and the simple moving average calculated over the previous 365 days in red.

See Appendix C for further examples.

Exponentially weighted moving average

For this moving average, we averaged over the past values of the process, while giving more recent values exponentially larger weights than those further in the past. As in previous chapters, for time constant τ we computed the smoothing factor as $a = \frac{2}{\tau+1}$, from which the value of the moving average $\mathrm{EMA}(t)$ of the process $X(t)$ was calculated iteratively as $\mathrm{EMA}(1) = X(1)$ and $\mathrm{EMA}(t) = (1-a) \times \mathrm{EMA}(t-1) + a \times X(t)$ for $2 \leq t$. A smaller time constant therefore led to less smoothing and a more "reactive" EMA. While our definition of the exponential moving average allows us to calculate a moving average for the entire time period of the original process, the moving average will be less accurate for earlier values, as we start the moving average with an approximation at the same value as the original process. We therefore chose to crop all detrended series to the same length as for

the SMA, i.e. $n - \tau_{\max} + 1$.

See Appendix C for example graphs of some of the price series we analysed and their EMAs.

Parameter estimation

We estimated the parameters of the detrended processes $\{X_{\mathrm{EMA}_\tau,i}\}$ and $\{X_{\mathrm{SMA}_\tau,i}\}$ with $X_{\mathrm{EMA}_\tau,i} = X_i - \mathrm{EMA}_\tau, i$ and $X_{\mathrm{SMA}_\tau,i} = X_i - \mathrm{SMA}_\tau, i$ using the estimators

$$\hat{\alpha} = -\frac{1}{\Delta t} \log \frac{\sum_{i=1}^{N} (X_{i-1} X_i)}{\sum_{i=1}^{N} (X_{i-1}^2)} \tag{6.2}$$

and

$$\hat{\sigma} = \sqrt{\frac{\sum_{i=1}^{N} (X_i^2) - 2e^{-\hat{\alpha}\Delta t} \sum_{i=1}^{N} (X_{i-1} X_i) + e^{-2\hat{\alpha}\Delta t} \sum_{i=1}^{N} (X_{i-1}^2) 2\hat{\alpha}}{N(1 - e^{-2\hat{\alpha}\Delta t})}}, \tag{6.3}$$

which corresponds to our method as described in 5.5.

See Figure 6.2 for the cropped daily Thomson Reuters CHF/JPY series detrended using an SMA over 60 days.

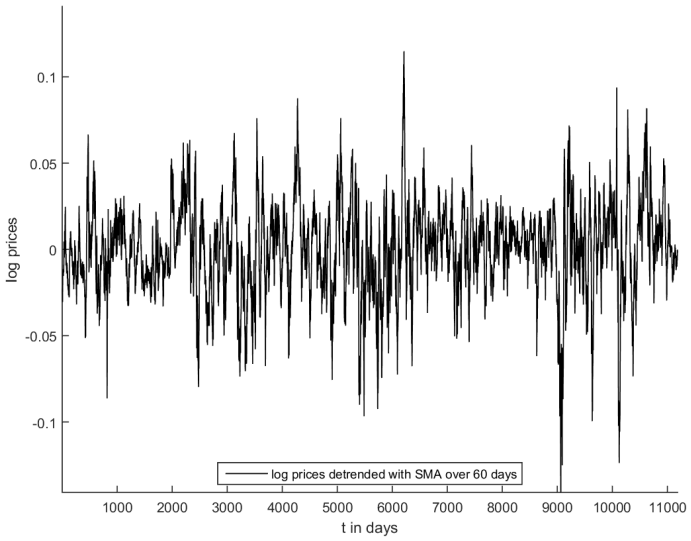

Figure 6.2: Daily CHF/JPY prices minus moving average calculated over previous 60 days

Figure 6.2 shows the cropped detrended interpolated daily log prices for CHF/JPY from Thomson Reuters in black, calculated by subtracting the 60-day simple moving average from the interpolated daily log prices.

See Appendix C for further example graphs of the series we analysed detrended with different τs.

6.2.2 Results

We found a consistent dependence of $\hat{\alpha}$ and $\frac{\hat{\sigma}^2}{2\hat{\alpha}}$ on τ. We conducted a linear regression on both dependencies on a log-log scale and found high correlation coefficients.

As an example, the logarithm of the ML-estimated mean reversion strengths in 1/days for Thomson Reuters CHF/JPY as a function of the logarithm of the SMA windows in days along with the regression line is presented in Figure 6.3.

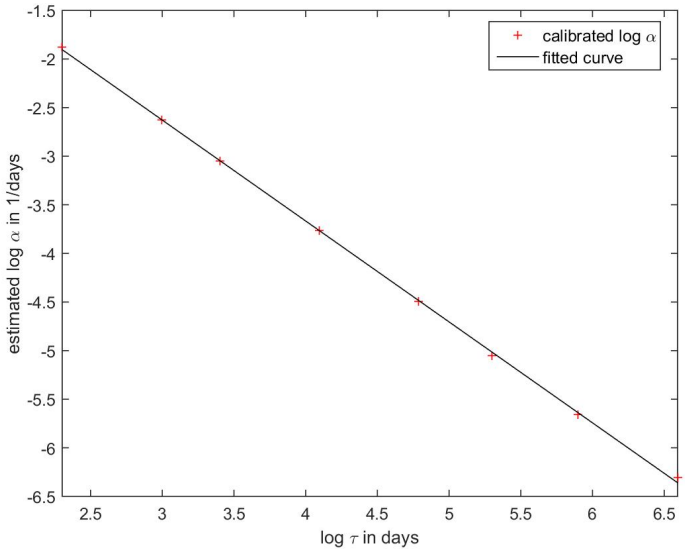

Figure 6.3: Log of estimated mean reversion strengths for detrended daily log CHF/JPY prices for different SMA windows

The fitted slope and therefore the scaling exponent in Figure 6.3 is $E_\alpha = -1.0382$ with $R_\alpha = -0.9999$.

The logarithm of the SMA ML-estimated long-term variance $\frac{\hat{\sigma}^2}{2\hat{\alpha}}$ for the same series as a function of the logarithm of τ along with a line fit is shown in Figure 6.4.

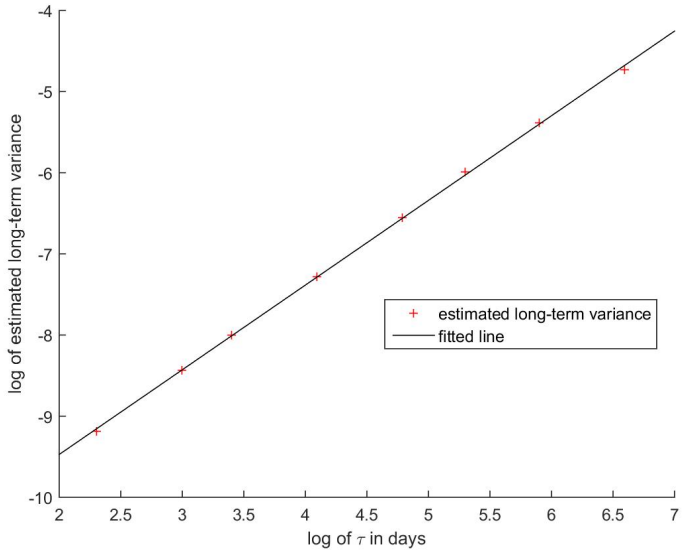

Figure 6.4: Log of estimated long-term variance for detrended daily log CHF/JPY prices for different SMA windows

The line fitted in Figure 6.4 has the slope $E_{\text{var}} = 1.0436$ with correlation coefficient $R_{\text{var}} = 0.9998$. Both line fits show a slight curvature, which is similar to that reported for Hurst exponent estimation methods in the literature. We did not find a significant dependence of $\log \hat{\sigma}$ on $\log \tau$ beyond a curvature like that found for $\hat{\alpha}$ and $\frac{\hat{\sigma}^2}{2\hat{\alpha}}$. The estimated mean reversion strengths, diffusion coefficients and long-term variances of the daily Thomson Reuters CHF/JPY data using ML for each of the eight τ_{SMA}s are presented in Table 6.1.

τ/days	$\hat{\alpha} \times$ day	$\hat{\sigma} \times \sqrt{\text{day}}$	$\hat{\sigma}^2/(2\hat{\alpha})$
10	0.1527	0.0056	1.0247E-04
20	0.0723	0.0056	2.1807E-04
30	0.0475	0.0056	3.3415E-04
60	0.0231	0.0056	6.9051E-04
120	0.0112	0.0056	1.4295E-03
200	0.0064	0.0057	2.5017E-03
365	0.0035	0.0057	4.5833E-03
730	0.0018	0.0057	8.8110E-03

Table 6.1: Estimated $\hat{\alpha}$s, $\hat{\sigma}$s and $\frac{\hat{\sigma}^s}{2\hat{\alpha}}$ for detrended daily Thomson Reuters CHF/JPY series with SMA window τ in days

We present a table of the best fit values for E_α and E_{var} using SMAs and EMAs for detrending for each Thomson Reuters currency pair, along with the correlation coefficients R_α and R_{var}, in Table 6.2 below.

	SMA				EMA			
	E_α	R_α	E_{var}	R_{var}	E_α	R_α	E_{var}	R_{var}
CAD	-1.0295	-0.9999	1.0355	0.9999	-1.0093	-0.9999	1.0544	0.9999
GBP	-1.0599	-0.9994	1.0676	0.9993	-1.0239	-0.9997	1.0730	0.9992
JPY	-1.1171	-0.9999	1.1247	0.9999	-1.0808	-1.0000	1.1289	0.9998
EUR/AUD	-0.9660	-0.9989	0.9709	0.9988	-0.9127	-0.9984	0.9578	0.9972
EUR/CAD	-1.0808	-0.9999	1.0879	0.9999	-1.0418	-0.9999	1.0895	0.9998
EUR/CHF	-1.0737	-0.9998	1.0745	0.9998	-1.0655	-0.9992	1.1026	0.9997
EUR/GBP	-1.0256	-1.0000	1.0292	1.0000	-0.9956	-1.0000	1.0367	0.9999
EUR/JPY	-1.1412	-1.0000	1.1491	1.0000	-1.1005	-0.9999	1.1489	0.9998
EUR	-1.0964	-1.0000	1.1045	0.9999	-1.0652	-1.0000	1.1131	0.9999
EUR/NOK	-1.0004	-0.9999	1.0001	0.9999	-0.9602	-0.9998	0.9936	0.9994
EUR/SEK	-1.0345	-0.9998	1.0385	0.9997	-0.9886	-0.9996	1.0308	0.9991
GBP/AUD	-1.0101	-0.9995	1.0176	0.9994	-0.9740	-0.9998	1.0218	0.9991
GBP/CAD	-1.0268	-0.9996	1.0339	0.9995	-0.9925	-0.9998	1.0406	0.9993
GBP/CHF	-1.0805	-0.9998	1.0872	0.9998	-1.0579	-0.9999	1.1060	0.9999
GBP/EUR	-1.0246	-1.0000	1.0281	1.0000	-0.9947	-1.0000	1.0355	0.9999
GBP/JPY	-1.1353	-0.9999	1.1430	0.9999	-1.1051	-0.9998	1.1555	1.0000
CHF/JPY	-1.0382	-0.9999	1.0436	0.9998	-0.9955	-0.9998	1.0411	0.9993

Table 6.2: Fitted E_αs and R_αs, E_{var}s and R_{var}s for SMA and EMA detrended Thomson Reuters data

The table of all best fit values E_α and E_{var} along with the correlation coefficients R_α and R_{var} for the fits using SMAs and EMAs for each Commerzbank currency pair and source found in this way can be seen below in Table 6.3.

		SMA				EMA			
	source	E_α	R_α	E_{var}	R_{var}	E_α	R_α	E_{var}	R_{var}
AUD/JPY	LN	-0.9571	-0.9998	0.9571	0.9998	-0.9574	-0.9999	0.9592	0.9999
	NY	-0.9494	-0.9998	0.9495	0.9998	-0.9503	-0.9999	0.9522	0.9999
AUD/USD	LN	-0.9315	-0.9998	0.9316	0.9998	-0.9293	-0.9999	0.9311	0.9999
	NY	-0.9291	-0.9998	0.9292	0.9998	-0.9271	-0.9999	0.9290	0.9999
EUR/USD	LN	-1.0857	-0.9991	1.0853	0.9991	-1.0604	-0.9995	1.0613	0.9995
	NY	-1.0309	-0.9977	1.0310	0.9977	-1.0166	-0.9983	1.0182	0.9983
USD/BRL	LN	-0.9505	-0.9992	0.9508	0.9992	-0.9528	-0.9995	0.9551	0.9995
	NY	-0.9527	-0.9992	0.9531	0.9992	-0.9548	-0.9995	0.9571	0.9995
USD/CAD	LN	-0.8721	-0.9963	0.8722	0.9963	-0.8654	-0.9971	0.8674	0.9971
	NY	-0.8804	-0.9970	0.8806	0.9970	-0.8735	-0.9975	0.8756	0.9974
USD/CHF	LN	-0.9794	-0.9989	0.9795	0.9989	-0.9667	-0.9995	0.9683	0.9995
	NY	-0.9691	-0.9990	0.9688	0.9990	-0.9564	-0.9995	0.9575	0.9994
USD/CNH	LN	-1.0407	-1.0000	1.0410	1.0000	-1.0324	-1.0000	1.0345	1.0000
	NY	-1.0308	-0.9999	1.0311	0.9999	-1.0253	-0.9999	1.0275	0.9999

Table 6.3: Fitted E_αs, R_αs, E_{var}s and R_{var}s for SMA and EMA detrended Commerzbank data

See Appendix C for further example graphs of the calibrated reversion strength and example graphs of the long-term variance as a function of τ.

6.3 Detrending moving average analysis

Finally, we conducted a DMA on the daily Thomson Reuters data, and compared the estimated Hurst exponent to the scaling exponent of the estimated long-term variance as a function of τ found in Section 6.2.

6.3.1 Methodology

We conducted the DMA according to the algorithm outlined originally in Alessio et al.'s paper [81]. This was done in the following way: Starting with the daily Thomson Reuters time series $\{X_i\}_{1\leq i\leq n}$, we chose a $\tau_{\max} = 500 \ll n$ to be the largest MA window we would analyse in days. For each MA window τ we next computed the series' simple lagging moving averages $\{\overline{X}_{i,\tau}\}_{\tau\leq i\leq n}$ where

$$\overline{X}_{i,\tau} = \frac{1}{\tau}\sum_{k=0}^{\tau-1} X_{i-k}\,. \tag{6.4}$$

We did this for $2 \leq \tau \leq \tau_{\max}$. The scaling quantity $\sigma^2(\tau)$ was then computed as

$$\sigma^2(\tau) = \frac{1}{n-\tau_{\max}}\sum_{i=\tau_{\max}}^{n}\left[X_i - \overline{X}_{i,\tau}\right]^2. \tag{6.5}$$

This makes $\sigma^2(\tau)$ the variance of the SMA_τ-detrended series, where each detrended series is cropped to be the length $n-\tau_{\max}+1$ of the shortest detrended series. We then conducted a line fit to $\log\sigma^2(\tau)$ as a function of $\log\tau$ in order to determine the slope $2H$. In other words, we calibrated the relationship

$$\sigma^2(\tau) = c\tau^{2H}\,, \tag{6.6}$$

making H the Hurst exponent of the series. Due to the multiscaling property of FX data it should be noted that H in this case refers to $H(2)$, i.e. the second-order Hurst exponent, which does not equal the $H(1)$ we determined in Chapter 4.

See Figure 6.5 for a plot of $\log\sigma^2(\tau)$ as a function of $\log\tau$ for CHF/JPY.

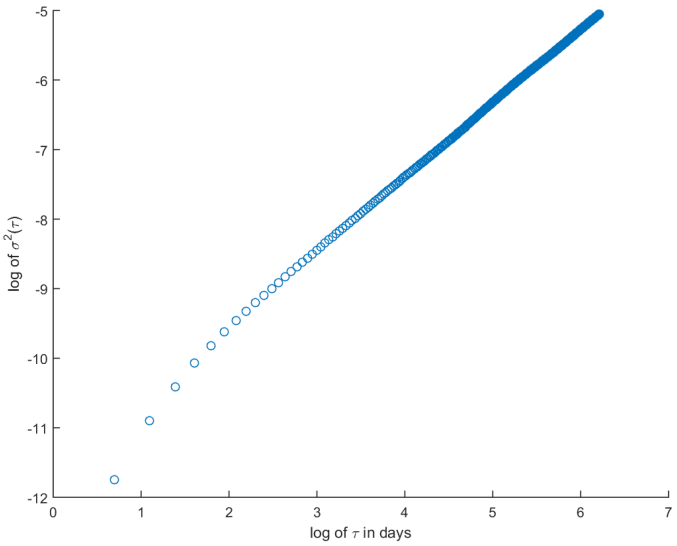

Figure 6.5: Log of σ^2_{DMA} of CHF/JPY as a function of log of τ in days

Note that interpolation of weekends may affect the variance of the series detrended over small numbers of days. Furthermore, we observe a curvature as reported in the literature for methods of estimating the Hurst exponent. See Appendix C for more example graphs.

6.3.2 Results

We used the DMA method to find the Hurst exponents of all series in the Thomson Reuters data set, and compared the computed $2H_{\text{DMA}}$ to the scaling exponent E_{var} of the SMA estimators found in Section 6.2. See Table 6.4 for these values side by side.

	$2H_{\text{DMA}}$	E_{var}
CAD	1.0674	1.0355
GBP	1.1077	1.0676
JPY	1.1281	1.1247
EURAUD	0.9942	0.9709
EURCAD	1.1124	1.0879
EURCHF	1.0998	1.0745
EURGBP	1.0507	1.0292
EURJPY	1.1760	1.1491
EUR	1.1157	1.1045
EURNOK	1.0352	1.0001
EURSEK	1.0660	1.0385
GBPAUD	1.0100	1.0176
GBPCAD	1.0764	1.0339
GBPCHF	1.1460	1.0872
GBPEUR	1.0493	1.0281
GBPJPY	1.1746	1.1430
CHFJPY	1.0770	1.0436

Table 6.4: Estimated $2H_{\text{DMA}}$ and E_{var} for Thomson Reuters data

We found a very strong linear relationship between $\log \sigma^2_{\mathrm{DMA}}(\tau)$ and $\log \tau$, as would be expected due to the well-known fractal properties of FX series. More interestingly, we found a strong correlation between $2H_{\mathrm{DMA}}$ and E_{var}, with a correlation coefficient of 0.9573.

6.4 Discussion

We have calibrated a model of an OUP with time-dependent reversion level to FX data. We have observed a clear and systematic dependence of the calibrated model parameters on the time constant used to detrend the process. Thus we conclude that when calibrating this model to a time series using methods such as those described in Chapter 5, or when using trading strategies where mean reversion to a moving average is predicted, we are faced with a choice of what MA, or what reversion strength, we want to calibrate. In other words, the MA or the reversion strength of the process becomes an input parameter of the calibration, and we have in this chapter shown the effects of this parameter. Furthermore, we have shown that the effects of this input parameter are determined by the Hurst exponent of the time series.

It should be noted that this part of the research is a calibration rather than a parameter estimation study, as we do not know whether the time series really follow such a process, and the results should be interpreted accordingly. It would be beneficial to a more complete understanding of these results to conduct the same analysis on a simulated OUP with time-dependent reversion level.

The implications of this for trading strategies need to be further explored, but our findings support the trading of FX rates on multiple time scales at once, and a clear recommendation is to take the Hurst exponent into account when choosing the width of bands around a moving average. Furthermore, the term "mean reversion-based trading strategies", when applied to FX rates, may be slightly misleading since it is not clear whether the moving average does represents a true reversion level or an arbitrarily chosen time scale.

Of course subtracting a moving average acts as a high-pass filter, and therefore our method effectively separates the frequencies occurring in the time series into those contributing to the underlying reversion level, and those that are the overlayered mean-reverting process. This makes intuitive sense, as the lowest contributing frequencies will be things such as political changes, and the highest will be noise generated by algorithmic high-frequency trading, with things such as economic factors, seasonality factors, and news events all lying somewhere on this scale, and choosing which of these levels are seen as "underlying" and which are overlayered in some ways is an arbitrary decision, with the separation of the nominal exchange rate into the real exchange rate and the PPP rate being just one quantifiable separation.

Chapter 7

Conclusions and future work

This chapter presents the conclusions that may be drawn from the research conducted as part of this thesis. We will also make some recommendations for potential future work to build on the research, and summarize the thesis's contributions to science.

7.1 Scaling of log returns

We observed the scaling of mean absolute log returns in our real-world FX data, and in doing so have extended the ranges of intervals over which we know the law to hold. Using simulated data, we have shown that not only Brownian motion, but also an Ornstein–Uhlenbeck process with time-dependent reversion level obeys this scaling law, albeit not with the same exponents as found in FX data. We have shown that after detrending by subtracting a moving average, the dependence of the mean absolute returns of log FX rates on the observation steps resembles that found in a standard Ornstein–Uhlenbeck model, which on a log-log scale is a linear relationship for small intervals which flattens for larger observation steps. The same is true both for a detrended Wiener process and a detrended Ornstein–Uhlenbeck process with time-dependent reversion level. However, we have shown that in the detrended series the level at which the process flattens depends on the time constant used to compute the moving average.

We conclude from our findings that there is no evidence of raw logarithmic FX rates being mean reverting with constant reversion level on the time scales we can currently observe. However, depending on the shape of the underlying reversion level, a model of FX rates being mean reverting to a time-dependent reversion level appears not incompatible with the scaling laws observed in the real-world data, although modifications, such as introducing fractional noise, would have to be made to the model to adjust the scaling exponent. It should also be noted that while this model appears feasible, a simple Brownian motion also displays these behaviours, meaning that the decision to choose a model of FX rates with a mean reverting component over, say, a fractal Brownian motion model, is only motivated by external factors such as models of FX rate determination or the performance of known trading strategies.

Future work

Due to the fast-changing nature of the foreign exchange market and technology, it is interesting of itself to re-test for the standard scaling law as the market ages and evolves, and smaller and larger time intervals become available. In order to reduce the bias of interpolation, which becomes particularly troublesome for high-frequency data, other ways of testing for the power law may be used. This could for example be done by treating each price change in the series as an individual data point to which we then fit the scaling law, although the computational cost of this has to be considered.

Different detrending methods, such as subtracting price levels known from external data from the series, could be used to detrend the process.

The models we used for the logarithmic FX data, namely an Ornstein–Uhlenbeck process with random walk reversion level and a Brownian motion, could be refined by introducing fractal noise in order to adjust the scaling exponent to that found in FX data. In this case, the models could be fitted to the real-world series and their goodness of fit could be compared. Different types of reversion level and more complex mean reverting processes could also be tested.

7.2 OUP parameter estimation under various conditions

We observed a variety of effects of the process and observation parameters on the reliability of standard parameter estimators of the standard OUP based on finite samples, using synthetic data. In particular, we found that non-regular observation of the process caused in some cases a qualitative change in the mean errors and mean square errors of the process estimators. The interdependence between the factors is clearly quite complex and means that when dealing with finite and irregular, incomplete or interpolated observations, the literature on the ME and MSE of the estimators in case of regular observations no longer applies, and we may be dealing with unknown errors in our estimates.

We also tested two methods for estimating the parameters of an OUP with unknown time-dependent reversion level, using a simulated OUP with an underlying sine function. We found both methods to greatly outperform the standard estimators. However, both methods rely on the computation of a moving average of the series, which requires the input of a time constant, which we chose arbitrarily. Yet, the outcome of the estimation greatly depends on this parameter. This means that currently these methods may be best suited to cases where external knowledge informs the choice of this time constant. Furthermore, both methods employ a symmetrical moving average. This means that they cannot be applied in real-time, although the methods could be adapted to employ lagging MAs.

Future work

Since there is a great number of factors affecting the reliability of estimators, and since effects additionally depend on the orders of magnitude of the parameters, there remains great scope for further analysis. An exhaustive study of these effects should, for example, include an analysis of the dependence of estimator MSEs and MEs on the observation window when keeping the number of observations constant, the effect of the initial displacement of the process, as well as an analysis of the non-near-unit-root case. Furthermore, the level of irregularity of observations could be quantified, for example as the size of the time window around the regular sampling point, so that the dependence of the MEs and MSEs of the estimators on this irregularity parameter could be observed. Some of the methods proposed in the literature for improving parameter estimates could also be tested, and a case where the reversion level is known would be of interest. Additionally, an analytical description of these effects would provide great insight.

A weakness of the two estimation methods for OUPs with time-dependent reversion level is the arbitrary input parameter of the moving average. Finding a way of determining an optimal time constant, or even a different convolution altogether, would be invaluable in improving these methods. Additionally, this should be done for a variety of underlying reversion levels, as well as process and observation parameters. For real-time application both methods would have to be adapted by using a lagging moving average.

7.3 Time-dependent OUP reversion levels and the Hurst exponent

Using our estimation method from Part 2, we calibrated a model of an OUP with time-dependent reversion level to our real-world FX data sets. We found a clear dependence of the calibrated process parameters on the input parameter of the calibration method, i.e. the time constant of the moving average. We then conducted a detrending moving average analysis on the real-world data and showed that the thus obtained Hurst exponent describes the dependence of the calibrated long-term variance of the OUP on the input parameter of the calibration method. One possible interpretation of this is that rather than there being one true underlying reversion level, the self-similarity of the process means that it is instead mean-reverting on a spectrum of time scales, i.e. the mean reversion is scale-free. Alternatively, it may mean that the mean reversion is inferred into the data by the calibration itself. In both cases our findings are particularly relevant to mean reversion based trading strategies.

Future work

A deeper understanding of our findings could be gathered by conducting the same analysis on a variety of simulated processes with known properties. Also, before calibrating the OUP parameters to the detrended series, a mean reversion test such as a Dickey–Fuller test

could be applied to the series. When describing the calibrated parameters as functions of the time constant, the fitting of alternative functions to the relationship may be possible. It may also be worth exploring whether there is a relationship between the calibrated reversion strength and the Hurst exponent.

Further insight could be gained by exploring how our findings may improve mean reversion based trading strategies using moving averages as approximations of the fundamental value.

7.4 Contributions to science

We have contributed to science by taking a step towards bridging the gap between the self-similarity of FX time series and models of FX rates being mean reverting. In addition to extending the range of intervals over which we know the scaling law of FX log returns to hold, we have demonstrated that a model of log nominal exchange rates following a mean reverting process with time-dependent reversion level is compatible with the scaling law we observe in real-world FX data. We have found a dependence of the calibrated parameters of this model on the way the reversion level is defined, and have shown a relationship between this dependence and the Hurst exponent of the series, which to the best of our knowledge has never been shown before. These findings may help refine models of FX rates and trading strategies. Furthermore, we have shed some light on the reliability of standard parameter estimators of the OUP in the case of finite, irregular, incomplete, or interpolated observations. Even though in practical application data sets are imperfect, the literature on the properties of estimators has so far mostly been focused on perfectly regular data sets. Finally, we have tested two methods for estimating the parameters of Ornstein–Uhlenbeck processes with time-dependent reversion level. The literature on estimating the parameters of such processes where the reversion level is unknown is very scarce, and we hope to contribute towards developing methods to solve this problem.

In Part 1, the scaling law relating the volatility of exchange prices to the time interval over which it is measured was verified using a novel data set and a greater range of intervals than we have found reported in the literature. We thus have extended our knowledge of the ranges of intervals over which the scaling law holds. We also showed that the scaling law may be consistent with a model of FX rates reverting to a time-dependent underlying value, and that the mean absolute returns of detrended data resemble those of an Ornstein–Uhlenbeck process. This helps bridge the gap between this scaling behaviour, which has so far been reported as a stylized fact in the literature, and the construction of a stochastic model of FX rates.

In Part 2, we presented numerical findings regarding the accuracy of standard parameter estimators of the Ornstein–Uhlenbeck process in the case of irregular observations. As far as we know, the effect of the true parameters of the OUP on estimator accuracy in the case of irregular observations and interpolation has never been reported before. These findings are very relevant wherever OUP parameters are estimated on imperfect

data, as we have shown significant effects of the irregularity, and a qualitative difference between the effect of parameters on estimator accuracy between the regular, irregular, interpolated and business time cases. Secondly, we have proposed a method of estimating the parameters of OUPs with time-dependent reversion level which we have not found reported elsewhere, and have tested this method against another method reported in the literature, which to the best of our knowledge has not been tested before, showing that the two perform similarly. There is currently very little literature on the subject of estimating the parameters of an OUP with unknown time-dependent reversion level, and our research may help in developing and refining such methods, which have a great number of potential applications not only in finance but also in a wide range of other areas.

In Part 3, we have shown that the calibration of a model of an OUP reverting to a time-dependent reversion level, which relies on detrending the process, depends heavily on the detrending method used, and shown empirically the relationships between the calibrated parameters and the detrending parameter. These findings are relevant not only to the calibration of OUPs with time-dependent reversion level, but also to the parameter estimation of such processes. We also conducted a detrending moving average analysis on FX series and determined the Hurst exponent of the series and showed that the dependence of the calibrated parameters on the detrending parameter is directly related to the Hurst exponent of the series. To the best of our knowledge, this has never been done before, and we suggest that it may be of great use for improving mean reversion based trading strategies and models of FX time series.

Bibliography

[1] R. Gençay, G. Ballocchi, M. Dacorogna, R. Olsen, and O. Pictet. Real-time trading models and the statistical properties of foreign exchange rates. *International Economic Review*, 43(2):463–491, 2002.

[2] M. Susai and Y. Yoshida. We missed it again! why do so many market orders in high-frequency fx trading fail to be executed? In G. N. Gregoriou, editor, *Handbook of high frequency trading*, chapter 13, pages 215–235. Elsevier, London, UK, 2015.

[3] M. Aloud, M. Fasli, E. Tsang, A. Dupuis, and R. Olsen. Stylized facts of the FX market transactions data: An empirical study. *Journal of Finance and Investment Analysis*, 2(4):145–183, 2013.

[4] H. H. Lean, V. Mishra, and R. Smyth. The relevance of heteroskedasticity and structural breaks when testing for a random walk with high-frequency financial data: Evidence from asean stock markets. In G. N. Gregoriou, editor, *Handbook of high frequency trading*, chapter 4, pages 59–74. Elsevier, London, UK, 2015.

[5] G. Oh, S. Kim, and C. Eom. Market efficiency in foreign exchange markets. *Physica A: Statistical Mechanics and its Applications*, 382(1):209–212, 2007.

[6] G. Gözgör, C. Memiş, and G. Karabulut. The application of stochastic processes in currency exchangerate forecasting and benchmarking for usd-tl and euro-tl exchange rates. In *International Conference On Applied Economics 2010*, 2010.

[7] J. James, I. W. Marsh, and L. Sarno, editors. *Handbook of Exchange Rates*. John Wiley & Sons, Inc., Hoboken, New Jersey, 2012.

[8] Bank for International Settlements. Triennial central bank survey. `www.bis.org/statistics/rpfx19_fx.pdf`, September 2019. Accessed: September, 2019.

[9] D. M. Guillaume, M. M. Dacorogna, R. R. Davé, U. A. Müller, R. B. Olsen, and O. V. Pictet. From the bird's eye to the microscope: A survey of new stylized facts of the intra-daily foreign exchange markets. *Finance and Stochastics*, 1(2):95–129, 1997.

[10] M. R. King, C. Osler, and D. Rime. Foreign exchange market structure, players, and evolution. In J. James, I. W. Marsh, and L. Sarno, editors, *Handbook of Exchange Rates*, chapter 1, pages 3–44. John Wiley & Sons, Inc., Hoboken, New Jersey, 2012.

[11] C. J. Neely and P. A. Weller. Technical analysis in the foreign exchange market. In J. James, I. W. Marsh, and L. Sarno, editors, *Handbook of Exchange Rates*, chapter 12, pages 343–373. John Wiley & Sons, Inc., Hoboken, New Jersey, 2012.

[12] V. Charvin, J. Fullwood, and J. James. The fair value of FX options. Do you get what you pay for? *Quantitative Finance*, 14(1):15–23, 2014.

[13] C. Attfield, M. Glod, and J. James. Options and forwards compete for best hedge. *Quantitative Finance*, 1(1):9–11, 2001.

[14] A. Buckley. *International finance*. Pearson, Harlow, UK, 2012.

[15] Bank for International Settlements. High-frequency trading in the foreign exchange market. `https://www.bis.org/publ/mktc05.pdf`, September 2011. Accessed: September, 2019.

[16] M. D. D. Evans and D. Rime. Micro approaches to foreign exchange determination. In J. James, I. W. Marsh, and L. Sarno, editors, *Handbook of Exchange Rates*, chapter 3, pages 73–110. John Wiley & Sons, Inc., Hoboken, New Jersey, 2012.

[17] M. D. Chinn. Macro approaches to foreign exchange determination. In J. James, I. W. Marsh, and L. Sarno, editors, *Handbook of Exchange Rates*, chapter 2, pages 45–71. John Wiley & Sons, Inc., Hoboken, New Jersey, 2012.

[18] K. Cuthbertson and D. Nitzsche. *Quantitative Financial Economics*. John Wiley & Sons, Ltd, Chichester, UK, 2004.

[19] L. Sarno and M. P. Taylor. Purchasing power parity and the real exchange rate. *IMF Staff Papers*, 49(1):65–105, 2002.

[20] P. De Grauwe and P. Rovira Kaltwasser. The exchange rate in a behavioral finance framework. In J. James, I. W. Marsh, and L. Sarno, editors, *Handbook of Exchange Rates*, chapter 4, pages 111–132. John Wiley & Sons, Inc., Hoboken, New Jersey, 2012.

[21] J. M. Poterba and L. H. Summers. Mean reversion in stock prices: Evidence and implications. *Journal of Financial Economics*, 22(1):27–59, 1988.

[22] A. E. Kocagil, N. R. Swanson, and T. Zeng. A new definition for time-dependent price mean reversion in commodity markets. *Economics Letters*, 71(1):9–16, 2001.

[23] C. S. Asness, T. J. Moskowitz, and L. H. Pedersen. Value and momentum everywhere. *The Journal of Finance*, 68(3):929–985, 2013.

[24] I. W. Marsh, E. Passari, and L. Sarno. Purchasing power parity in tradable goods. In J. James, I. W. Marsh, and L. Sarno, editors, *Handbook of Exchange Rates*, chapter 7, pages 189–220. John Wiley & Sons, Inc., Hoboken, New Jersey, 2012.

[25] J. R. Lothian and M. P. Taylor. Real exchange rate behavior: The recent float from the perspective of the past two centuries. *The Journal of Political Economy*, 104(3):488–509, 1996.

[26] R. C. B. da Fonseca, R. Y. Matsushita, M. T. de Castro, and A. Figueiredo. On the time-homogeneous Ornstein—Uhlenbeck process in the foreign exchange rates. *Physics Letters A*, 379(37):2154–2168, 2015.

[27] N. Jegadeesh and S. Titman. Returns to buying winners and selling losers: Implications for stock market efficiency. *The Journal of Finance*, 48(1):65–91, 1993.

[28] L. Menkhoff and M. P. Taylor. The obstinate passion of foreign exchange professionals: Technical analysis. *Journal of Economic Literature*, 45(4):936–972, 2007.

[29] J. James. Robustness of simple trend-following strategies. *Quantitative Finance*, 3(6):C114–C116, 2003.

[30] A. F. Serban. Combining mean reversion and momentum trading strategies in foreign exchange markets. *Journal of Banking & Finance*, 34(11):2720–2727, 2010.

[31] G. E. Uhlenbeck and L. S. Ornstein. On the theory of the Brownian motion. *Physical Review*, 36(5):823–841, 1930.

[32] A. N. Borodin. *Stochastic Processes*. Springer International Publishing AG, Cham, Switzerland, 2013.

[33] A. Einstein. Zur Theorie der Brownschen Bewegung. *Annalen der Physik*, 4(19):371–381, 1906.

[34] S. M. Iacus. *Simulation and Inference for Stochastic Differential Equations*. Springer Science+Business Media, LLC, New York, New York, 2008.

[35] S. Asmussen and P. W. Glynn. *Stochastic Simulation*. Springer Science+Business Media, LLC, New York, New York, 2007.

[36] M. Jeanblanc, M. Yor, and Chesney M. *Mathematical methods for financial markets*. Springer-Verlag London Limited, Heidelberg, Germany, 2009.

[37] P. C. B. Phillips and J. Yu. Maximum likelihood and Gaussian estimation of continuous time models in finance. In T. G. Andersen, R. A. Davis, J.-P. Kreiß, and T. Mikosch, editors, *Handboook of Financial Time Series*, pages 497–530. Springer-Verlag Berlin Heidelberg, Heidelberg, 2009.

[38] D.-P. Brandes. Continuous time autoregressive moving average processes with random Lévy coefficients. *ALEA, Latin American Journal of Probability and Mathematical Statistics*, 14:219–244, 2017.

[39] O. Vasicek. An equilibrium characterization of the term structure. *Journal of Financial Economics*, 5(2):177–188, 1977.

[40] J. Hull and A. White. Pricing interest-rate-derivative securities. *The review of financial studies*, 3(4):573–592, 1990.

[41] L. M. Ricciardi and L. Sacerdote. The Ornstein-Uhlenbeck process as a model for neuronal activity. *Biological Cybernetics*, 35(1):1–9, 1979.

[42] R. Kobayashi, S. Shinomoto, and P. Lansky. Estimation of time-dependent input from neuronal membrane potential. *Neural Computation*, 23(12):3070–3093, 2011.

[43] A. Zapranis and A. Alexandridis. Modeling temperature time-dependent mean reversion with neural networks in the context of derivatives pricing. In *HERCMA, Athens, Greece*, 2007.

[44] F. H. Marín Sánchez and J. S. Palacio. Gaussian estimation of one-factor mean reversion processes. *Journal of Probability and Statistics*, 2013. Article ID 239384.

[45] E. Kreyszig. *Statistische Methoden und ihre Anwendungen*. Vandenhoeck & Ruprecht, Göttingen, Germany, 1991.

[46] C. Y. Tang and S. X. Chen. Parameter estimation and bias correction for diffusion processes. *Journal of Econometrics*, 149(1):65–81, 2009.

[47] P. C. B. Phillips and J. Yu. Jackknifing bond option prices. *The Review of Financial Studies*, 18(2):707–742, 2005.

[48] W. Smith. On the simulation and estimation of the mean-reverting Ornstein-Uhlenbeck process. `https://commoditymodels.files.wordpress.com/2010/02/estimating-the-parameters-of-a-mean-reverting-ornstein-uhlenbeck-process1.pdf`, February 2010. Accessed: July, 2019.

[49] M. Arató, A. Kuki, and A. Szabó. Exact distribution of estimators of parameters in Ornstein-Uhlenbeck processes. *Computers & Mathematics with Applications*, 31(11):45–54, 1996.

[50] M. Arató and S. Fegyverneki. New statistical investigations of the Ornstein-Uhlenbeck process. *Computers and Mathematics with Applications*, 44(5-6):677–692, 2002.

[51] D. Florens-Landais and H. Pham. Large deviations in estimation of an Ornstein–Uhlenbeck model. *Journal of Applied Probability*, 36(1):60–77, 1999.

[52] J. Yu. Bias in the estimation of the mean reversion parameter in continuous time models. *Journal of Econometrics*, 169(1):114–122, 2012.

[53] S. Rieder. Robust parameter estimation for the Ornstein—Uhlenbeck process. *Statistical Methods & Applications*, 21(4):411–436, 2012.

[54] J. C. Cox, J. E. Ingersoll, Jr., and S. A. Ross. A theory of the term structure of interest rates. *Econometrica*, 53(2):385–407, 1985.

[55] K. C. Chan, G. A. Karolyi, F. A. Longstaff, and A. B. Sanders. An empirical comparison of alternative models of the short-term interest rate. *The Journal of Finance*, 47(3):1209–1227, 1992.

[56] E. Martin, U. Behn, and G. Germano. First-passage and first-exit times of a Bessel-like stochastic process. *Physical Review E*, 83(5):051115–1–051115–16, 2011.

[57] K. B. Nowman. Gaussian estimation of single-factor continuous time models of the term structure of interest rates. *The Journal of Finance*, 52(4):1695–1706, 1997.

[58] J. Yu and P. C. B. Phillips. A Gaussian approach for continuous time models of the short-term interest rate. *The Econometrics Journal*, 4(2):210–224, 2001.

[59] S. Sun and X. Zhang. Empirical likelihood estimation of discretely sampled processes of OU type. *Science in China Series A: Mathematics*, 52(5):908–931, 2009.

[60] O. E. Barndorff-Nielsen and N. Shephard. Non-Gaussian Ornstein–Uhlenbeck-based models and some of their uses in financial economics. *Journal of the Royal Statistical Society: Series B (Statistical Methodology)*, 63(2):167–241, 2001.

[61] H. Mai. Efficient maximum likelihood estimation for Lévy-driven Ornstein–Uhlenbeck processes. *Bernoulli*, 20(2):919–957, 2014.

[62] S. Zhang and X. Zhang. A least squares estimator for discretely observed Ornstein—Uhlenbeck processes driven by symmetric α-stable motions. *Annals of the Institute of Statistical Mathematics*, 65(1):89–103, 2013.

[63] Y. Hu and H. Long. Parameter estimation for Ornstein-Uhlenbeck processes driven by α-stable Lévy motions. *Communications on Stochastic Analysis*, 1(2):175–192, 2007.

[64] Y. Hu and H. Long. Least squares estimator for Ornstein–Uhlenbeck processes driven by α-stable motions. *Stochastic Processes and their Applications*, 119(8):2465–2480, 2009.

[65] O. E. Barndorff-Nielsen and A. Basse-O'Connor. Quasi Ornstein–Uhlenbeck processes. *Bernoulli*, 17(3):916–941, 2011.

[66] K. Kubilius, Y. Mishura, K. Ralchenko, and O. Seleznjev. Consistency of the drift parameter estimator for the discretized fractional Ornstein–Uhlenbeck process with Hurst index $H \in (0, \frac{1}{2})$. *Electronic Journal of Statistics*, 9(2):1799–1825, 2015.

[67] B. Bercu, L. Coutin, and N. Savy. Sharp large deviations for the non-stationary Ornstein—Uhlenbeck process. *Stochastic Processes and their Applications*, 122(10):3393–3424, 2012.

[68] M. Maejima and K. Yamamoto. Long-memory stable Ornstein-Uhlenbeck processes. *Electronic Journal of Probability*, 8:19:1–19:18, 2003.

[69] Y. Hu, C. Lee, M. H. Lee, and J. Song. Parameter estimation for reflected Ornstein–Uhlenbeck processes with discrete observations. *Statistical Inference for Stochastic Processes*, 18(3):279–291, 2015.

[70] A. Gloter. Parameter estimation for a discrete sampling of an integrated Ornstein–Uhlenbeck process. *Statistics*, 35:225–243, 2001.

[71] A. Gloter. Parameter estimation for a discretely observed integrated diffusion process. *Scandinavian Journal of Statistics*, 33(1):83–104, 2006.

[72] G. Matulewicz. *Statistical inference of Ornstein-Uhlenbeck processes: generation of stochastic graphs, sparsity, applications in finance.* PhD thesis, Université Paris-Saclay, 2017.

[73] D. Dehay. Parameter maximum likelihood estimation problem for time periodic modulated drift Ornstein Uhlenbeck processes. *Statistical Inference for Stochastic Processes*, 18(1):69–98, 2015.

[74] C. Thierfelder. The trending Ornstein-Uhlenbeck process and its applications in mathematical finance. Master's thesis, Hertford College, University of Oxford, 2015.

[75] F. H. Marín Sánchez and V. M. Gallego. Parameter estimation in mean reversion processes with deterministic long-term trend. *Journal of Probability and Statistics*, 2016. Article ID 5191583.

[76] A. Dupuis and R. B. Olsen. High frequency finance: Using scaling laws to build trading models. In J. James, I. W. Marsh, and L. Sarno, editors, *Handbook of Exchange Rates*, chapter 20, pages 563–584. John Wiley & Sons, Inc., Hoboken, New Jersey, 2012.

[77] P. Embrechts and M. Maejima. *Selfsimilar Processes*. Princeton University Press, Princeton, New Jersey, 2002.

[78] T. Di Matteo. Multi-scaling in finance. *Quantitative Finance*, 7(1):21–36, 2007.

[79] H. E Hurst. The problem of long-term storage in reservoirs. *Hydrological Sciences Journal*, 1(3):13–27, 1956.

[80] R. Hardstone, S.-S. Poil, G. Schiavone, R. Jansen, V. V. Nikulin, H. D. Mansvelder, and K. Linkenkaer-Hansen. Detrended fluctuation analysis: a scale-free view on neuronal oscillations. *Frontiers in Physiology*, 3:1–13, 2012. Article ID 450.

[81] E. Alessio, A. Carbone, G. Castelli, and V. Frappietro. Second-order moving average and scaling of stochastic time series. *The European Physical Journal B*, 27(2):197–200, 2002.

[82] U. A. Müller, M. M. Dacorogna, R. B. Olsen, O. V. Pictet, M. Schwarz, and C. Morgenegg. Statistical study of foreign exchange rates, empirical evidence of a price change scaling law, and intraday analysis. *Journal of Banking and Finance*, 14(6):1189–1208, 1990.

[83] B. Mandelbrot. The variation of certain speculative prices. *The Journal of Business*, 36(4):394–419, 1963.

[84] J. B. Glattfelder, A. Dupuis, and R. B. Olsen. Patterns in high-frequency FX data: discovery of 12 empirical scaling laws. *Quantitative Finance*, 11(4):599–614, 2011.

[85] S. Galluccio, G. Caldarelli, M. Marsili, and Y.-C. Zhang. Scaling in currency exchange. *Physica A: Statistical Mechanics and its Applications*, 245(3-4):423–436, 1997.

[86] M. Aloud, E. Tsang, R. Olsen, and A. Dupuis. A directional-change event approach for studying financial time series. *Economics: The Open-Access, Open-Assessment E-Journal*, 6(36):1–17, 2012.

[87] R. N. Mantegna and H. E. Stanley. Scaling behaviour in the dynamics of an economic index. *Nature*, 376:46–49, 1995.

[88] G. Ballocchi, M. M. Dacorogna, C. M. Hopman, U. A. Müller, and R. B. Olsen. The intraday multivariate structure of the Eurofutures markets. *Journal of Empirical Finance*, 6(5):479–513, 1999.

[89] T. Di Matteo, T. Aste, and Michel M. Dacorogna. Long-term memories of developed and emerging markets: Using the scaling analysis to characterize their stage of development. *Journal of Banking & Finance*, 29(4):827–851, 2005.

Appendix A

Additional graphs relating to Chapter 4

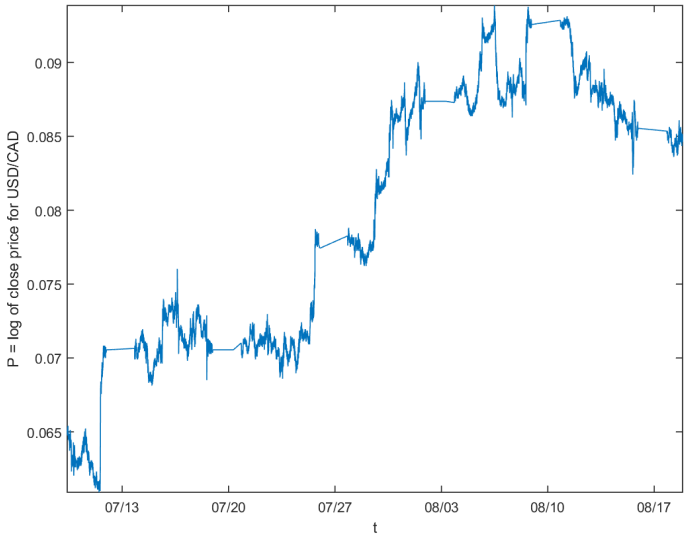

Figure A.1: Minutely logarithmic CAD/USD prices from Thomson Reuters

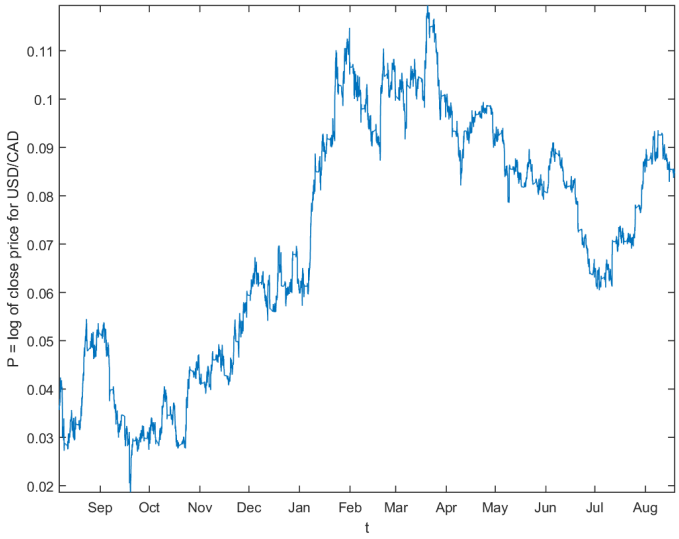

Figure A.2: Hourly logarithmic CAD/USD prices from Thomson Reuters

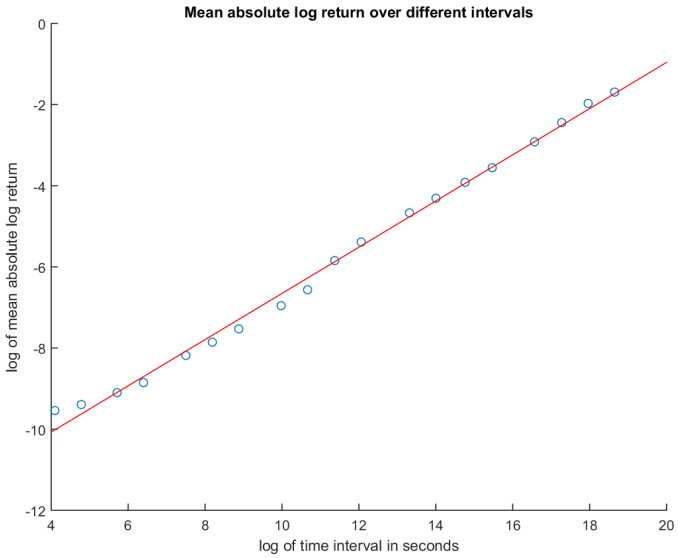

Figure A.3: Scaling of mean absolute log returns in Thomson Reuters data GBP/CHF

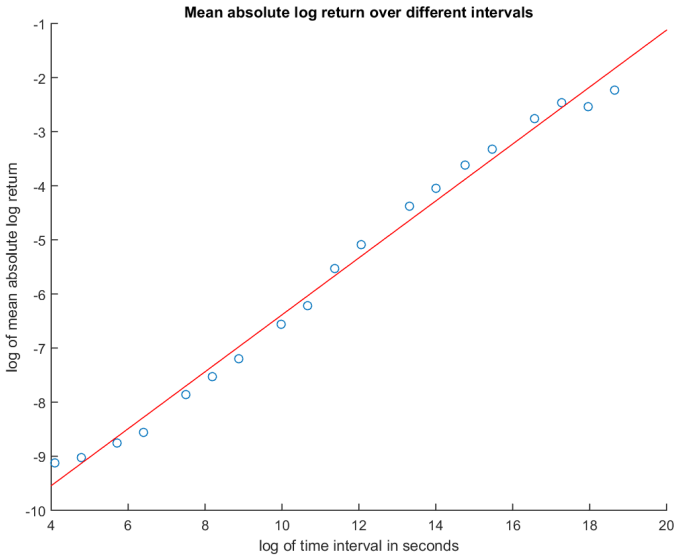

Figure A.4: Scaling of mean absolute log returns in Thomson Reuters data EUR/AUD

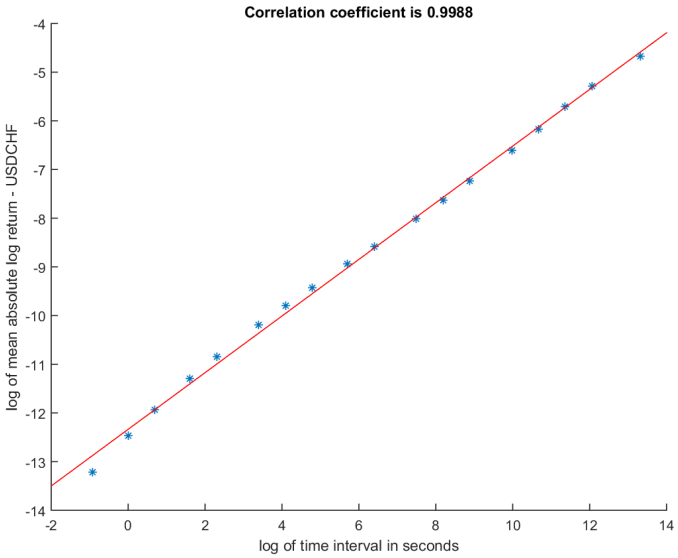

Figure A.5: Scaling of mean absolute returns in LN source Commerzbank data USD/CHF

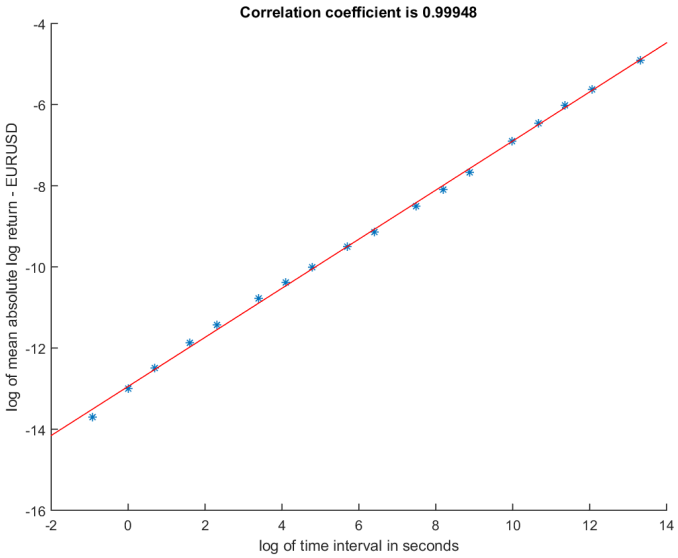

Figure A.6: Scaling of mean absolute log returns in NY source Commerzbank data EUR/USD

Appendix B

Additional tables relating to Chapter 5

α	method	MSE($\hat{\mu}$)	MSE($\hat{\alpha}$)	MSE($\hat{\sigma}$)	ME($\hat{\mu}$)	ME($\hat{\alpha}$)	ME($\hat{\sigma}$)
1.00E-09	stnd	2.04497	1.63E-15	1.19E-15	-0.37933	3.01E-08	1.16E-09
	intp	4,013.27653	7.24E-16	4.05E-12	2.15519	1.90E-08	-2.01E-06
	b-time	4.52535	4.05E-15	6.46E-12	-0.51016	4.77E-08	2.53E-06
6.00E-09	stnd	39.65148	2.19E-16	1.07E-15	0.07869	7.71E-09	-2.51E-10
	intp	27.99999	1.43E-16	4.05E-12	-0.04432	4.84E-09	-2.01E-06
	b-time	12.53743	6.29E-16	6.51E-12	-0.16918	1.55E-08	2.54E-06
1.10E-08	stnd	12.11843	6.82E-17	1.19E-15	-0.08140	3.33E-09	4.81E-10
	intp	30.98837	5.53E-17	4.05E-12	-0.10019	1.93E-09	-2.01E-06
	b-time	416.08171	2.68E-16	6.56E-12	-0.61133	1.14E-08	2.55E-06
1.60E-08	stnd	0.00956	4.95E-17	1.18E-15	-0.00192	2.68E-09	-6.53E-10
	intp	0.01204	4.19E-17	4.06E-12	0.01237	1.53E-09	-2.01E-06
	b-time	0.00956	2.77E-16	6.73E-12	-0.00156	1.32E-08	2.59E-06
2.10E-08	stnd	0.00410	5.26E-17	1.13E-15	-0.00092	2.52E-09	-7.91E-10
	intp	0.00461	4.53E-17	4.05E-12	0.00667	1.43E-09	-2.01E-06
	b-time	0.00411	3.59E-16	6.80E-12	-0.00054	1.57E-08	2.60E-06
2.60E-08	stnd	0.00180	4.61E-17	1.13E-15	-0.00019	1.93E-09	-1.17E-09
	intp	0.00192	4.07E-17	4.06E-12	0.00483	8.34E-10	-2.01E-06
	b-time	0.00181	4.11E-16	6.84E-12	0.00017	1.76E-08	2.61E-06
3.10E-08	stnd	0.00105	4.73E-17	1.19E-15	-0.00125	2.04E-09	1.80E-10
	intp	0.00109	4.15E-17	4.05E-12	0.00243	8.89E-10	-2.01E-06
	b-time	0.00105	5.24E-16	6.97E-12	-0.00093	2.05E-08	2.63E-06
3.60E-08	stnd	0.00070	4.71E-17	1.20E-15	-0.00123	1.83E-09	-5.58E-10
	intp	0.00072	4.18E-17	4.06E-12	0.00170	6.05E-10	-2.01E-06
	b-time	0.00071	6.30E-16	6.98E-12	-0.00091	2.29E-08	2.63E-06
4.10E-08	stnd	0.00054	5.16E-17	1.23E-15	-0.00073	1.87E-09	-1.15E-09
	intp	0.00055	4.59E-17	4.06E-12	0.00167	5.68E-10	-2.01E-06
	b-time	0.00054	7.77E-16	7.13E-12	-0.00044	2.57E-08	2.66E-06
4.60E-08	stnd	0.00044	5.29E-17	1.07E-15	-0.00100	1.93E-09	-1.63E-09
	intp	0.00045	4.67E-17	4.06E-12	0.00104	5.38E-10	-2.01E-06
	b-time	0.00044	9.32E-16	7.22E-12	-0.00072	2.86E-08	2.68E-06
5.10E-08	stnd	0.00031	6.05E-17	1.15E-15	-0.00040	1.84E-09	-3.71E-10
	intp	0.00032	5.43E-17	4.06E-12	0.00138	3.53E-10	-2.01E-06
	b-time	0.00031	1.10E-15	7.33E-12	-0.00013	3.11E-08	2.70E-06
5.60E-08	stnd	0.00024	6.27E-17	1.18E-15	-0.00050	1.66E-09	-8.96E-10
	intp	0.00024	5.69E-17	4.06E-12	0.00108	7.93E-11	-2.01E-06
	b-time	0.00024	1.27E-15	7.40E-12	-0.00024	3.35E-08	2.71E-06
6.10E-08	stnd	0.00021	6.36E-17	1.16E-15	-0.00046	1.83E-09	1.72E-09
	intp	0.00021	5.72E-17	4.05E-12	0.00095	1.54E-10	-2.01E-06
	b-time	0.00021	1.47E-15	7.54E-12	-0.00021	3.65E-08	2.74E-06

Table B.1: Mean errors and MSEs of estimators for varying αs in case of observation gaps in a standard OUP with $\mu = 1$, $\sigma =$ 1.00E-05, $X_0 = 0.5$, $\Delta t_{\text{sim}} =$ 3,600, $\Delta t_{\text{obs}} =$ 3,600, $n_{\text{obs}} =$ 43,801, 1,000 paths

n_{obs}	Δt_{obs}	method	MSE($\hat{\mu}$)	MSE($\hat{\alpha}$)	MSE($\hat{\sigma}$)	ME($\hat{\mu}$)	ME($\hat{\alpha}$)	ME($\hat{\sigma}$)
2,628,001	60	stnd	37.0273	1.72E-16	2.15E-17	-0.12549	6.98E-09	4.09E-10
		intp	38.1845	1.18E-16	3.91E-12	-0.87597	4.49E-09	-1.98E-06
		b-time	10.0698	4.95E-16	6.10E-12	-0.07397	1.43E-08	2.46E-06
1,314,001	120	stnd	1.8602	2.01E-16	3.52E-17	-0.04876	6.22E-09	6.57E-10
		intp	100.2804	1.35E-16	3.91E-12	0.96300	3.63E-09	-1.98E-06
		b-time	1.4624	5.65E-16	6.19E-12	-0.07384	1.32E-08	2.48E-06
525,600	300	stnd	2.2204	2.30E-16	8.20E-17	0.09888	8.35E-09	3.48E-10
		intp	2.2045	1.40E-16	3.92E-12	-0.28491	5.12E-09	-1.98E-06
		b-time	3.3647	6.62E-16	6.31E-12	0.13648	1.65E-08	2.50E-06
262,800	600	stnd	2.1890	2.34E-16	2.22E-16	-0.27345	7.10E-09	1.02E-09
		intp	4.9157	1.55E-16	3.93E-12	-0.16300	4.37E-09	-1.98E-06
		b-time	1.9477	6.48E-16	6.30E-12	-0.31989	1.45E-08	2.50E-06
131,400	1,200	stnd	1.7782	2.01E-16	4.12E-16	-0.08256	6.18E-09	-2.55E-09
		intp	2.5683	1.39E-16	3.97E-12	-0.05571	3.47E-09	-1.99E-06
		b-time	2.7938	5.70E-16	6.31E-12	-0.05366	1.32E-08	2.51E-06
87,600	1,800	stnd	1.4948	1.06E-16	6.62E-16	0.09321	5.48E-09	-5.26E-11
		intp	13.1267	7.81E-17	3.97E-12	-0.47999	3.32E-09	-1.99E-06
		b-time	1.0914	3.29E-16	6.40E-12	0.06096	1.21E-08	2.52E-06
43,800	3,600	stnd	1.7117	1.53E-16	1.11E-15	0.06823	5.72E-09	3.36E-09
		intp	14.1926	1.12E-16	4.03E-12	-0.28331	3.39E-09	-2.01E-06
		b-time	2.9223	4.46E-16	6.63E-12	0.13343	1.25E-08	2.57E-06
21,900	7,200	stnd	10.0447	1.49E-16	2.81E-15	-0.29807	5.91E-09	-3.53E-09
		intp	0.6362	1.09E-16	4.22E-12	-0.18731	3.51E-09	-2.05E-06
		b-time	9.8830	4.50E-16	6.69E-12	-0.44594	1.30E-08	2.58E-06
7,300	21,600	stnd	1.4454	1.82E-16	7.63E-15	-0.25518	7.56E-09	-7.77E-09
		intp	216.3876	1.19E-16	4.88E-12	-1.50011	4.70E-09	-2.21E-06
		b-time	5.4700	6.05E-16	8.03E-12	-0.21633	1.64E-08	2.82E-06
3,650	43,200	stnd	13.7395	1.79E-16	1.36E-14	-0.33195	7.68E-09	9.23E-10
		intp	2.0404	1.05E-16	5.89E-12	-0.07059	4.46E-09	-2.42E-06
		b-time	4.9732	7.00E-16	1.08E-11	-0.22568	1.82E-08	3.27E-06

Table B.2: Mean errors and MSEs of estimators for varying Δts in case of observation gaps in a standard OUP with $\mu = 1$, $\sigma =$ 1.00E-05, $\alpha =$6.34E-09, $X_0 = 0.5$, $\Delta t_{\text{sim}} = 60$, 100 paths

σ	method	MSE($\hat{\mu}$)	MSE($\hat{\alpha}$)	MSE($\hat{\sigma}$)	ME($\hat{\mu}$)	ME($\hat{\alpha}$)	ME($\hat{\sigma}$)
1.00E-07	stnd	1.05E-07	4.58E-21	1.19E-19	0.00002	-4.15E-12	9.01E-12
	intp	1.05E-07	4.58E-21	4.05E-16	0.00002	-4.41E-12	-2.01E-08
	b-time	2.43E-07	3.14E-16	2.75E-12	0.00037	1.77E-08	1.66E-06
1.10E-06	stnd	1.32E-05	5.18E-19	1.29E-17	-0.00015	4.23E-11	-3.74E-11
	intp	1.32E-05	5.17E-19	4.90E-14	-0.00010	2.77E-11	-2.21E-07
	b-time	1.32E-05	3.18E-16	1.28E-12	0.00020	1.78E-08	1.13E-06
2.10E-06	stnd	4.93E-05	1.85E-18	5.24E-17	0.00011	6.38E-11	9.22E-11
	intp	4.95E-05	1.84E-18	1.79E-13	0.00028	1.10E-11	-4.23E-07
	b-time	4.97E-05	3.22E-16	1.13E-12	0.00046	1.78E-08	1.06E-06
3.10E-06	stnd	9.49E-05	3.93E-18	1.14E-16	-0.00069	2.22E-10	-2.12E-10
	intp	9.49E-05	3.87E-18	3.90E-13	-0.00034	1.07E-10	-6.24E-07
	b-time	9.48E-05	3.36E-16	1.35E-12	-0.00035	1.81E-08	1.16E-06
4.10E-06	stnd	1.90E-04	8.09E-18	1.89E-16	-0.00037	4.07E-10	-3.36E-10
	intp	1.91E-04	7.88E-18	6.82E-13	0.00025	2.07E-10	-8.25E-07
	b-time	1.91E-04	3.56E-16	1.75E-12	-0.00003	1.84E-08	1.32E-06
5.10E-06	stnd	2.74E-04	1.13E-17	2.93E-16	0.00021	4.32E-10	-6.09E-10
	intp	2.77E-04	1.09E-17	1.06E-12	0.00117	1.25E-10	-1.03E-06
	b-time	2.75E-04	3.65E-16	2.31E-12	0.00055	1.84E-08	1.51E-06
6.10E-06	stnd	3.72E-04	1.64E-17	4.44E-16	-0.00040	7.91E-10	9.81E-11
	intp	3.77E-04	1.56E-17	1.51E-12	0.00097	3.52E-10	-1.23E-06
	b-time	3.73E-04	3.97E-16	3.01E-12	-0.00006	1.90E-08	1.73E-06
7.10E-06	stnd	4.93E-04	2.18E-17	6.04E-16	-0.00070	9.64E-10	-4.06E-10
	intp	5.01E-04	2.04E-17	2.05E-12	0.00115	3.71E-10	-1.43E-06
	b-time	4.94E-04	4.20E-16	3.80E-12	-0.00035	1.92E-08	1.94E-06
8.10E-06	stnd	6.75E-04	3.01E-17	8.08E-16	-0.00066	1.33E-09	-9.40E-10
	intp	6.92E-04	2.76E-17	2.66E-12	0.00172	5.62E-10	-1.63E-06
	b-time	6.76E-04	4.60E-16	4.79E-12	-0.00032	1.98E-08	2.18E-06
9.10E-06	stnd	9.31E-04	3.78E-17	8.85E-16	-0.00149	1.77E-09	-1.49E-09
	intp	9.57E-04	3.36E-17	3.36E-12	0.00146	7.96E-10	-1.83E-06
	b-time	9.34E-04	5.03E-16	5.87E-12	-0.00116	2.05E-08	2.42E-06

Table B.3: Mean errors and MSEs of estimators for varying σs in case of observation gaps in a standard OUP with $\mu = 1$, $\alpha =$ 3.17E-08, $X_0 = 0.5$, $\Delta t_{\text{sim}} =$ 3,600, $\Delta t_{\text{obs}} =$ 3,600, $n_{\text{obs}} =$ 43,801, 1,000 paths

α	method	MSE($\hat{\mu}$)	MSE($\hat{\alpha}$)	MSE($\hat{\sigma}$)	ME($\hat{\mu}$)	ME($\hat{\alpha}$)	ME($\hat{\sigma}$)
1.00E-09	regular	0.81363	1.64E-15	1.25E-14	-0.40359	3.03E-08	5.36E-09
	off 1	1.01554	1.63E-15	1.26E-14	-0.44035	3.03E-08	4.37E-09
	off 4	231.35356	1.63E-15	1.38E-14	0.07411	3.03E-08	5.52E-09
	random	2.69461	1.64E-15	2.43E-14	-0.36794	3.02E-08	5.16E-09
6.00E-09	regular	99.52145	1.98E-16	1.16E-14	-0.22807	6.91E-09	2.14E-09
	off 1	72.72640	1.98E-16	1.15E-14	0.12836	6.91E-09	2.99E-09
	off 4	117.10324	1.98E-16	1.34E-14	-0.65987	6.90E-09	-2.63E-09
	random	30.06861	1.97E-16	2.18E-14	-0.06244	6.89E-09	-2.39E-09
1.10E-08	regular	1.69080	7.69E-17	1.07E-14	0.06377	3.53E-09	-1.96E-09
	off 1	1.70400	7.69E-17	1.16E-14	0.06430	3.53E-09	7.51E-10
	off 4	2.05522	7.69E-17	1.20E-14	0.07043	3.53E-09	-9.08E-10
	random	7.78971	7.69E-17	2.13E-14	0.03099	3.54E-09	1.01E-08
1.60E-08	regular	0.27435	5.54E-17	1.13E-14	0.02786	2.60E-09	-2.93E-09
	off 1	0.29228	5.54E-17	1.13E-14	0.02842	2.60E-09	-1.41E-09
	off 4	0.30288	5.54E-17	1.26E-14	0.02869	2.61E-09	3.91E-09
	random	0.76016	5.63E-17	2.17E-14	0.03870	2.62E-09	2.02E-08
2.10E-08	regular	0.00346	4.61E-17	1.19E-14	-0.00080	2.38E-09	-4.85E-09
	off 1	0.00346	4.61E-17	1.22E-14	-0.00080	2.38E-09	-4.52E-09
	off 4	0.00347	4.61E-17	1.34E-14	-0.00082	2.38E-09	1.84E-09
	random	0.00345	4.52E-17	2.14E-14	-0.00084	2.33E-09	1.96E-08
2.60E-08	regular	0.00178	4.63E-17	1.12E-14	-0.00346	2.27E-09	9.78E-10
	off 1	0.00178	4.63E-17	1.11E-14	-0.00347	2.27E-09	2.15E-09
	off 4	0.00178	4.64E-17	1.41E-14	-0.00346	2.27E-09	2.55E-09
	random	0.00180	4.7E-17	2.45E-14	-0.00339	2.26E-09	3.46E-08
3.10E-08	regular	0.00110	4.81E-17	1.14E-14	-0.00085	2.07E-09	-1.09E-09
	off 1	0.00110	4.81E-17	1.16E-14	-0.00086	2.07E-09	-1.21E-10
	off 4	0.00110	4.81E-17	1.27E-14	-0.00086	2.07E-09	1.39E-09
	random	0.00109	4.92E-17	2.36E-14	-0.00089	2.11E-09	3.46E-08
3.60E-08	regular	0.00078	5.17E-17	1.13E-14	-0.00252	2.22E-09	-6.45E-09
	off 1	0.00078	5.17E-17	1.16E-14	-0.00252	2.22E-09	-4.79E-09
	off 4	0.00078	5.18E-17	1.26E-14	-0.00253	2.23E-09	2.65E-09
	random	0.00078	5.53E-17	2.47E-14	-0.00255	2.30E-09	4.03E-08
4.10E-08	regular	0.00053	5.07E-17	1.07E-14	-0.00109	2.29E-09	-6.99E-09
	off 1	0.00053	5.07E-17	1.15E-14	-0.00110	2.29E-09	-5.93E-09
	off 4	0.00053	5.08E-17	1.29E-14	-0.00111	2.30E-09	4.08E-09
	random	0.00053	5.32E-17	2.42E-14	-0.00104	2.25E-09	3.58E-08
4.60E-08	regular	0.00044	5.51E-17	1.12E-14	-0.00199	2.03E-09	1.61E-09
	off 1	0.00044	5.52E-17	1.15E-14	-0.00200	2.03E-09	2.08E-09
	off 4	0.00044	5.52E-17	1.26E-14	-0.00201	2.04E-09	9.69E-09
	random	0.00044	5.99E-17	2.70E-14	-0.00201	2.14E-09	6.08E-08
5.10E-08	regular	0.00031	5.72E-17	1.11E-14	0.00000	1.33E-09	-5.95E-09
	off 1	0.00031	5.72E-17	1.16E-14	-0.00001	1.33E-09	-4.75E-09
	off 4	0.00031	5.72E-17	1.25E-14	-0.00001	1.33E-09	1.16E-09
	random	0.00031	6.3E-17	2.47E-14	0.00003	1.34E-09	5.38E-08
5.60E-08	regular	0.00025	5.53E-17	1.07E-14	-0.00044	1.36E-09	-3.83E-09
	off 1	0.00025	5.53E-17	1.12E-14	-0.00044	1.36E-09	-4.23E-09
	off 4	0.00025	5.53E-17	1.27E-14	-0.00045	1.37E-09	1.25E-08
	random	0.00025	6.03E-17	2.62E-14	-0.00039	1.32E-09	6.35E-08
6.10E-08	regular	0.00021	6.38E-17	1.22E-14	-0.00047	1.38E-09	-8.06E-10
	off 1	0.00021	6.38E-17	1.24E-14	-0.00046	1.38E-09	-1.97E-09
	off 4	0.00021	6.39E-17	1.37E-14	-0.00048	1.39E-09	1.19E-08
	random	0.00022	7.24E-17	2.66E-14	-0.00047	1.38E-09	7.13E-08

Table B.4: Mean errors and MSEs of estimators for varying αs in case of irregular observations in a standard OUP with $\mu = 1$, $\sigma =$ 1.00E-05, $X_0 = 0.5$, $\Delta t_{\text{sim}} =$ 3,600, $\Delta t_{\text{obs}} =$ 36,000, $n_{\text{obs}} =$ 4,380, 1,000 paths

α	method	MSE($\hat{\mu}$)	MSE($\hat{\alpha}$)	MSE($\hat{\sigma}$)	ME($\hat{\mu}$)	ME($\hat{\alpha}$)	ME($\hat{\sigma}$)
1.00E-08	regular	3.11E+00	7.38E-17	1.16E-14	6.72E-02	4.08E-09	-5.54E-09
	off 1	1.90E+00	7.38E-17	1.23E-14	5.41E-02	4.09E-09	-3.84E-09
	off 4	9.59E-01	7.38E-17	1.33E-14	2.83E-02	4.09E-09	1.97E-09
	random	1.69E+00	7.43E-17	2.28E-14	3.69E-03	4.11E-09	9.67E-09
6.01E-06	regular	1.73E-08	6.77E-15	1.10E-14	-5.30E-07	4.01E-09	-1.12E-09
	off 1	1.72E-08	1.30E-14	1.63E-14	-8.56E-07	6.56E-09	5.66E-08
	off 4	1.75E-08	6.17E-14	4.21E-13	-3.28E-06	3.61E-08	5.53E-07
	random	2.33E-08	6.41E-12	1.18E-11	1.17E-05	6.65E-08	2.78E-06
1.20E-05	regular	4.37E-09	1.92E-14	1.17E-14	-2.57E-06	-5.74E-09	2.61E-10
	off 1	4.42E-09	1.28E-13	1.95E-14	-2.45E-06	-1.59E-08	5.68E-08
	off 4	4.49E-09	1.07E-12	5.07E-13	-3.92E-06	9.38E-08	5.37E-07
	random	6.54E-09	4.41E-11	1.50E-11	6.18E-06	-3.12E-09	2.72E-06
1.80E-05	regular	2.07E-09	4.59E-14	1.24E-14	-7.81E-07	7.57E-09	-9.70E-09
	off 1	2.08E-09	5.50E-13	2.27E-14	-6.39E-07	2.38E-08	2.90E-08
	off 4	2.21E-09	5.16E-12	3.76E-13	-1.62E-06	1.69E-07	3.67E-07
	random	3.25E-09	1.32E-10	1.58E-11	6.56E-06	-2.58E-08	2.35E-06
2.40E-05	regular	1.12E-09	9.64E-14	1.35E-14	-1.14E-06	-1.19E-08	3.14E-09
	off 1	1.14E-09	1.46E-12	3.73E-14	-1.17E-06	-7.36E-09	1.92E-08
	off 4	1.23E-09	1.39E-11	2.98E-13	-1.12E-07	-6.50E-08	2.01E-07
	random	1.86E-09	1.90E-10	1.18E-11	2.92E-06	-1.81E-06	1.52E-06
3.00E-05	regular	8.18E-10	2.03E-13	1.47E-14	-2.76E-07	1.94E-08	-2.01E-09
	off 1	8.38E-10	2.88E-12	5.29E-14	-5.16E-08	-2.34E-08	1.24E-09
	off 4	8.51E-10	2.61E-11	3.54E-13	-6.14E-08	-6.97E-08	6.13E-08
	random	1.31E-09	2.71E-10	1.12E-11	4.15E-06	-3.47E-06	1.17E-06
3.60E-05	regular	5.7E-10	4.38E-13	1.69E-14	-5.08E-07	-6.97E-09	-1.25E-09
	off 1	5.59E-10	4.55E-12	6.75E-14	-2.19E-07	-9.88E-08	-6.56E-09
	off 4	5.78E-10	4.02E-11	4.62E-13	6.57E-07	-4.34E-07	-4.27E-08
	random	9.1E-10	4.02E-10	1.05E-11	3.41E-06	-4.77E-06	7.55E-07
4.20E-05	regular	4.02E-10	7.98E-13	2.10E-14	6.57E-07	-1.22E-09	-3.06E-09
	off 1	4.14E-10	6.47E-12	8.06E-14	1.15E-06	-3.99E-08	-1.37E-08
	off 4	4.46E-10	5.09E-11	5.09E-13	4.14E-07	-7.98E-07	-1.14E-07
	random	6.98E-10	5.42E-10	1.05E-11	3.86E-06	-6.86E-06	4.24E-07
4.80E-05	regular	3.42E-10	1.60E-12	2.64E-14	-1.82E-07	9.84E-08	-6.86E-10
	off 1	3.42E-10	8.38E-12	8.60E-14	-3.29E-08	-2.02E-07	-3.14E-08
	off 4	3.56E-10	6.41E-11	5.80E-13	6.03E-07	-2.13E-06	-2.48E-07
	random	5.79E-10	6.66E-10	9.61E-12	2.22E-06	-8.58E-06	6.89E-08
5.40E-05	regular	2.87E-10	2.92E-12	3.17E-14	4.65E-07	3.52E-08	3.33E-09
	off 1	2.89E-10	1.00E-11	8.32E-14	4.28E-07	-4.03E-07	-3.77E-08
	off 4	2.8E-10	7.43E-11	5.97E-13	2.87E-07	-3.09E-06	-3.22E-07
	random	4.47E-10	7.97E-10	8.46E-12	1.87E-06	-1.20E-05	-3.16E-07
6.00E-05	regular	2.35E-10	5.14E-12	4.49E-14	-8.60E-07	7.08E-08	-1.14E-09
	off 1	2.4E-10	1.30E-11	9.15E-14	-5.23E-07	-5.24E-07	-5.28E-08
	off 4	2.65E-10	8.80E-11	6.12E-13	-1.29E-07	-4.88E-06	-4.39E-07
	random	3.76E-10	9.16E-10	8.05E-12	3.87E-07	-1.56E-05	-6.26E-07
6.60E-05	regular	2.12E-10	9.72E-12	6.20E-14	-1.05E-07	6.74E-08	-5.22E-11
	off 1	2.06E-10	1.73E-11	1.07E-13	-3.38E-07	-7.05E-07	-5.95E-08
	off 4	2.22E-10	1.03E-10	6.22E-13	3.92E-07	-6.46E-06	-5.24E-07
	random	3.41E-10	1.14E-09	8.79E-12	1.78E-06	-1.84E-05	-8.75E-07

Table B.5: Mean errors and MSEs of estimators for larger αs in case of irregular observations in a standard OUP with $\mu = 1$, $\sigma =$ 1.00E-05, $X_0 = 0.5$, $\Delta t_{\text{sim}} =$ 3,600, $\Delta t_{\text{obs}} =$ 36,000, $n_{\text{obs}} =$ 4,380, 1,000 paths

σ	method	MSE($\hat{\mu}$)	MSE($\hat{\alpha}$)	MSE($\hat{\sigma}$)	ME($\hat{\mu}$)	ME($\hat{\alpha}$)	ME($\hat{\sigma}$)
1.00E-07	regular	6.33E-13	1.61E-18	1.25E-18	2.56E-08	-4.65E-11	1.43E-11
	off 1	1.25E-11	6.29E-14	1.17E-12	-2.14E-07	1.47E-08	1.02E-06
	off 4	1.23E-10	6.43E-13	1.31E-11	-2.10E-06	1.16E-07	3.42E-06
	random	2.37E-09	5.16E-11	7.84E-11	1.11E-05	5.88E-07	8.02E-06
1.10E-06	regular	7.60E-11	1.87E-16	1.38E-16	4.71E-08	-3.00E-10	2.09E-10
	off 1	8.84E-11	6.15E-14	2.71E-13	-2.45E-07	1.74E-08	4.61E-07
	off 4	2.05E-10	6.15E-13	8.20E-12	-1.49E-06	7.36E-08	2.61E-06
	random	2.15E-09	4.58E-11	6.49E-11	7.48E-06	7.20E-07	7.11E-06
2.10E-06	regular	3.02E-10	6.94E-16	4.78E-16	-2.95E-07	-4.25E-10	-6.35E-10
	off 1	3.08E-10	6.22E-14	1.10E-13	-4.57E-07	1.40E-08	2.86E-07
	off 4	4.17E-10	6.16E-13	5.28E-12	-2.19E-06	1.19E-07	2.04E-06
	random	2.47E-09	5.03E-11	5.09E-11	5.86E-06	1.07E-06	6.14E-06
3.10E-06	regular	6.88E-10	1.59E-15	1.09E-15	1.09E-06	-1.48E-09	-8.87E-10
	off 1	7.04E-10	6.29E-14	5.14E-14	1.09E-06	5.43E-09	1.92E-07
	off 4	8.01E-10	6.51E-13	3.25E-12	-1.27E-06	1.54E-07	1.57E-06
	random	3.20E-09	4.62E-11	4.24E-11	8.54E-06	9.17E-07	5.51E-06
4.10E-06	regular	1.09E-09	2.63E-15	2.04E-15	9.57E-07	4.31E-10	-2.21E-09
	off 1	1.11E-09	5.93E-14	3.67E-14	8.08E-07	1.97E-08	1.59E-07
	off 4	1.22E-09	6.32E-13	2.48E-12	-1.19E-06	1.43E-07	1.34E-06
	random	3.53E-09	4.33E-11	3.72E-11	8.87E-06	8.33E-07	5.07E-06
5.10E-06	regular	1.66E-09	3.82E-15	2.92E-15	-1.40E-06	3.62E-09	7.80E-10
	off 1	1.65E-09	6.35E-14	2.52E-14	-1.73E-06	1.71E-08	1.28E-07
	off 4	1.73E-09	6.28E-13	1.68E-12	-3.74E-06	1.43E-07	1.10E-06
	random	4.04E-09	4.64E-11	2.97E-11	5.32E-06	9.36E-07	4.53E-06
6.10E-06	regular	2.31E-09	5.30E-15	4.30E-15	1.75E-06	1.59E-09	-8.05E-10
	off 1	2.34E-09	6.08E-14	2.06E-14	1.54E-06	1.18E-08	1.05E-07
	off 4	2.41E-09	5.91E-13	1.34E-12	-2.73E-07	1.02E-07	9.66E-07
	random	4.54E-09	3.72E-11	2.61E-11	9.65E-06	4.61E-07	4.17E-06
7.10E-06	regular	3.30E-09	7.88E-15	5.71E-15	-1.27E-06	7.41E-09	-3.87E-09
	off 1	3.32E-09	6.44E-14	1.79E-14	-1.90E-06	3.65E-08	8.79E-08
	off 4	3.42E-09	5.62E-13	1.03E-12	-3.52E-06	1.24E-07	8.37E-07
	random	6.04E-09	4.07E-11	2.17E-11	4.43E-06	7.95E-07	3.71E-06
8.10E-06	regular	4.14E-09	1.02E-14	7.25E-15	2.85E-06	1.21E-09	-5.59E-09
	off 1	4.10E-09	5.99E-14	1.62E-14	2.59E-06	-1.13E-09	7.19E-08
	off 4	4.26E-09	5.55E-13	7.94E-13	1.15E-06	1.10E-07	7.29E-07
	random	6.71E-09	3.71E-11	2.00E-11	8.01E-06	5.96E-07	3.46E-06
9.10E-06	regular	5.61E-09	1.23E-14	9.51E-15	-3.03E-06	4.08E-10	9.79E-10
	off 1	5.64E-09	6.34E-14	1.77E-14	-3.30E-06	1.35E-08	6.74E-08
	off 4	5.76E-09	5.37E-13	6.16E-13	-4.93E-06	7.71E-08	6.29E-07
	random	8.14E-09	4.15E-11	1.92E-11	4.04E-06	8.97E-07	3.24E-06

Table B.6: Mean errors and MSEs of estimators for varying σs in case of irregular observations in a standard OUP. $\mu = 1$, $\alpha =$ 1.00E-5, $X_0 = 0.5$, $\Delta t_{\text{sim}} =$ 3,600, $\Delta t_{\text{obs}} =$ 36,000, $n_{\text{obs}} =$ 4,380, 1,000 paths.

σ	method	MSE($\hat{\mu}$)	MSE($\hat{\alpha}$)	MSE($\hat{\sigma}$)	ME($\hat{\mu}$)	ME($\hat{\alpha}$)	ME($\hat{\sigma}$)
0.000001	regular	6.33E-11	1.61E-16	1.25E-16	2.56E-07	-4.43E-10	1.37E-10
	off 1	7.38E-11	6.27E-14	3.39E-13	1.76E-08	1.44E-08	5.19E-07
	off 4	1.85E-10	6.42E-13	8.40E-12	-1.88E-06	1.16E-07	2.67E-06
	random	2.38E-09	5.12E-11	6.56E-11	1.14E-05	5.79E-07	7.20E-06
0.010001	regular	0.00627	1.91E-13	1.67E-08	0.00036	5.06E-08	9.98E-06
	off 1	0.00627	1.85E-13	1.60E-08	0.00023	2.70E-08	-9.88E-07
	off 4	0.00647	2.16E-13	3.22E-08	-0.00013	-1.98E-07	-1.19E-04
	random	0.00694	1.83E-12	4.90E-07	0.00039	-1.29E-06	-6.84E-04
0.020001	regular	0.02735	1.94E-13	5.98E-08	-0.00292	1.71E-08	-5.96E-07
	off 1	0.02712	1.94E-13	6.42E-08	-0.00240	-2.62E-09	-1.75E-05
	off 4	0.02719	2.36E-13	1.22E-07	-0.00229	-2.22E-07	-2.41E-04
	random	0.02949	1.91E-12	1.98E-06	0.00084	-1.31E-06	-1.38E-03
0.030001	regular	0.06436	1.97E-13	1.47E-07	0.01015	2.23E-08	2.83E-06
	off 1	0.06425	1.96E-13	1.47E-07	0.01147	1.11E-09	-2.89E-05
	off 4	0.06406	2.34E-13	2.73E-07	0.01048	-2.07E-07	-3.44E-04
	random	0.07462	1.87E-12	4.37E-06	0.00803	-1.30E-06	-2.05E-03
0.040001	regular	0.10329	1.80E-13	2.65E-07	0.00937	3.82E-08	2.69E-06
	off 1	0.10391	1.77E-13	2.65E-07	0.01074	1.42E-08	-4.42E-05
	off 4	0.10578	2.07E-13	4.83E-07	0.01161	-1.91E-07	-4.60E-04
	random	0.12110	1.84E-12	7.90E-06	0.00871	-1.29E-06	-2.75E-03
0.050001	regular	0.15913	2.05E-13	3.93E-07	-0.01300	4.14E-08	3.68E-05
	off 1	0.15772	2.05E-13	3.84E-07	-0.01441	1.69E-08	-2.33E-05
	off 4	0.15712	2.36E-13	7.90E-07	-0.01390	-2.06E-07	-5.86E-04
	random	0.18317	1.82E-12	1.19E-05	-0.01245	-1.28E-06	-3.38E-03
0.060001	regular	0.22293	1.83E-13	5.58E-07	0.01748	1.95E-08	8.74E-06
	off 1	0.22280	1.80E-13	5.66E-07	0.01741	-2.33E-09	-5.54E-05
	off 4	0.22318	2.27E-13	1.14E-06	0.01467	-2.24E-07	-7.30E-04
	random	0.25915	1.86E-12	1.76E-05	0.01411	-1.31E-06	-4.10E-03
0.070001	regular	0.32174	1.86E-13	7.82E-07	-0.01108	3.73E-08	-4.48E-06
	off 1	0.32156	1.84E-13	8.08E-07	-0.01337	1.46E-08	-7.73E-05
	off 4	0.32592	2.19E-13	1.54E-06	-0.01349	-1.96E-07	-8.22E-04
	random	0.38718	1.79E-12	2.39E-05	-0.00739	-1.28E-06	-4.78E-03
0.080001	regular	0.40434	2.01E-13	1.02E-06	0.02820	4.61E-08	1.68E-06
	off 1	0.40011	1.94E-13	1.06E-06	0.02558	2.13E-08	-9.04E-05
	off 4	0.40488	2.23E-13	2.01E-06	0.02957	-1.92E-07	-9.47E-04
	random	0.46755	1.80E-12	3.16E-05	0.01896	-1.28E-06	-5.50E-03
0.090001	regular	0.54887	1.89E-13	1.25E-06	-0.03016	-9.39E-09	-4.51E-06
	off 1	0.54937	1.90E-13	1.29E-06	-0.03040	-3.12E-08	-1.15E-04
	off 4	0.55731	2.39E-13	2.51E-06	-0.03456	-2.51E-07	-1.09E-03
	random	0.63207	1.90E-12	3.95E-05	-0.01673	-1.32E-06	-6.14E-03

Table B.7: Mean errors and MSEs of estimators for larger σs in case of irregular observations in a standard OUP with $\mu = 1$, $\alpha =$ 1.00E-5, $X_0 = 0.5$, $\Delta t_{\text{sim}} =$ 3,600, $\Delta t_{\text{obs}} =$ 36,000, $n_{\text{obs}} =$ 4,380, 1,000 paths

Appendix C

Additional graphs relating to Chapter 6

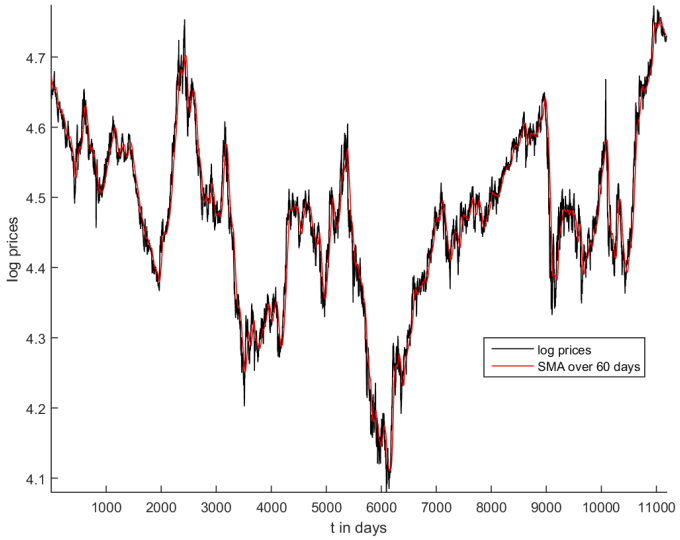

Figure C.1: Daily CHF/JPY log prices and simple moving average calculated over previous 60 days

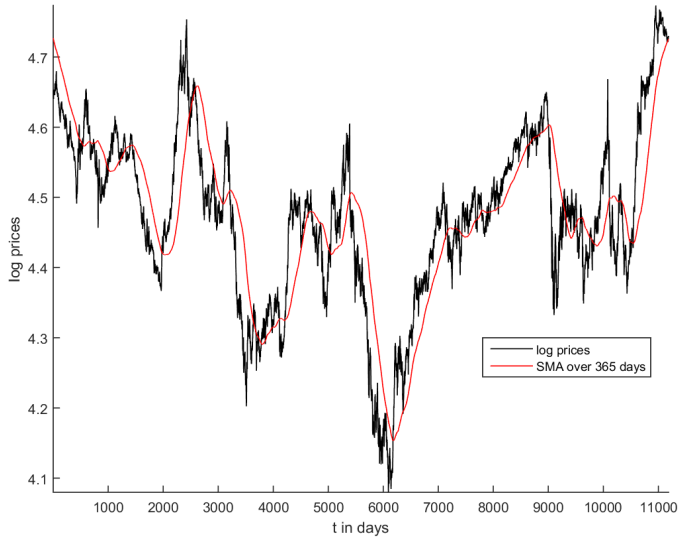

Figure C.2: Daily CHF/JPY log prices and simple moving average calculated over previous 365 days

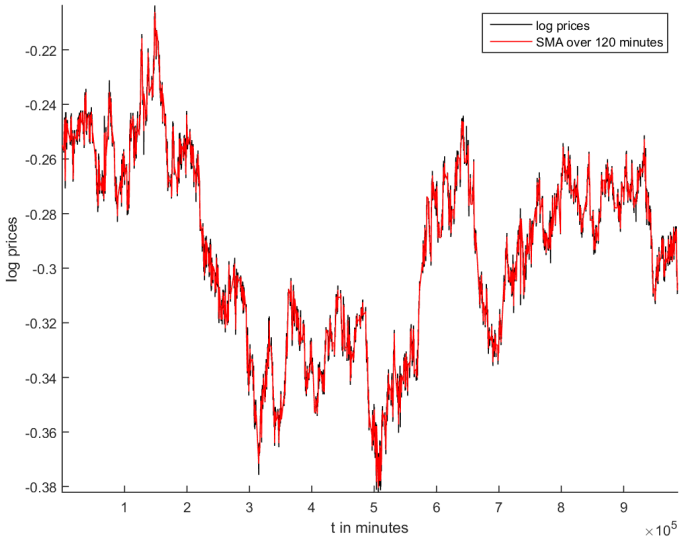

Figure C.3: Minutely AUD/USD LN log prices and simple moving average calculated over previous two hours

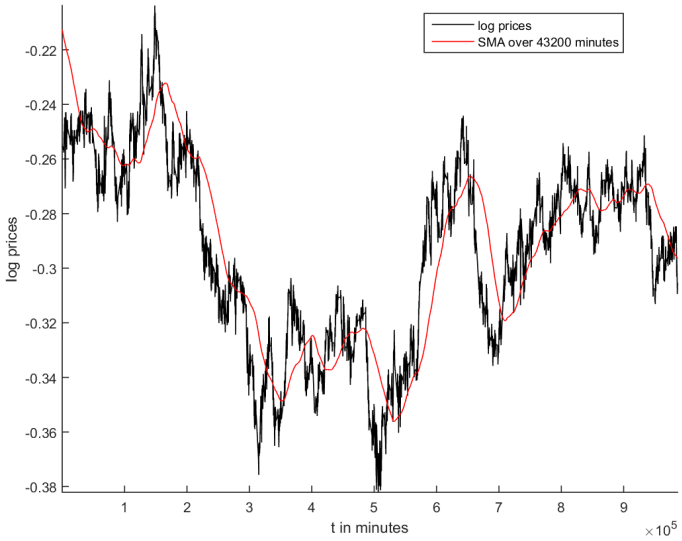

Figure C.4: Minutely AUD/USD LN log prices and simple moving average calculated over previous 30 days

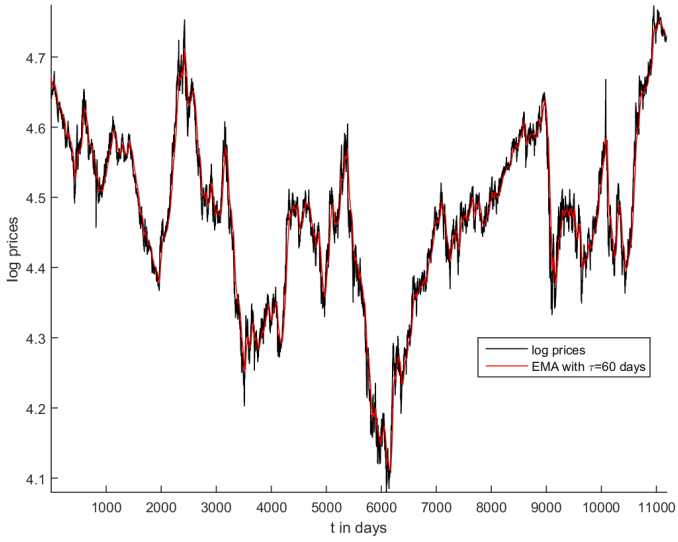

Figure C.5: Daily CHF/JPY log prices and lagging exponential moving average with time constant 60 days

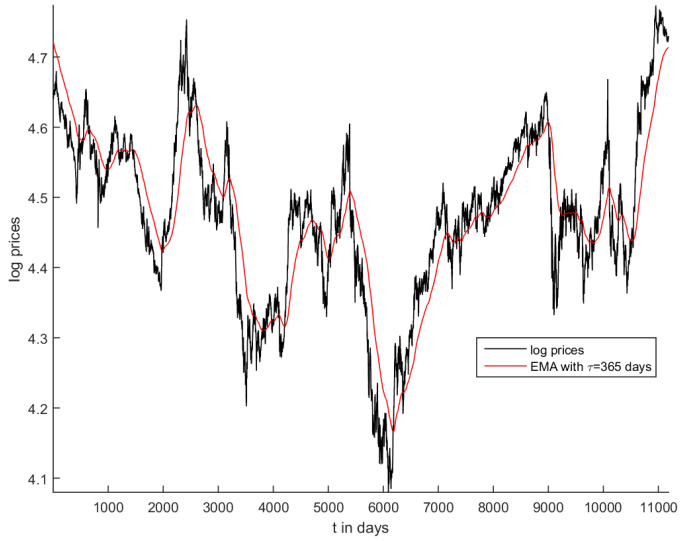

Figure C.6: Daily CHF/JPY log prices and lagging exponential moving average with time constant 365 days

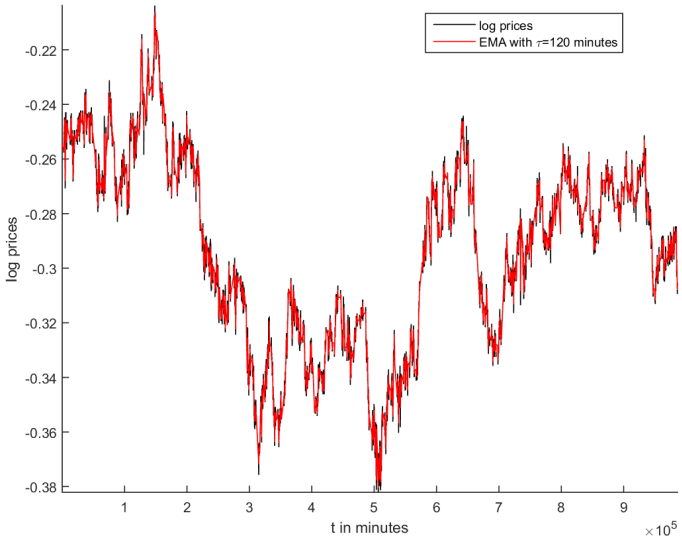

Figure C.7: Minutely AUD/USD LN log prices and lagging exponential moving average with time constant two hours

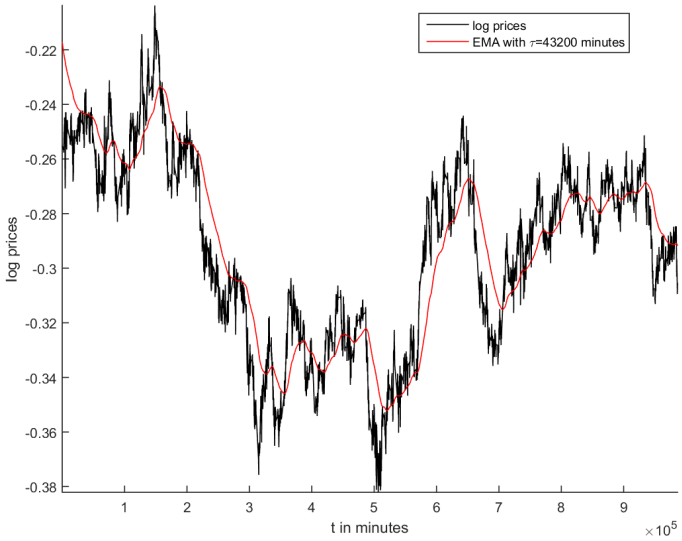

Figure C.8: Minutely AUD/USD LN log prices and lagging exponential moving average with time constant 30 days

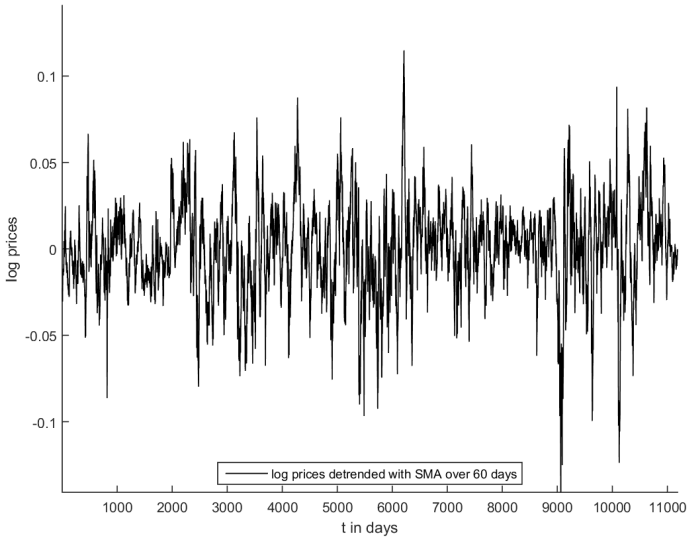

Figure C.9: Daily CHF/JPY log prices minus SMA calculated over previous 60 days

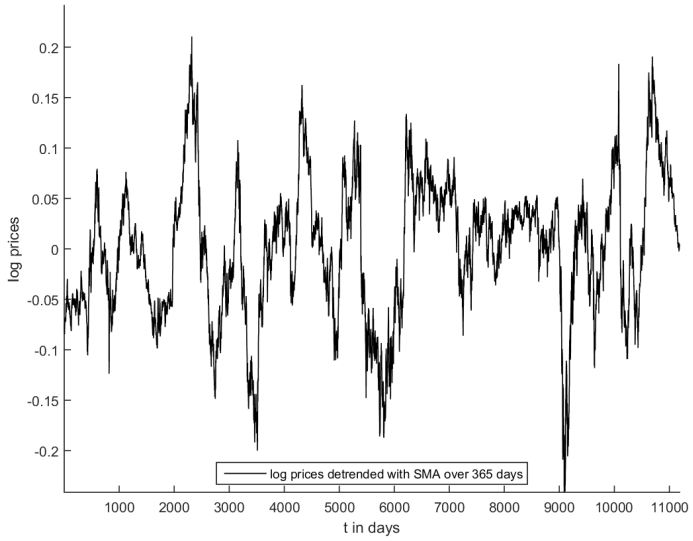

Figure C.10: Daily CHF/JPY log prices minus SMA calculated over previous 365 days

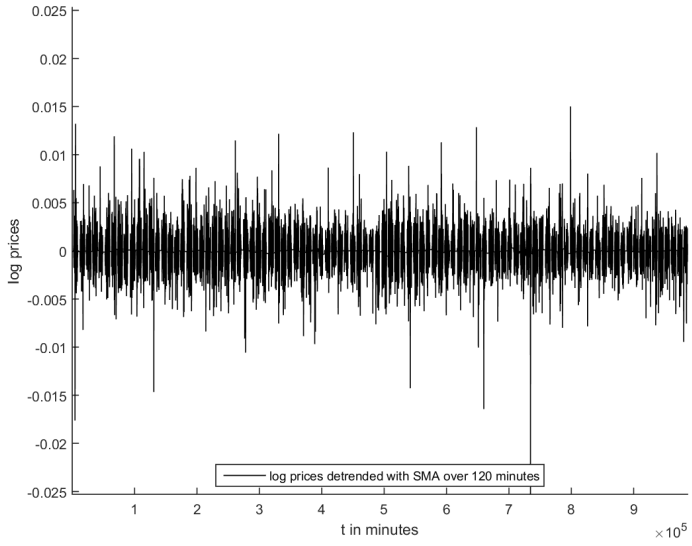

Figure C.11: Minutely AUD/USD LN log prices minus SMA calculated over two hours

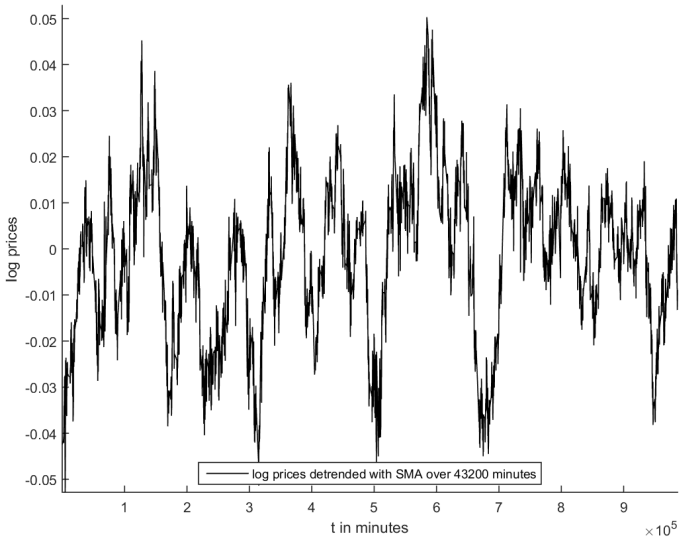

Figure C.12: Minutely AUD/USD LN log prices minus SMA calculated over 30 days

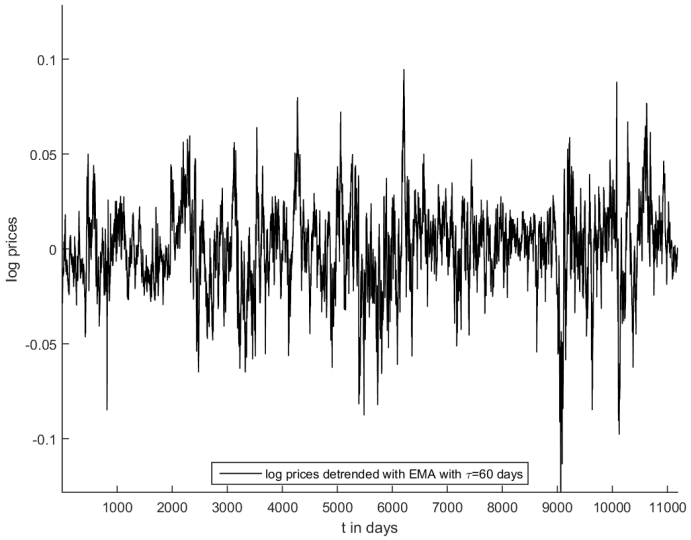

Figure C.13: Daily CHF/JPY log prices minus lagging exponential moving average with time constant 60 days

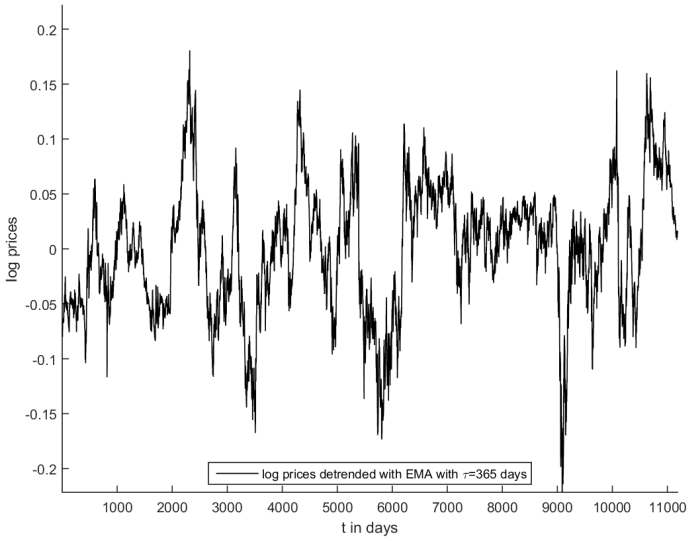

Figure C.14: Daily CHF/JPY log prices minus lagging exponential moving average with time constant 365 days

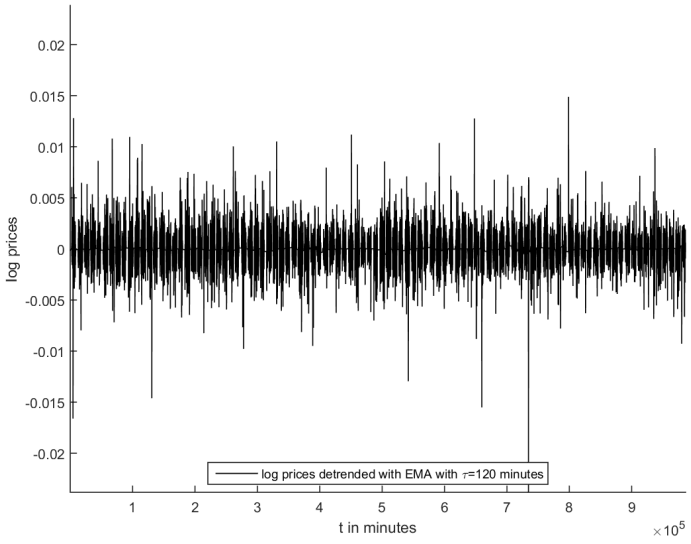

Figure C.15: Minutely AUD/USD LN log prices minus lagging exponential moving average with time constant two hours

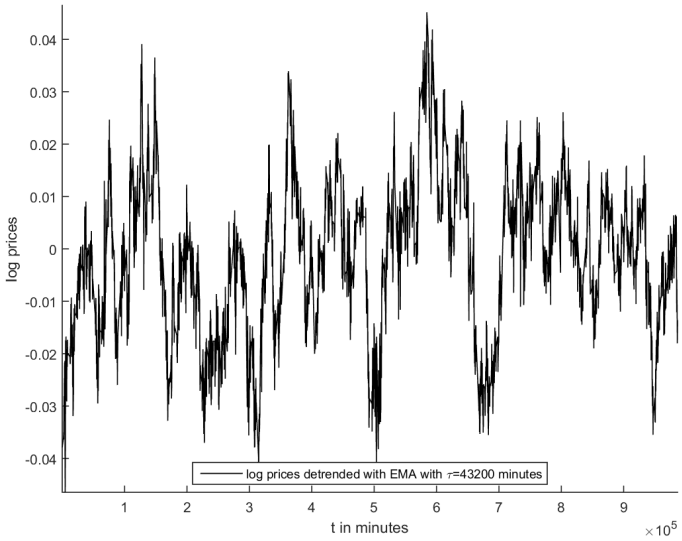

Figure C.16: Minutely AUD/USD LN log prices minus lagging exponential moving average with time constant 30 days

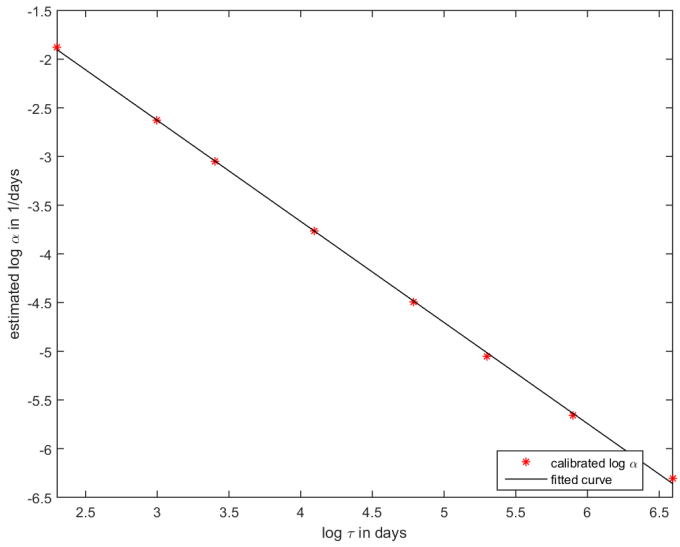

Figure C.17: Estimated mean log reversion strengths in 1/h for detrended daily log CHF/JPY prices for different log SMA windows

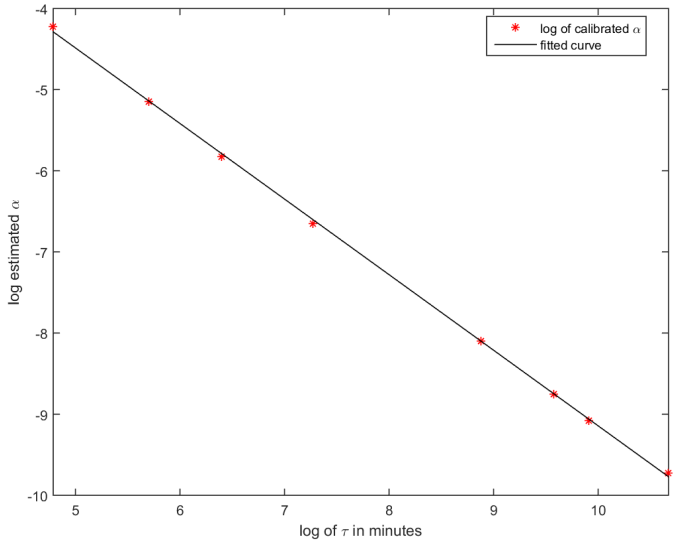

Figure C.18: Estimated log mean reversion strengths in 1/h for detrended minutely log AUD/USD LN prices for different log SMA windows

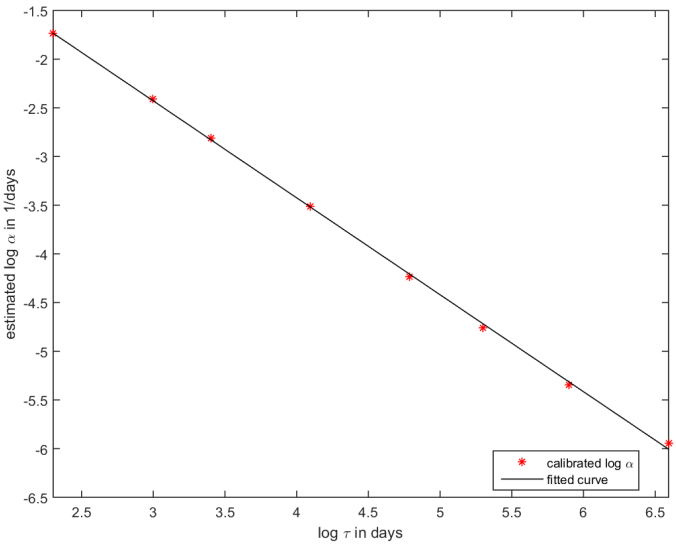

Figure C.19: Estimated log mean reversion strengths in 1/h for detrended daily log CHF/JPY prices for different log EMA time constants

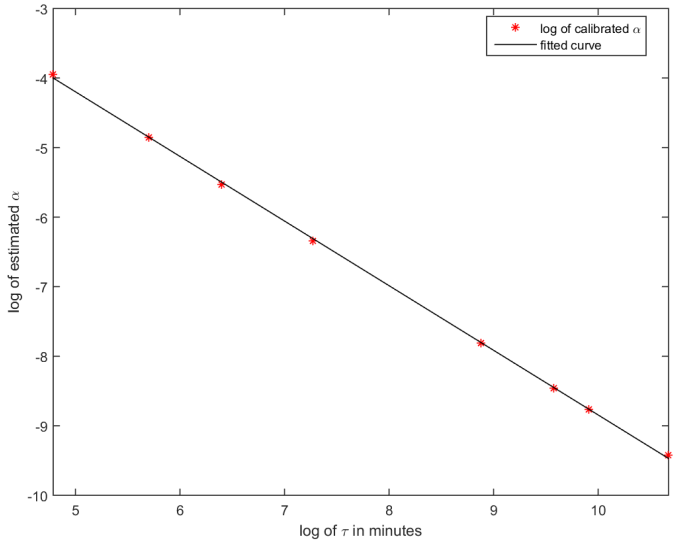

Figure C.20: Estimated log mean reversion strengths in 1/h for detrended minutely log AUD/USD LN prices for different log EMA time constants

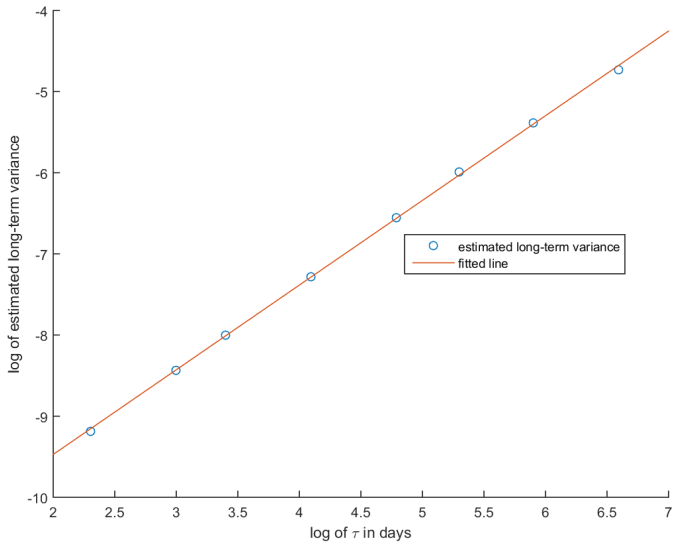

Figure C.21: Log of estimated long-term variances for detrended daily log CHF/JPY prices for different log SMA windows

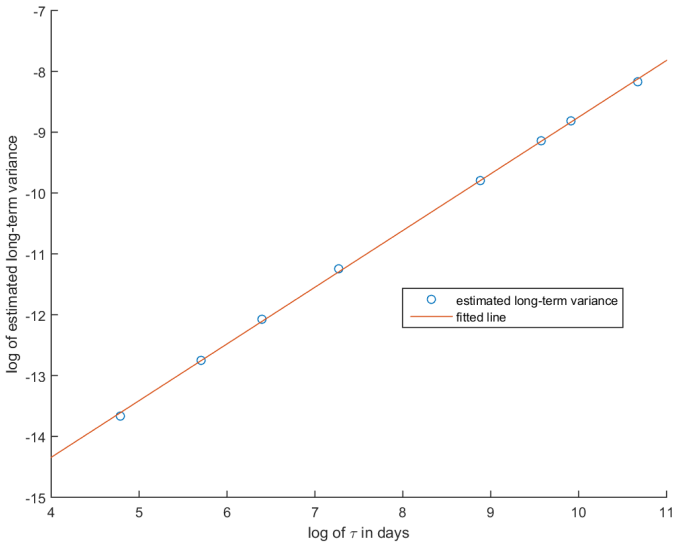

Figure C.22: Log of estimated long-term variances for detrended minutely log AUD/USD LN prices for different log SMA windows

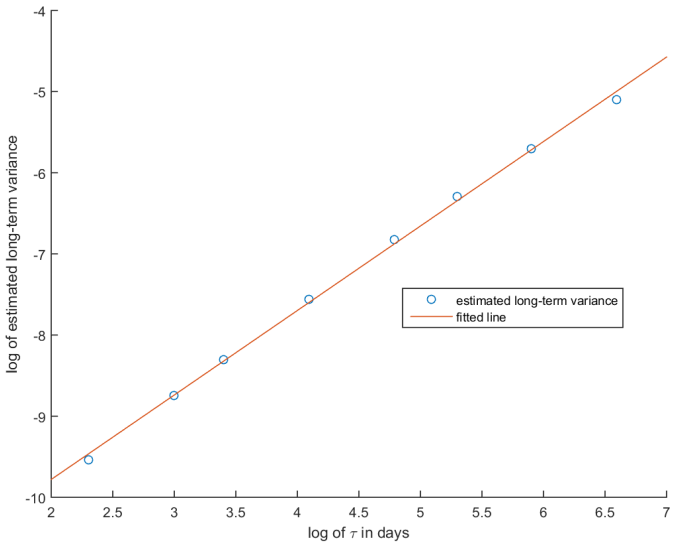

Figure C.23: Log of estimated long-term variances for detrended daily log CHF/JPY prices for different log EMA time constants

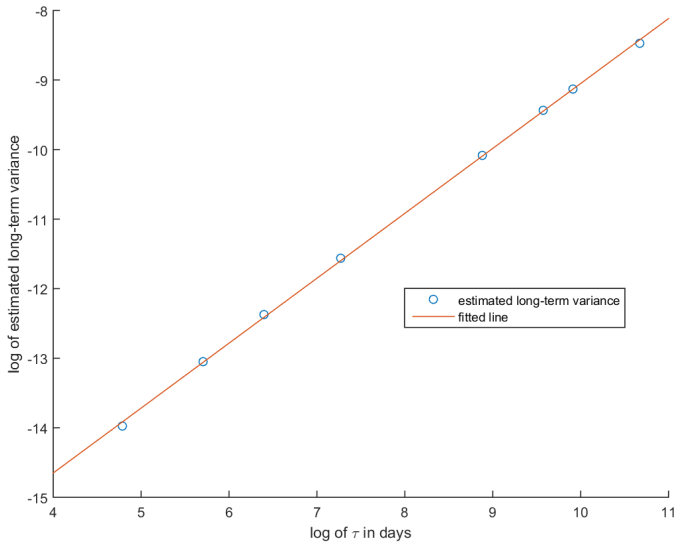

Figure C.24: Log of estimated long-term variances for detrended minutely log AUD/USD LN prices for different log EMA time constants

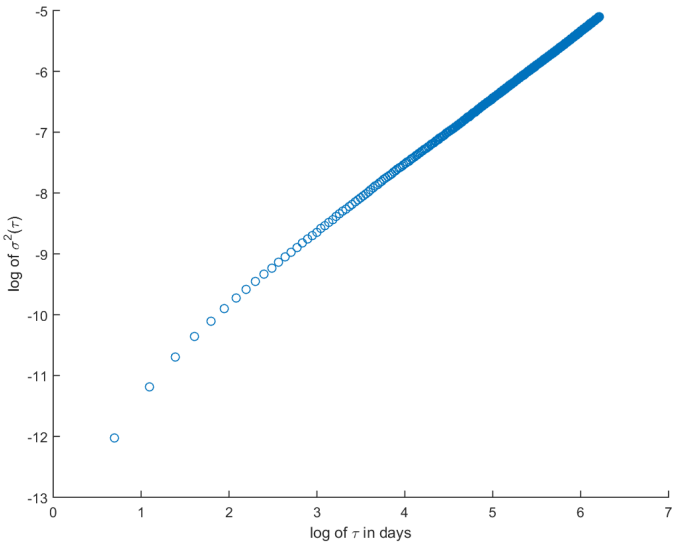

Figure C.25: Log of σ_{DMA} for USD/EUR as a function of log τ in days

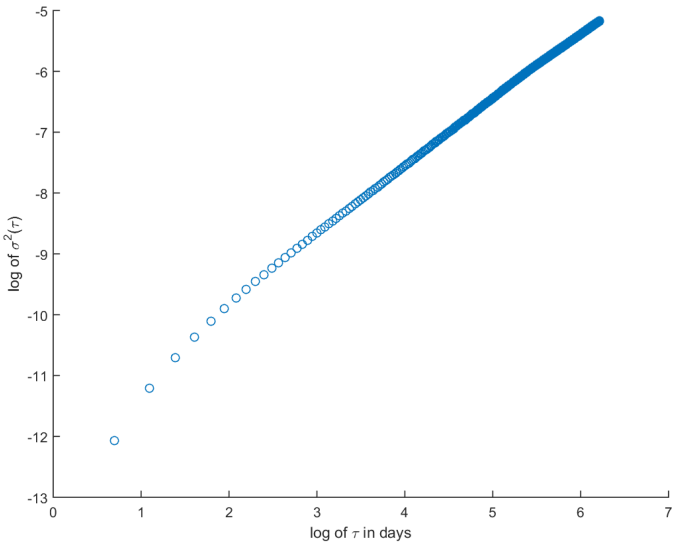

Figure C.26: Log of σ_{DMA} for USD/GBP as a function of log τ in days